IDŐJÁRÁS

QUARTERLY JOURNAL
OF THE HUNGARIAN METEOROLOGICAL SERVICE

CONTENTS

Szilvia Kugler, László Horváth, and *Tamás Weidinger:* Modeling dry flux of ammonia and nitric acid between the atmosphere and Lake Balaton 93

Csilla Péliné Németh, Judit Bartholy, and *Rita Pongrácz:* Homogenization of Hungarian daily wind speed data series.. 119

Agnieszka Wypych and *Ewelina Henek:* Spatial modeling of the climatic water balance index using GIS methods..... 133

Attila Kovács and *János Unger:* A modification of Tourism Climatic Index to Central European climatic conditions – examples 147

Andrea Móring and *László Horváth:* Long-term trend of deposition of atmospheric sulfur and nitrogen compounds in Hungary 167

****

http://www.met.hu/Journal-Idojaras.php

VOL. 118 * NO. 2 * APRIL – JUNE 2014

IDŐJÁRÁS

Quarterly Journal of the Hungarian Meteorological Service

Editorial Office: Kitaibel P.u. 1, H-1024 Budapest, Hungary
P.O. Box 38, H-1525 Budapest, Hungary
E-mail: journal.idojaras@met.hu
Fax: (36-1) 346-4669

Indexed and abstracted in Science Citation Index Expanded™ and Journal Citation Reports/Science Edition
Covered in the abstract and citation database SCOPUS®

Subscription by mail:
IDŐJÁRÁS, P.O. Box 38, H-1525 Budapest, Hungary
E-mail: journal.idojaras@met.hu

IDŐJÁRÁS

Quarterly Journal of the Hungarian Meteorological Service
Vol. 118, No. 2, April – June, 2014, pp. 93–118

Modeling dry flux of ammonia and nitric acid between the atmosphere and Lake Balaton

Szilvia Kugler[1,2], **László Horváth***[3,4], and **Tamás Weidinger**[1]

[1]*Department of Meteorology, Eötvös Loránd University, Pázmány Péter sétány 1/A, 1117 Budapest, Hungary*

[2]*Institute for Solid State Physics and Optics, Wigner Research Centre for Physics, Hungarian Academy of Sciences, Konkoly-Thege Miklós út 29-33, 1121 Budapest, Hungary*

[3]*Hungarian Meteorological Service, Gilice tér 39, 1181 Budapest, Hungary*

[4]*MTA-SZIE Plant Ecology Research Group, Szent István University, Páter K. u. 1, 2103 Gödöllő, Hungary*

**Corresponding author E-mail:* horvath.l@met.hu

(Manuscript received in final form January 30, 2014)

Abstract—N-deposition from atmosphere contributes to the eutrophication of Lake Balaton (Hungary). To estimate the share of N-input compared to the effect of other sources, measurements have started in the 70's of the last century. However, in previous calculations the flux of N-gases (NH_3 and HNO_3) was estimated using deposition velocity parameters determined for terrestrial ecosystems. These simplifications were accompanied by an overestimation of the role of these compounds. According to our results for years 2001–2004, ammonia has a mean net emission flux from the lake (32.7 t N $year^{-1}$), while nitric acid deposition takes –21.8 t N $year^{-1}$ that are one order of magnitude lower than sum of other deposition forms (esp. wet N-deposition). The pH range in lake water (pH = 8.3–8.9) allows the bi-directional flux for ammonia. Ammonia exchange can act as a buffering system, i.e., in case of a high N-load to the lake from other sources (rivers, waste water, run-off, etc.) N-accumulations can be buffered through nitrogen emission in form of NH_3 as a consequence of the elevated compensation-point concentration. From this reason, eutrophication of Lake Balaton is phosphorus limited. Comparing the measured ammonia flux with the fluxes calculated by compensation-point models based on single Henry's law theory and by Hales-Drewes theory, it can be concluded that in our case latter theory describes better the exchange processes, suggesting that effect of carbon dioxide on the solubility of ammonia can not be excluded. However, in contrast with Hales and Drewes who suggested a decreased solubility of ammonia in presence of CO_2, we find an opposite effect, i.e., CO_2 favors the solubility of ammonia in the slight alkaline pH-range representative to the lake.

Key-words: eutrophication, FLake model, Monin-Obukhov theory, resistance model, compensation-point model, ammonia flux, nitric acid flux

1. Introduction

Atmospheric load of trace materials is one of the most important nutrient sources for freshwater ecosystems. Nutrient enrichment causes change of ecosystem structure and function; this process is termed eutrophication (*Durand et al.*, 2011). Generally, the two limiting elements in eutrophication are the nitrogen and the phosphorus. According to an international survey (*ICLF*, 2010), Lake Balaton nowadays is co-limited; i.e., both N and P are limiting factors for eutrophication.

The mean surface of Lake Balaton is 598 km^2 with a contributing area of 5775 km^2. Being a shallow lake (mean depth of water is 3 m), Balaton is especially sensitive to nutrient loading (*Jordan et al.*, 2005). The first serious extinction of fish caused by algal bloom as a consequence of nutrient enrichment was observed in 1975 (*Herodek*, 1977).

Since then, intensive investigations have been started to estimate the source and strength of nutrient loading to the lake for mitigation purposes. *Jolánkai* and *Bíró* (2005) compiled the load of N and P into the lake from different sources for a three-decade period between 1975 and 2004. According to this work, the atmospheric nitrogen deposition has varied within a wide range between 300 and 1,800 t N $year^{-1}$. The reason of this large variation is the lack of direct measurement of dry deposition of nitrogen compounds to the surface of the lake. In all of previous studies, dry deposition of nitrate and ammonium particles and nitric acid vapor was estimated by the inferential method taking into account deposition velocities determined for terrestrial surfaces (*Horváth et al.*, 1981; *Horváth*, 1990). It led to an overestimation of nitrogen load, especially as the consequence of different surface characteristics (e.g., roughness) between terrestrial and water systems. To eliminate these discrepancies, a field campaign has started in 2002 to measure the dry deposition of nitrogen compounds also providing direct measurement data for validation of modeled fluxes. In a previous study (*Kugler* and *Horváth*, 2004), it was pointed out that dry deposition rates of nitrate and ammonium particles over Lake Balaton are much lower than it was supposed before and takes a nearly negligible share in the total atmospheric N-load to the lake.

In another paper (*Kugler et al.*, 2008), results of a preliminary analysis concerning the atmospheric dry deposition of nitric acid and net flux of ammonia for a year period (March 2002–February 2003) was reported based on a simple compensation-point model. It was found that deposition rate for nitric acid is less by one order of magnitude compared to grass surfaces, and ammonia has bi-directional flux resulting in either monthly average net emission or net deposition as the function of physical and chemical conditions in air and water. As ammonia has bi-directional flux, it is a key component in the nitrogen balance between the atmosphere and the lake, since compensation-point concentration and emission rate of ammonia is increasing parallel with increase

of N-load from other sources (waste water, rivers, creeks, leaching of fertilizers, etc.). It means a negative feedback mechanism which probably emits the excess nitrogen in the form of ammonia into the atmosphere (*Kugler et al.*, 2008). Moreover, in other case, in the lack of nutrient-N the atmosphere may act as nitrogen (ammonia) source for this aquatic ecosystem.

The aim of the paper is to investigate in more details the dry fluxes of gaseous nitrogen compounds and to estimate their share in total atmospheric N-load. Our investigations are based on sophisticated models for a four-year period (2001–2004) validated by flux data measured by the gradient method.

2. *Methodology*

2.1. Measurements

Meteorological and chemical parameters have been measured at the Storm Warning Observatory of Hungarian Meteorological Service, at the shore of lake (46° 54' 48.88" N; 18° 2' 19.76" E) in the town Siófok.

Meteorological measurements as wind direction and velocity, air temperature, relative humidity, and air pressure were observed by standard meteorological instruments. The global radiation and long wave radiation components were calculated by different parameterization schemes (*Holtslag* and *van Ulden,* 1983; *Mészáros*, 2002; *Foken*, 2006).

Measurement protocol for ammonia and nitric acid concentrations are: i) for the compensation-point model calculations: March 2002–February 2003 by 24-h continuous sampling at the height of 12.3 m above lake surface; ii) for the gradient measurements: July 12, 2002–July 25, 2012, 3-hour samplings, 8 times a day at two levels above the lake surface (12.3 and 2.8 m); iii) for interpolation of concentration data to Siófok: K-puszta and Farkasfa background air pollution monitoring stations (46° 58' N, 19° 33' E and 46° 55' N, 16° 18' E) (2001–2004). Ammonia and nitric acid were sampled by a NILU EK-type three-stage bulk filter-pack sampler (*EMEP*, 1996). Concentrations of nitrate and ammonium ions in the extract of filters water were determined by ion-chromatography and spectrophotometry, respectively. Minimum detection limit (MDL) was 0.1 $\mu g\, N\, m^{-3}$ for both ions. The bulk relative error of sampling and measurements is 10%.

The NH_3+NH_4^+ concentration (by spectrophotometry) and pH in the lake water were sampled and measured on the basis of bi-weekly samplings by the Middle Transdanubian Inspectorate for Environmental Protection, Natural Protection, and Water Management and by the VITUKI, Research Centre for Environmental Protection and Water Management. Sampling points were selected at Balatonakali, Keszthely, Siófok, and Szigliget settlements.

For validation of models, dry fluxes of ammonia and nitric acid were measured by the gradient method as described in Section 2.3.

2.2. The compensation-point model

Net dry flux of a gas having bi-directional exchange can be estimated by a modified compensation-point model (first described by *Farquhar et al.*, 1980):

$$F = -\left(C(z_{ref}) - C(z_0)\right) \cdot \left(\frac{1}{R_a + R_b}\right), \tag{1}$$

where F is the flux of gases, $C(z_{ref})$ is the atmospheric concentration of gases measured at the level z_{ref} (in our case 12.3 m), $C(z_0)$ is the compensation-point concentration at z_0 (roughness length) level, R_a and R_b are the resistances of turbulent and laminar layers, respectively. In case of ammonia and nitric acid vapor above water surfaces, the canopy resistance (R_c) can be neglected according to *Erisman et al.* (1994) and *Shahin et al.* (2002).

The net dry flux of nitric acid vapor can be calculated by Eq. (1), taking into account that in the slightly alkaline water HNO_3 molecules are completely dissociated, i.e., $C(z_0) = 0$ (*Kugler et al.*, 2008).

During the measurement campaign, the compensation-point concentrations for ammonia were calculated by two different methods. First, the simple Henry's law was used to determine the compensation-point concentration:

$$C(z_0) = \frac{C_w}{\left[H^+\right]\frac{K}{K_w}H_1 + H_1}, \tag{2}$$

where C_w and $[H^+]$ are concentrations of sum of ammonia+ ammonium and hydrogen ion in water phase, respectively, H_1 is the Henry's law constant of ammonia, K, K_w are constants at a given temperature (*Horváth*, 1982).

According to *Hales* and *Drewes* (1979), the simple Henry's law cannot be applied to calculate the compensation-point concentration, since carbon dioxide decreases the solubility of ammonia in water phase that must be taken into account in compensation-point calculation by the following formula:

$$C(z_0) = \frac{C_w(H_1H_2[CO_2]Q + 1)}{H_1H_2P[CO_2] + \left[H^+\right]\frac{K}{K_w}H_1 + H_1}, \tag{3}$$

where, Q, P, K, K_w are constants at a given temperature, H_2 is the Henry's law constant of carbon dioxide, $[CO_2]$ is the concentration of carbon dioxide in the air (calculated from the average mixing ratio of 380 ppm, in 2002–2003).

Later on, laboratory experiments (*Ayers et al.*, 1985; *Dasgupta* and *Dong*, 1986) demonstrated by laboratory experiments that theory of *Hales* and *Drewes* (1979) is not suitable, and the classical Henry's law should be used to calculate the compensation-point concentration. Due to the obvious contradiction among different authors and results between field and laboratory measurements, we have calculated the compensation-point concentrations using single Henry's law and the modified solubility theory of Hales-Drewes as well.

2.3. The gradient method

The gradient method was applied for validation of compensation-point models and in case of ammonia to verify two different outputs of models based on different solubility theories. The net gradient flux of a gas can be determined by the following equation supposed the similarity in exchange of heat and trace gases (*Weidinger et al.*, 2000; *Foken*, 2006):

$$F = -\rho_m \overline{K}_H \frac{\Delta C}{\Delta z}, \tag{4}$$

where $\overline{K}_H$ is the turbulent diffusion coefficient of the heat flux in a certain layer, ΔC is the concentration difference between two heights above surface, Δz is the difference between the two heights, ρ_m is the average density of the moist air. Turbulent diffusion coefficient at dimensionless height ($\zeta = (z-d)/L$) can be calculated using the similarity theory by the following formula:

$$K_H(\zeta) = \frac{\kappa u_* (z-d)}{\varphi_H(\zeta)}, \tag{5}$$

where κ is the Kármán constant (usually set to 0.4), u_* is the friction velocity, z is the height, d is the displacement height, L is the Monin-Obukhov length, φ_H is the universal function of sensible heat flux. Above water surface the displacement height is zero. Parameterizations of *Businger et al.* (1971) and *Dyer* (1974) were used for determination of the universal functions in different stratifications. The calculations of the friction velocity are described in Section 2.4.

2.4. The micrometeorological input

Turbulent diffusion coefficient for the gradient method and different resistances for compensation-point model were calculated by two different micrometeorological methods. First, we used the Monin-Obukhov theory to determine the turbulent sensible heat fluxes, the Monin-Obukhov length, and the friction velocity. It is named as resistance model (RM), since it was applied to

calculate the resistances (*Weidinger et al.*, 2000; *Ács* and *Szász*, 2002; *Ács*, 2003). Another model, namely the 1D numerical FLake model (FM) was also used to determine the same characteristics (*Mironov*, 2008).

At first, both models calculate the net radiation (Q_S) by the following equation:

$$Q_S = Q_H + Q_E + Q_G, \tag{6}$$

where Q_H, Q_E are the sensible and latent heat fluxes, Q_G is the heat flux into the water.

Calculation of momentum flux (τ), sensible heat flux (Q_H), latent heat flux (Q_E), and trace gas fluxes (Q_C) can be described by the following equations (*Foken*, 2006):

$$\tau = \rho_m u_*^2 = \rho_m K_M \frac{\partial \bar{u}}{\partial z}, \tag{7}$$

$$Q_H = -c_{pm}\rho_m u_* T_* = -\rho_m c_{pm} K_H \frac{\partial \bar{\theta}}{\partial z}, \tag{8}$$

$$Q_E = -\lambda \rho_m u_* q_* = -\lambda \rho_m K_E \frac{\partial \bar{q}}{\partial z}, \tag{9}$$

$$Q_C = -\rho_m u_* c_* = -\rho_m K_C \frac{\partial \bar{c}}{\partial z}, \tag{10}$$

where c_{pm} is the specific heat at constant pressure, λ is the phase transition energy, z is the height, $\bar{\theta}$, $\bar{q}$, $\bar{c}$, $\bar{u}$ are average potential temperature, specific humidity, trace gas concentration, and wind velocity, respectively, u_*, T_*, q_*, c_* are dynamical parameters for wind velocity, air temperature, specific humidity, and trace gas concentration, respectively. K_s is the turbulent diffusion coefficient of a certain property $s \in (M, H, E, C)$ as momentum, sensible, latent heat, and trace gas. We assume that eddy diffusivity coefficients of sensible and latent heat and trace gases are similar $K_H = K_E = K_C$.

With the knowledge of the gradient of certain micrometeorological parameters (*Weidinger et al.*, 2000; *Mészáros*, 2002), the universal functions of momentum, heat, humidity, and trace gases can be calculated as:

$$\frac{\partial \bar{u}}{\partial z} = \frac{u_*}{\kappa(z-d)} \varphi_M(\zeta), \tag{11}$$

$$\frac{\partial \bar{\theta}}{\partial z} = \frac{T_*}{\kappa(z-d)} \varphi_H(\zeta), \tag{12}$$

$$\frac{\partial \bar{q}}{\partial z} = \frac{q_*}{\kappa(z-d)} \varphi_E(\zeta), \tag{13}$$

$$\frac{\partial \bar{c}}{\partial z} = \frac{c_*}{\kappa(z-d)} \varphi_C(\zeta), \tag{14}$$

where $\zeta = (z-d)/L$ is the dimensionless height and L is the so-called Monin-Obukhov length. Other parameters have been described previously. φ_S $s \in (M, H, E, C)$ is the universal function of a certain property as momentum, heat, humidity, and trace gas.

The Monin-Obukhov length is determined by this formula:

$$L = \frac{u_*^2}{\kappa \beta T_*}, \tag{15}$$

where $\beta = g/\bar{\theta}$ is the stability parameter, g is the acceleration of gravity.

The general forms of universal functions (*Arya*, 2001) of momentum and sensible heat are described as:

$$\varphi_M = (1-\gamma_1\zeta)^{-\frac{1}{4}}, \qquad \text{if } 0 > \zeta \quad \text{(unstable)}, \tag{16}$$

$$\varphi_M = 1+\beta_1\zeta, \qquad \text{if } 0 \le \zeta \quad \text{(stable)}, \tag{17}$$

$$\varphi_H = \alpha(1-\gamma_2\zeta)^{-\frac{1}{2}}, \qquad \text{if } 0 > \zeta \quad \text{(unstable)}, \tag{18}$$

$$\varphi_H = \alpha + \frac{\beta_2}{\alpha}\zeta = \alpha(1+\beta_2\zeta), \qquad \text{if } 0 \le \zeta \quad \text{(stable)}, \tag{19}$$

where $\alpha, \beta_1, \beta_1, \gamma_1, \gamma_2$ are constants derived from the micrometeorological experiments of *Businger et al.* (1971) and *Dyer* (1974).

By integration of the Eqs. (11–12), turbulent characteristics for a certain layer are described as follows:

$$u(z_2)-u(z_1)=\frac{u_*}{\kappa}\left[ln\frac{z_2}{z_1}-\int_{\zeta_1}^{\zeta_2}(\varphi_M-1)\mathrm{d}ln\zeta\right]=\frac{u_*}{\kappa}\left[ln\frac{z_2}{z_1}-(\Psi_M(\zeta_2)-\Psi_M(\zeta_1))\right], \quad (20)$$

$$\theta(z_2)-\theta(z_1)=\frac{T_*}{\kappa}\left[ln\frac{z_2}{z_1}-\int_{\zeta_1}^{\zeta_2}(\varphi_H-\alpha)\mathrm{d}ln\zeta\right]=\frac{T_*}{\kappa}\alpha\left[ln\frac{z_2}{z_1}-(\Psi_H(\zeta_2)-\Psi_H(\zeta_1))\right], \quad (21)$$

where Ψ_M, Ψ_H are integral forms of stability function of momentum and sensible heat.

Stability functions in cases of stable and unstable stratifications are:

$$\Psi_M(\zeta)=ln\left[\left(\frac{1+x_M{}^2}{2}\right)\left(\frac{1+x_M}{2}\right)^2\right]-2tan^{-1}x_M+\frac{\pi}{2}, \quad \text{if } 0>\zeta, \quad (22)$$

$$\Psi_H=2ln\left(\frac{1+x_H{}^2}{2}\right), \quad \text{if } 0>\zeta, \quad (23)$$

$$\Psi_M=-\beta_1, \ \Psi_H=-\frac{\beta_2}{\alpha}, \quad \text{if } 0\le\zeta, \quad (24)$$

where $x_M=(1-\gamma_1\zeta)^{1/4}$, $x_H=(1-\gamma_2\zeta)^{1/4}$.

RM model uses Eqs. (16-19) for calculation, where the constants used have been measured at the Kansas experiment of *Businger et al.* (1971):

$$\alpha=0,74;\ \beta_1=4,7;\ \beta_2=4,7/\alpha;\ \gamma_1=15;\ \gamma_2=9. \quad (25)$$

After calculation of radiation balance, RM is resolving the Eqs. (15, 20–21). We considered $z_1=z_0=0.0003$ m, and water temperature was applied at height z_1. Model uses iteration method to calculate friction velocity (u_*), dynamic temperature (T_*), and sensible heat flux using Eq. (8). Sensible heat flux was calculated using the assumption that $\varphi_E=\varphi_H$ based on the difference in specific humidity. At the end of calculations, heat flux into the water is determined as residual term in radiation balance.

Since RM uses measured water temperatures at depth of 1 m for calculations, we tried to find a lake model which is able to predict the surface

temperature of a shallow lake. The FLake model (FM) is able to predict a vertical temperature structure in lakes at various depths on time scales from a few hours to a year.

The change in water temperature is described by the following equation in FM:

$$h\frac{\partial T_S}{\partial t} = \frac{1}{\rho_w \cdot c_w}[Q_W + I_W - Q_M - I(h)], \tag{26}$$

where h is the depth of mixed layer, T_s is the surface temperature of water (the same as the temperature in the upper water layer), ρ_w is the density of water, c_w is the specific heat capacity of water, Q_w is the heat flux through air-ice-water or air-water interface, I_w is the radiation flux through air-ice-water or air-water interface, Q_M is the heat flux at the bottom of mixed layer, $I(h)$ is the radiation flux at the bottom of depth layer (h). Terms Q_w and I_w are defined as $Q_G = Q_w + I_w$ for Q_G referring to Eq. (6).

FM uses the following method for calculations. First, prognostic and diagnostic values of the model are set to their initial values. As next step, the albedo of water, ice, and snow and also optical characteristics of water are determined. It follows the calculation of long wave radiation from surface and shortwave heat balance. With the Monin-Obkuhov theory momentum, sensible, and latent heat fluxes plus the dynamic velocity are derived. At the parameterization of the universal functions Eqs. (16–19), FM uses constants of *Dyer* (1974):

$$\alpha = 1; \beta_1 = \beta_2 = 5; \gamma_1 = \gamma_2 = 16\,. \tag{27}$$

For further calculations FM uses the Euler explicit scheme. In all time steps all model variables are derived. As the next step, heat flux through air-ice-water or air-water interface, a heat flux utilized in calculations of the convective boundary-layer evolution in the lake water, then heat flux through water-bottom sediment interface are computed. Later on, it follows to determine change in thickness and temperature of ice and snow, mean temperature of water column, mixed-layer depth, mixed-layer temperature, bottom temperature, and shape factor with respect to temperature profile in thermocline. Depth of upper layer of bottom sediments penetrated by thermal wave and temperature at that depth are computed. At the end, lake surface temperature is updated. That is set equal to either temperature of the water-surface temperature, or to surface temperature of ice or snow. The model applies a 10-step iteration method. More details for the FLake model description refer to *Mironov* (2008) and *Mironov et al.* (2010).

Both models determine the turbulent fluxes dynamic velocity, and also stratification. Then, aerodynamic resistances can be derived to solve the following equation (*Ács et al.*, 2000) using Eq. (5):

$$R_a = \int_{z_0}^{z} \frac{1}{K_H(z)} dz \,, \tag{28}$$

where K_H is the turbulent diffusion coefficient of sensible heat flux in a certain layer.

The boundary layer resistance can be calculated by the following formula (*Kramm et al.*, 1996):

$$R_b = \frac{2}{\kappa u_*} \left(\frac{\mathrm{Sc}}{\mathrm{Pr}} \right)^P , \tag{29}$$

where Sc is the Schmidt-number, Pr is the Prandtl-number, and P is an empirical constant (2/3). The quotient of Schmidt- to Prandtl-numbers are 0.96 for ammonia and 1.44 for nitric acid (*Hicks et al.*, 1987).

3. *Results and discussions*

3.1. Calculation of resistances and turbulent diffusion coefficients

Turbulent heat and momentum fluxes and diffusion coefficient were parallel determined by resistance (RM) and Flake models (FM) (*Ács* and *Szász*, 2002; *Mironov*, 2008) between January 2001 and December 2004 on hourly base.

Input data for resistance model are: water and air temperature, wetness characteristics (e.g., specific humidity), wind velocity and direction, cloudiness, and global radiation. Output data are: hourly averages of momentum flux (τ), sensible (Q_H) and latent (Q_E) heat fluxes, turbulent diffusion coefficients (K_H), resistances (R_a, R_b), and Monin-Obukhov length (L) on the basis of methods described by *Ács et al.* (2000), *Weidinger et al.* (2000), and *Foken* (2006).

Input data for FLake model are: rate of snow accumulation, global radiation, longwave radiation, wind velocity, and temperature, humidity, and pressure of air. Initial conditions (*Table 1*) were determined by *Vörös et al.* (2010) based on measurements and sensitivity analysis. Initial mean water temperature was always set to the measured water temperature of the lake.

Table 1. Initial conditions and predicted variables in FLake model

Type	Symbol	Name	Setting/ initialization
Initial conditions	$Depth_{\_w}$	Depth of lake*	0.9 m
	Fetch	Wind fetch	3000 m
	T_{bs0}	Sediment temperature	283.15 K
	$Depth_{\_bs}$	Depth of sediment	3 m
	Latitude	Geographical situation	47°
	Albedo	Albedo	0.095
Prognostic variables	T_{snow}	Snow temperature	273.15 K
	T_{ice}	Ice temperature	273.15 K
	T_{mnw}	Mean water temperature	274.25 K
	T_{wML}	Temperature in boundary layer	274.25 K
	T_{bot}	Temperature at boundary of water/sediment	274.25 K
	T_{B1}	Temperature at the bottom of upper sediment	283.15 K
	C_θ	Shape factor	0.50
	h_{snow}	Snow depth	0 m
	h_{ice}	Ice depth	0 m
	h_{ML}	Thickness of mixing layer	0.9 m
	h_{B1}	Depth of upper layer of sediment	3 m
	T_{sfc}	Temperature in the previous time step	274.25 K

*Based on the sensitivity analysis of FLake model for Lake Balaton after *Vörös et al.* (2010)

Output data of FLake model are: turbulent fluxes over lake, turbulent diffusion coefficient of sensible heat flux, aerodynamic and boundary layer resistances, and Monin-Obukhov length.

Data of calculated hourly energy balance components by the two methods were governed mainly by the water temperature and input meteorological variables. Extreme figures caused by i) difference of measured (RM) and modeled (FM) water temperature, ii) high negative value of sensible heat flux during stable conditions at high wind velocity, and iii) by overestimation of latent heat flux during very unstable stratifications were filtered. Corrections were applied for cases with extreme large deviations between the figures calculated by the two methods caused by unreliable output data at least from one of the methods. Filtration criteria were as follows:

i) radiation balance must not be lower than -120 W m^{-2},
ii) latent heat flux must not reach 450 W m^{-2},
iii) lower and upper thresholds for sensible heat flux were -75 W m^{-2} and 175 W m^{-2}, respectively.

Application of these criteria is justified by, e.g., *Liu et al.* (2011) in calculation of direct fluxes for a water reservoir. Data over or below these limits

were replaced by the limit figure itself. Hourly energy balance was closed in these cases by change of heat flux into water.

Corrections were applied in cases when difference in heat fluxes into water was larger than 200 W m^{-2}. In these cases by proportional variation of sensible and latent heat fluxes – keeping the Bowen-ratio constant calculated by the two methods –, the difference between heat flux into water was kept below 200 W m^{-2}. According to the criteria above, corrections were applied in 3 to 6% of cases in the different years.

For validation of results we compared the monthly evaporation rates with that of calculated by Central-Transdanubian Water Directorate on the basis of Meyer-formula (*Anda* and *Varga*, 2010), for the period of 2001–2004. According to *Kovács* (2011) and *Szilágyi* and *Kovács* (2011), the Meyer-formula (MF) simulates well the real evaporation for Balaton. The monthly evaporation rates calculated by the different methods can be seen in *Fig. 1*. Correlations between model results (MF)–(FM) and (MF)–(RM) are r=0.93 and r=0.80, respectively, both are significant relations at p=0.01 probability level.

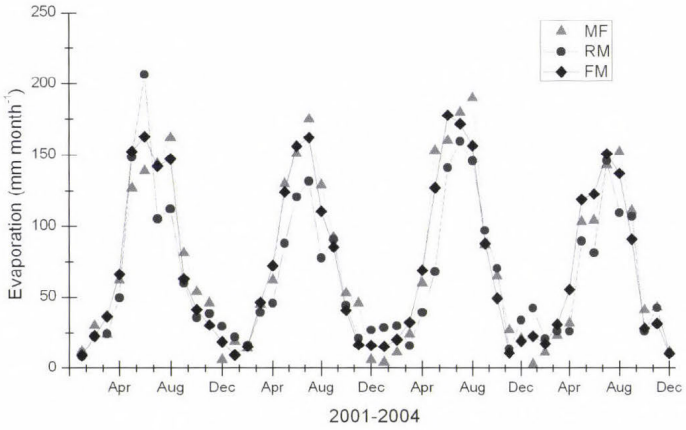

Fig. 1. Monthly evaporation rate calculated by three different ways for Lake Balaton (MF: Meyer-formula, FM: FLake model, RM: resistance model)

Yearly sum of evaporation calculated by the three different methods can be seen in *Table 2*. There is a good agreement between the mean values of MF an FM models, while RM underestimates the evaporation in comparison to others. The deviations among the mean values of three models are below 20%.

Table 2. Yearly evaporation (in mm) calculated by three different methods ((MF: Meyer-formula, FM: FLake model, RM: resistance model)

Year	MF	FM	RM
2001	887	892	841
2002	922	855	725
2003	982	938	843
2004	778	817	728
Mean	**892**	**876**	**784**

Mean monthly sensible heat fluxes were also determined by both FM and RM methods (*Fig. 2a*). It is generally a small value for lakes in comparison to radiation balance (*Fig. 2b*), because the stratifications over the lake are close to the neutral. The differences probably derive from differences between measured (RM) and calculated (FM) water surface temperatures.

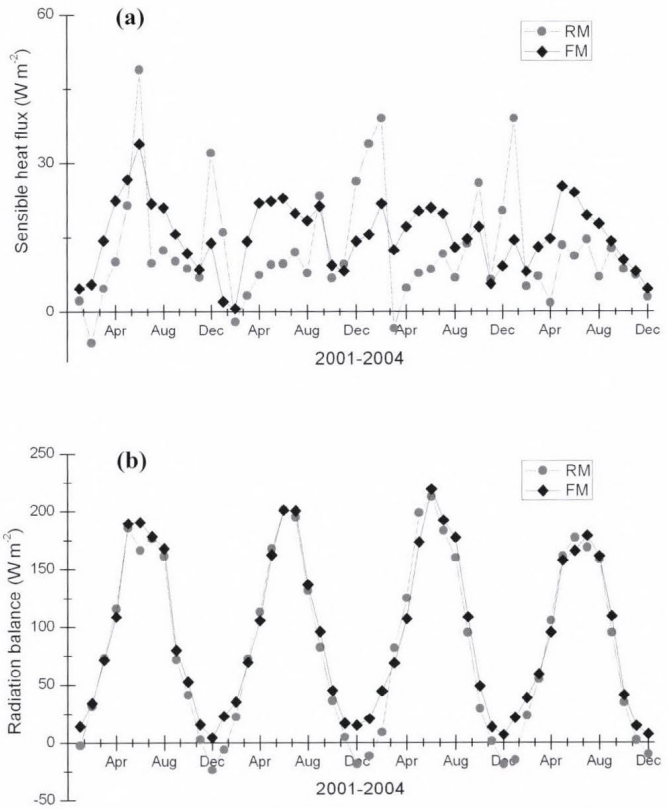

Fig. 2. Variation of monthly mean of sensible heat flux, Q_H (a) and radiation balance, Q_S (b) calculated by two different models (FM: FLake model, RM: resistance model)

Fig. 2b shows the course of monthly mean of radiation balance. Parameterization of surface energy budget components can be described by Eq. (6). The agreement between the two models is appropriate. Calculated turbulent diffusion coefficient of sensible heat between the heights of 12.3 and 2.8 meters using FM and RM methods for the period of experiment carried out in July 2002 gives also a good agreement as it can be seen in *Fig. 3a*. By the knowledge of K_H, we can estimate the exchange rate of gases by the gradient method supposing that exchange for heat and for trace gases are similar as mentioned above. Correlation between the diffusion coefficients determined by the two methods is $r=0.96$ ($p=0.01$).

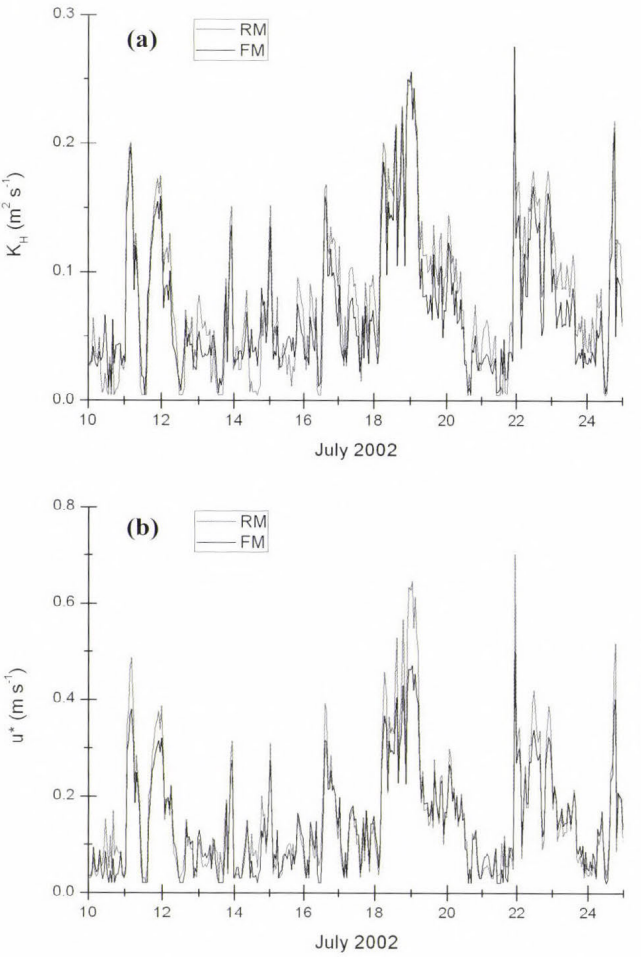

Fig. 3. Turbulent diffusion coefficients of sensible heat flux, K_H for the height between 12.3 and 2.8 meters (a) and friction velocity (b) calculated by the two different methods (July 10–25, 2002)

Finally, friction velocities (u_*) were also compared derived from RM and FM models (*Fig. 3b*). Agreement is good between results of the two models; systematic deviations can only be observed in case of higher values. Correlation is significant, $p=0.97$ ($p=0.01$).

In summary, it can be stated that the agreement between turbulent fluxes calculated by the two models is reasonable providing appropriate input data for determination of gas fluxes.

3.2. Modeling of fluxes

Ammonia and nitric acid fluxes were modeled at first for the period of July 12–25, 2002 for intercomparison (validation) of modeled fluxes by the results of gradient flux measurements conducted in the same period (*Figs. 4a,b*).

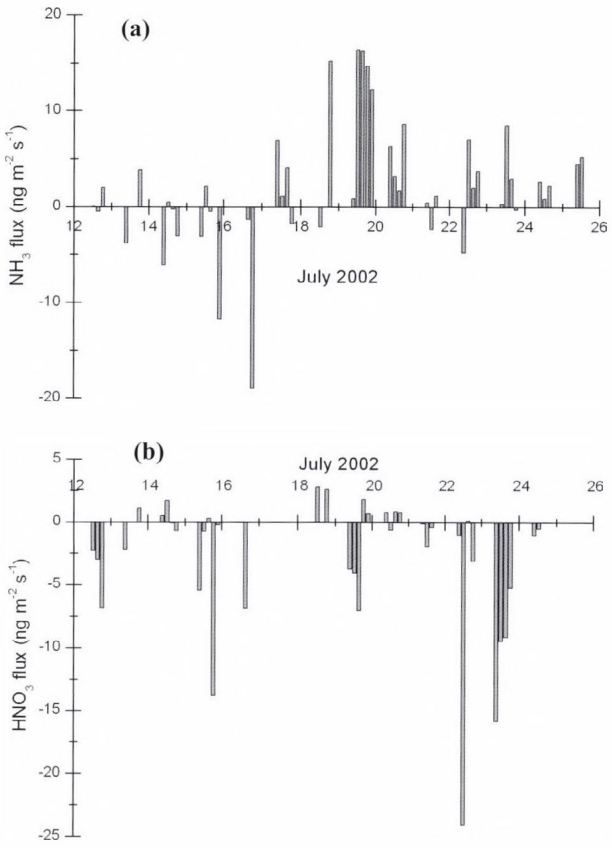

Fig. 4. Ammonia (a) and nitric acid (b) fluxes measured by the gradient method during a summer campaign at Siófok observatory

Ammonia exchange between the lake and the atmosphere was calculated on the basis of hourly micrometeorological parameters and 3-hour measured concentrations by means of the compensation-point model Eq. (1) using RM and FM methods for calculation of resistances. Only good fetch cases (wind from lake dominantly during duration of 3-hour samplings) were taken into consideration in evaluation. Compensation-point concentration of ammonia was calculated parallel by using the simple Henry's law equation and by the modified solubility theory of Hales-Drewes taking into account the effect of carbon dioxide on the solubility of ammonia in water at low concentrations. Ammonia concentration in air (at $h = 12.3$ m above water surface), ammonium+ammonia concentration and pH in water were measured as described in Section 2.1. Average of the 3-hour eddy diffusion coefficients for sensible heat was used in calculation.

The pH is a crucial parameter in controlling ratio the of ammonia to ammonium in diluted water solutions. It follows form Eqs. (2) and (3), that one unit decrease in pH results in one order decrease in compensation-point concentration. Ammonia in acidic solutions ($pH < 7$) – being a weak base – exists dominantly in protonated form (NH_4^+) prohibiting the escape of ammonia gas from the water. In the range of pH of the lake (pH=8.3–8.9), ammonia and ammonium exist together making the bi-directional change (either volatilization or absorption) of ammonia between the water and the atmosphere possible. Sign of the flux is determined by the difference in compensation-point and atmospheric concentration of ammonia according to the Eq. (1).

Other two input parameters of compensation-point model were the aerodynamic and boundary-layer resistances; they were calculated using both the resistance and FLake models as described in Section 2.4. Average resistances calculated by the two models were used (for details refer to 3.5).

Flux of nitric acid was modeled by the same way as of ammonia, the only difference is that HNO_3 does not exist in molecular form in diluted solutions, especially in the pH range of 8.3–8.9. It follows, that in Eq. (1) the compensation-point concentration of nitric acid equals to zero. Nitric acid concentrations in air were sampled by 3-hour sampling and analyzed as described in Section 2.1.

3.3. Measurement of fluxes of ammonia and nitric acid by the gradient method

For validation of models, dry fluxes of ammonia and nitric acid were measured during a summer campaign at the shore of the lake by the gradient method between July 12 and 25, 2002. Concentration gradients were determined by concentrations measured at 2.8 m and 12.3 m heights near/above the water surface by 3-hour samplings according to Eq. (4). Turbulent diffusion coefficient was derived from Eq. (5). Averages of 3-hour diffusion coefficient were used in calculation. Fluxes of ammonia and nitric acid by the gradient

method during expedition can be seen in *Figs. 4a,b*. The 3-hour mean fluxes were varied between -18.9 ng m^{-2} s^{-1} and 16.3 ng m^{-2} s^{-1} for ammonia and between 2.8 ng m^{-2} s^{-1} and -24.1 ng m^{-2} s^{-1} for nitric acid. (Positive figures derive from the 10% uncertainty of nitric acid concentration measurements.) Certainly, only good fetch cases (wind dominantly from lake during the duration of 3-hour samplings) were taken into consideration in the evaluation. Concentrations – especially for nitric acid – sometimes were below the detection limit; in these cases fluxes were not computed.

3.4. Validation, comparison of modeled and measured fluxes

The 3-hour mean of ammonia fluxes measured by the gradient method and modeled by the compensation-point model (using both resistance and FLake models for calculation of resistances) were compared for the period of summer campaign in 2002. The regression of the measured and modeled fluxes can be seen in *Figs. 5a,b*. Compensation-point concentrations for models were calculated both by simple Henry's law and Hales-Drewes solubility theory. Three-hour averages of calculated and modeled fluxes were plotted. Modeled fluxes are calculated as the mean of the results of the resistance and the FLake models. (The deviation between results of resistance and FLake models can be seen in *Table 2*.)

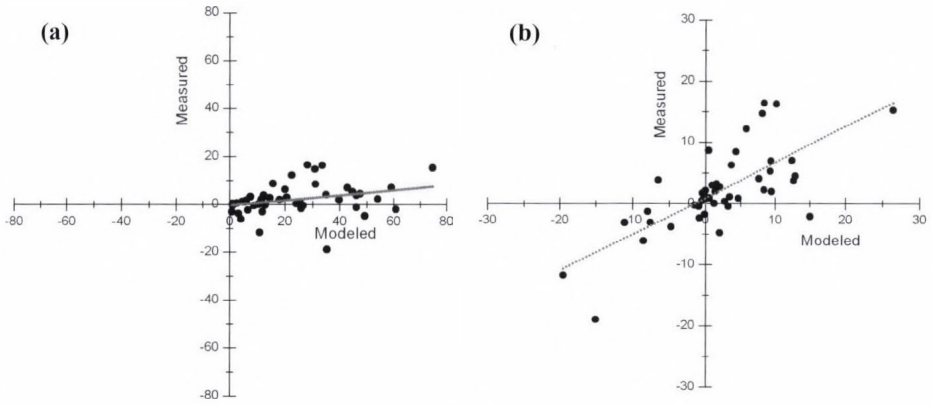

Fig. 5. Comparison of measured ammonia fluxes with results of compensation-point model used a) Henry's law; and b) Hales-Drewes theory for calculation of compensation-point concentration in ng m^{-2} s^{-1} for the period of July 12–25, 2002

The main parameters of comparison can be seen in *Table 3*. According to *Fig. 5* and *Table 3*, the difference between results of the two solubility theories

is significant. In contrast of finding of *Ayers et al.* (1985) and *Dasgupta* and *Dong* (1986), who demonstrated by laboratory measurement that classical Henry's law is applicable for solubility of ammonia, it seems that modeled fluxes by the theory of Hales and Drewes ranges much better with our gradient method measurements. Though, according to theory of *Hales* and *Drewes* (1979), carbon dioxide decreases the solubility of ammonia (increases the compensation-point concentration as a probable effect of carbamic acid), a reversed picture can be observed from our results. As *Fig. 5* and *Table 3* show, the fluxes are much lower calculated by Hales-Drewes theory suggesting that solubility of ammonia is rather increasing in the pH regime representative for the lake water. The supposed effect of carbon dioxide as the function of pH is illustrated in *Fig. 6* calculated at 20° C with the average $[NH_4^+]_w+[NH_3]_w$ concentrations measured in the modeled period ($1.61\ 10^{-6}$ M) by Eq. (3). As it can be seen, the effect of carbon dioxide strongly depends on the pH. At pH < 8.25, CO_2 enhances the volatilization of ammonia above that the influence turns to the inverse. This relationship explains our results, because during the summer experiment the pH of lake water was always above 8.65.

Table 3. Mean parameters in comparison of ammonia fluxes measured and modeled by the two solubility theories

	Hales-Drewes theory	**Henry's law**
Water temperature	22–29 °C	
pH	8.65–8.72	
C_w (ammonia + ammonium)	48–58 μM	
Mean flux	2.21 ng m^{-2} s^{-1}	24.4 ng m^{-2} s^{-1}
Degree of freedom	46	
Correlation	r = 0.72	r = 0.24
Significance (probability level)	p = 0.01	Non significant

Data in *Table 3* suggest the applicability of Hales-Drewes solubility theory instead of the classical Henry's law in calculation of compensation-point concentration in flux modeling, since correlation is significant, furthermore, the measured (2.11 ng m^{-2} s^{-1}) and modeled (2.21 ng m^{-2} s^{-1}) average fluxes were practically the same (SD=6.59 and 8.08, respectively). In contrast, modeled fluxes using the single Henry's law equilibrium constant only for ammonia (excluding CO_2) gives a mean flux higher by one order without significant relationship with the measured fluxes. Deviation from single Henry's law solubility theory was found in earlier investigations as well (*Lau* and *Charlson*, 1977; *Horváth*, 1982), underlying the disagreement among field and laboratory measurements in estimating the effect of CO_2 on the solubility of ammonia. To clarify the reason of this disagreement, further research is needed in this field.

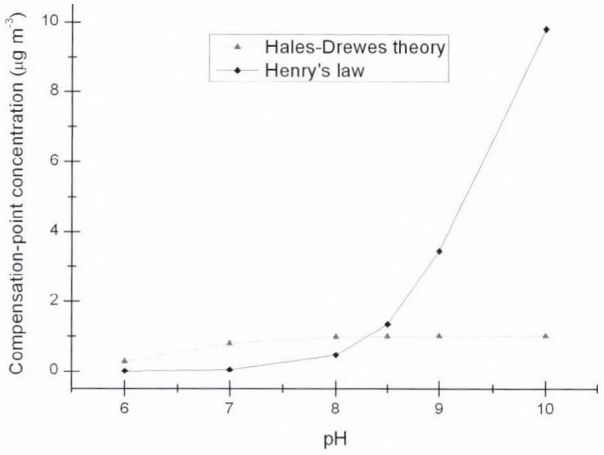

Fig. 6. Compensation-point concentration of ammonia in diluted water solution at 20 °C in the function of pH calculated by the Henry's law and the Hales-Drewes theory at $[NH_4^+]_w + [NH_3]_w = 1.61\ 10^{-6}$ M

Modeled fluxes of nitric acid were verified by fluxes measured by the gradient method similarly to ammonia. Samplings, gradient measurements, and gradient flux calculations were the same. Regression is illustrated by *Fig. 7*. The correlation between the calculated and modeled fluxes is $r=0.68$ ($p=0.01$).

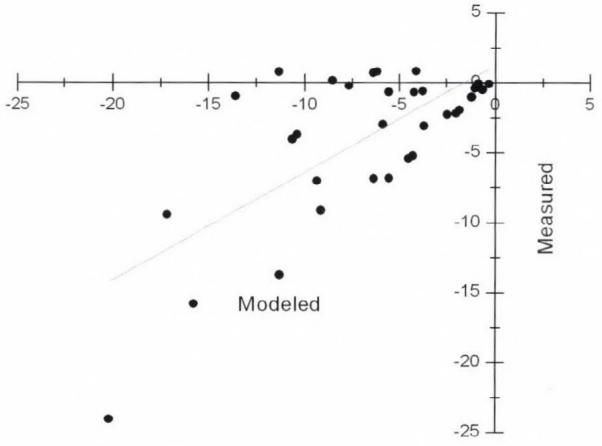

Fig. 7. Comparison of measured nitric acid fluxes with results of compensation-point model (ng m^{-2} s^{-1}) for the period of July 12–25, 2002

3.5. Flux calculation by the RM and FM models using new solubility theory

Ammonia exchange between the lake and the atmosphere was modeled on the basis of hourly micrometeorological parameters and daily concentration measurement of atmospheric ammonia between 2001 and 2004 by the compensation-point model Eq.(1) using the RM and FM models for calculation of resistances. Daily ammonia concentrations were measured near the lake between March 2002 and February 2003, while for the remaining period, interpolated data were used from two Hungarian background air pollution monitoring stations (*Farkasfa* and *K-puszta*). The agreement is relatively good (*Fig. 8a*), showing a uniform pattern of background ammonia concentration all over Hungary.

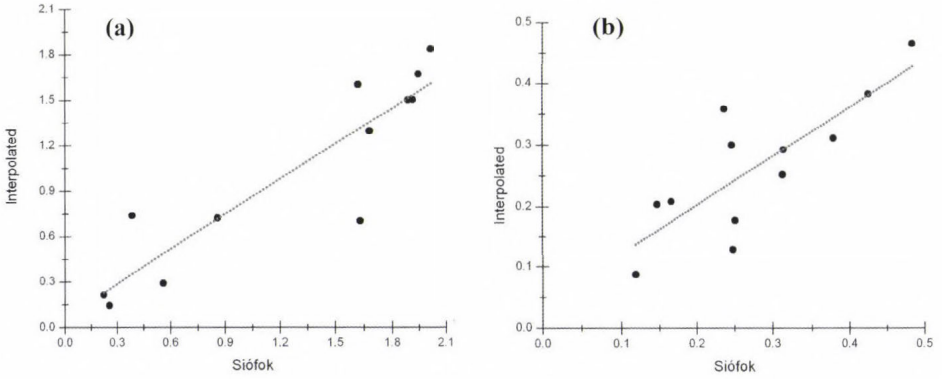

Fig. 8. Comparison of monthly mean ammonia (a) and nitric acid (b) concentrations in μg N m^{-3} measured near the lakeside (Siófok) and the average of two background air pollution monitoring stations (K-puszta, Farkasfa) in μg m^{-3}, between March 2002 and February 2003 (r = 0.90 and 0.78 for ammonia and nitric acid, respectively, and $p = 0.01$)

For calculation of the compensation-point concentration, the knowledge of pH, and sum of NH_3 and NH_4^+ concentrations in water were necessary. They were provided by the Middle Transdanubian Inspectorate for Environmental Protection, Natural Protection, and Water Management, measured on the basis of periodic measurement at five sampling points around the lake (*Figs. 9a,b*).

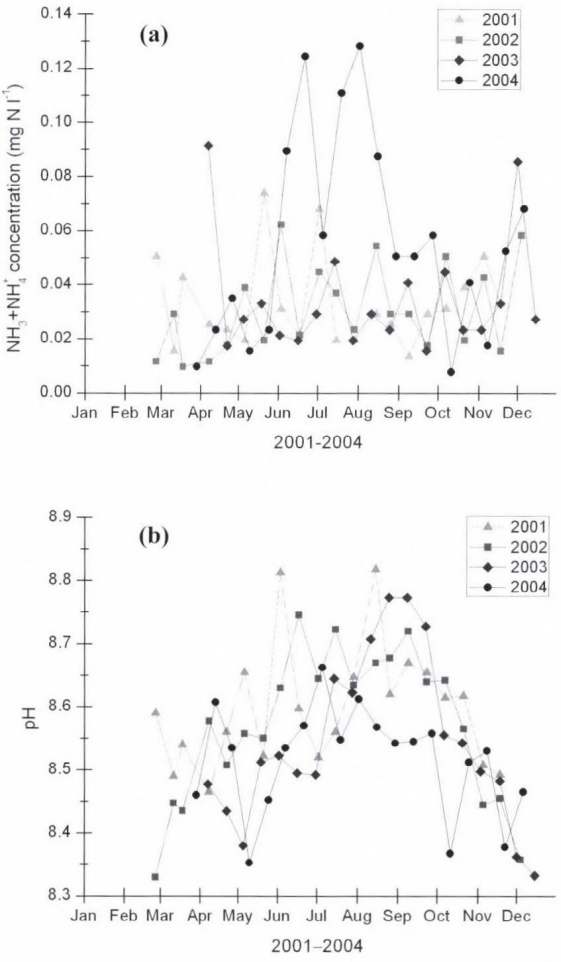

Fig. 9. Concentration of ammonia + ammonium (a) and pH (b) in the lake water, mean of 5 sampling points

Flux rates calculated by the two models had to be selected according to the wind direction. Determined by the location of the measurement point, the fetch criteria (homogeneous open water surface within at least 1 km) are fulfilled in the sector of 203 to 68 degrees clockwise. In the "wrong" sector, air temperature and wind velocity – both determining the exchange processes – are different from parameters measured in the "good fetch" sector.

Fluxes by the compensation-point model based on RM and FM were calculated on hourly base. Mean monthly fluxes can be seen in *Fig. 10a*. The compensation-point concentration of ammonia was generally higher in summer

half-year compared to the atmospheric concentrations resulting in emission peaks in this season. As a yearly average, net flux can be calculated in each year.

Deposition model of nitric acid is similar to the compensation-point model of ammonia. Only difference is that compensation-point concentration of nitric acid is zero in Eq. (1). Calculation method of nitric acid fluxes was the same as for ammonia using direct concentration measurements (March 2002–February 2003) and interpolated concentrations from the 2 background monitoring stations. The correlation between direct measurements and interpolated concentrations can be seen in *Fig. 8b*. *Fig. 10b* shows the mean monthly nitric acid fluxes for the four-year period.

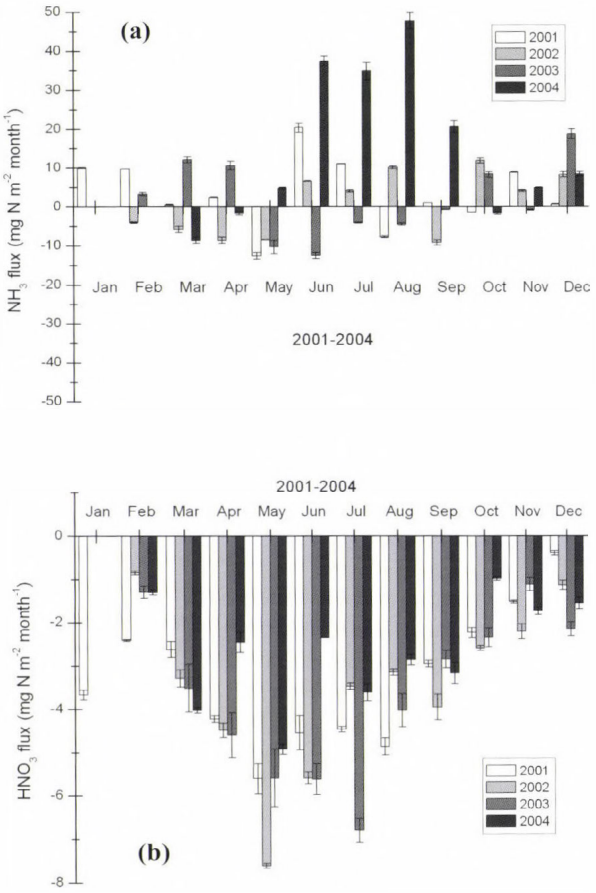

Fig. 10. Modeled mean monthly rates of ammonia (a) and nitric acid (b) fluxes (error bars denote the difference between two modeled fluxes by RM and FM)

In frozen periods (typically between the end of December to middle of February), fluxes were not computed since compensation-point concentration of ammonia is unambiguously zero, because the frozen surface prevents emission. Theoretically, deposition (adsorption) is possible onto ice surface probably followed by emission (desorption). Moreover, concentrations of ammonia and nitric acid in winter season are much lower since the equilibrium of $(NH_3)_{gas}+(HNO_3)_{gas}\leftrightarrow(NH_4NO_3)_{particle}$ process highly depends on air temperature and humidity (*Stelson* and *Seinfeld*, 1982). Low temperature and high humidity favor aerosol formation in frozen periods. For these reasons, deposition during frozen lake event was estimated to be negligible.

Yearly average of ammonia (by Hales-Drewes theory) and nitric acid dry fluxes calculated by FLake (FM) and resistance (RM) models are compiled in *Table 4*. For ammonia, upward (emission) fluxes were modeled in each year with large difference among years caused by extremely high ammonia+ammonium concentrations in lake water in different years (*Fig. 9a*). For nitric acid, the pattern is more even, there are no large differences among years.

Table 4. Yearly mean of ammonia and nitric acid fluxes over Lake Balaton (2001–2004) using the different turbulence models (FM: Flake model, RM: resistance model)

models	**2001**	**2002**	**2003**	**2004**	***mean***
			(mg N m^{-2} $year^{-1}$)		
FM NH_3	42.6	6.01	17.3	138	*51.0*
RM NH_3	43.8	12.5	23.4	156	*58.9*
mean	**43.2**	**9.27**	**20.4**	**147**	***54.9***
FM HNO_3	–38.3	–37.8	–39.7	–28.5	*–36.1*
RM HNO_3	–40.6	–38.9	–40.0	–29.4	*–37.2*
mean	**–39.5**	**–38.3**	**–39.9**	**–29.0**	***–36.7***

4. Conclusions

Dry flux of ammonia gas and nitric acid vapor were modeled both by a simple resistance model and by the more sophisticated FLake model.

Between the years of 2001 and 2004, net yearly ammonia emission and nitric acid deposition were observed at Lake Balaton. Calculated net NH_3 emission and HNO_3 deposition to the whole surface of lake between 2001 and 2004 were 32.7 t N $year^{-1}$ and –21.8 t N $year^{-1}$, respectively. The magnitude of these figures is less by one order of magnitude compared to nitrogen load from wet deposition and from dry deposition of aerosol particles that takes

–437 t N $year^{-1}$ in the same period (*Kugler* and *Horváth*, 2008). It means that dry fluxes of ammonia and nitric acid do not play important role in the N-budget and in the eutrophication of Lake Balaton in those years.

The pH range in the lake water allows bi-directional flux of ammonia. Direction of net flux (emission or deposition) depends mainly on concentrations in the water and air. Ammonia exchange can act as a buffering system, i.e., in case of a high N-load into the lake from other sources (rivers, waste water, run-off, etc.), the effect can be buffered through nitrogen emission in form of NH_3 as a consequence of the elevated compensation-point concentration. In contrast, in lack of enough nitrogen for living systems, ammonia can be absorbed (deposited) parallel with decrease of compensation-point concentration controlled by the water. The main consequence of this phenomenon can be that eutrophication of Lake Balaton (and probably of other lakes with similar pH) is probably phosphorus limited.

Comparing the measured ammonia flux with the fluxes calculated by compensation-point model based on the single Henry's law theory and by the modified solubility theory of Hales-Drewes, it can be concluded that in our case latter theory describes better the exchange processes, suggesting that effect of carbon dioxide on the solubility of ammonia can not be excluded. However, in contrast with Hales-Drewes, who suggested the decrease the solubility of ammonia in presence of CO_2, we find an opposite effect, i.e., CO_2 favors the solubility of ammonia in the pH-range of the lake. To eliminate the obvious contradiction among the different solubility theories, further researches are needed in the future.

Acknowledgements—Our research was supported by the OTKA K46824 project.

References

Ács, F., Hantel, M., and *Unegg, J.W.*, 2000: Climate Diagnostics with the Budapest-Vienna Land-Surface Model SURFMOD. Austrian Contributions to the Global Change Program Volume 3, Austrian Academy of Sciences, Vienna.

Ács, F. and *Szász, G.* 2002: Characteristics of microscale evapotranspiration: a comparative analysis. *Theor. Appl. Climatol. 73,* 189–205.

Ács, F. 2003: On the relationship between the spatial variability of soil properties and transpiration. *Időjárás 10*, 257–272.

Anda, A. and *Varga, B.*, 2010: Analysis of precipitation on Lake Balaton catchments from 1921 to 2007. *Időjárás 114,* 187–201.

Arya, S.P., 2001: Introduction to micrometeorology, 2nd edition. Academic Press, San Diego, London.

Ayers, G.P., Gillett, R.W., and *Caeser, E.R.*, 1985: Solubility of ammonia in water in the presence of atmospheric CO_2. *Tellus 37B*, 35–40.

Businger, J.A., Wyngaard, J.C., Izumi, Y., and *Bradley, E.F.*, 1971: Flux-Profile Relationships in the Atmospheric Surface Layer. *J. Atmos. Sci. 28*, 181–189.

Dasgupta, P.K. and *Dong, S.*, 1986: Solubility of Ammonia in Liquid Water and Generation of Trace Levels of Standard Gaseous Ammonia. *Atmos. Environ. 20*, 565–570.

Durand, P., Breuer, L., Johnes, P.J., Billen, G., Butturini, A., Pinay, G., van Grinsven, H., Garnier, J., Rivett, M., Reay, D.S., Curtis, C., Siemens, J., Maberly, S., Kaste, O., Humborg, C., Loeb, R., de Klein, J., Hejzlar, J., Skoulikidis, N., Kortelainen, P., Lepisto, A., and *Wright, R.*, 2011: Nitrogen processes in aquatic ecosystems. In (Eds. *Sutton, M. A., Howard, C. M., Erisman, J. W., Billen, G., Bleeker, A., Grennfelt, P., van Grinsven, H.,* and *Grizzetti, B.*) The European Nitrogen Assessment Cambridge University Press, Cambridge, U.K., 126–146.

Dyer, A.J., 1974: A review of flux-profile relationships. *Bound-Lay.Meteorol. 7*, 363–372.

EMEP, 1996: EMEP Manual for sampling and chemical analysis. EMEP/CCC-Report 1/95, NILU, Kjeller, Norway.

Erisman, J.W., van Pul, A. and *Wyers, P.*, 1994: Parameterization of dry deposition mechanisms for the quantification of atmospheric input to ecosystems. *Atmos. Environ. 28*, 2595–2607.

Farquhar, G.D., Firth, P.M., Wetselaar, R., and *Weir, B.*, 1980: On the Gaseous Exchange of Ammonia between Leaves and the Environment: Determination of the Ammonia Compensation Point. *Plant Physiol. 66*, 710–714.

Foken, Th., 2006: Angewandte Meteorologie. Springer-Verlag, Berlin, Heidelberg, New York.

Hales, J.M. and *Drewes, D.R.*, 1979: Solubility of ammonia at low concentrations. *Atmos. Environ.13*, 1133–1147.

Herodek S., 1977: A balatoni fitoplankton kutatás újabb eredményei. *Ann. Inst. Biol.(Tihany) Hun. Acad. Scient. 44*, 181–198.

Hicks, B.B., Baldocchi, D.D., Meyers, T.P., Hosker, R.P., and *Matt, D.R.*, 1987: A preliminary multiple resistance routine for deriving dry deposition velocities from measured quantities. *Water Air Soil Poll. 36*, 311–330.

Holtslag, A.A.M. and *van Ulden, A.P.*, 1983: A simple scheme for daytime estimates of the surface fluxes from routine weather data. *J. Climate Appl. Meteorol. 22*, 517–529.

Horváth, L., Mészáros, Á., Mészáros, E., and *Várhelyi, G.*, 1981: On the atmospheric deposition of nitrogen and phosphorus into Lake Balaton. *Időjárás 85*, 194–200.

Horváth, L., 1982: On the vertical flux of gaseous ammonia above water and soil surfaces. In (eds. Georgii, H-W. and Pankrath, J.) Deposition of Atmospheric Pollutants. D. Reidel Publishing Company, Dordrecht, Boston, London, 17–22.

Horváth L., 1990: Légköri szennyező anyagok töménysége és ülepedése a Balaton térségében. *Vízügyi Közlemények 77*, 204–208.

International Committee Lake Foundation, 2010: World Lakes Database, http://www.ilec.or.jp/.

Jolánkai G. and *Bíró I.*, 2005: A Balaton tápanyag terhelésének mérlege, mérése és modellezése, 2004. A munka második részének zárójelentése. Témaszám: 714/31/648601. VITUKI Kht. Vízminőség-védelmi Szakágazat, 77p. (In Hungarian)

Jordan, Gy., van Rompaey, A., Szilassi, P., Csillag, G., Mannaerts, C., and *Woldai, T.*, 2005: Historical land use changes and their impact on sediment fluxes in the Balaton basin (Hungary). *Agric. Ecosyst. Environ. 108*, 119–133.

Kovács, Á.D., 2011: Tó- és területi párolgás becslésének pontosítása és magyarországi alkalmazásai.PhD értekezés. BME, Budapest, 101p. (In Hungarian)

Kramm, B., Dlugi, R., Foken, Th., Mölders, N., Müller, H., and *Paw U.K.T.*, 1996: On the determination of the sublayer Stanton numbers of heat and matter for different types of surfaces. *Contrib. Atmos. Phys. 69*, 417–430.

Kugler, Sz. and *Horváth, L.*, 2004: Estimation of the nitrogen loading from the atmospheric dry deposition of ammonium and nitrate aerosol particles to Lake Balaton. *Időjárás 108*, 155–162.

Kugler, Sz., Horváth, L., and *Machon, A.*, 2008: Estimation of nitrogen balance between the atmosphere and Lake Balaton and a semi natural grassland in Hungary. *Environ. Poll. 154*, 498–503.

Lau, N.-Ch. and *Charlson, R.J.*, 1977: On the discrepancy between background atmospheric ammonia gas measurements and the existence of acid sulfates as a dominant atmospheric aerosol. *Atmospheric Environment 11*, 475–478.

Liu, H., Blanken, P.D., Weidinger, T., Nordbo, A., and *Vesala, T.*, 2011: Variability in cold front activities modulating cool-season evaporation from a southern inland water in the USA. *Environ. Res. Lett. 6*, 024022.

Mészáros R., 2002: A felszínközeli ózon száraz ülepedésének meghatározása különböző felszíntípusok felett. PhD értekezés, ELTE, Budapest, 113p. (In Hungarian)

Mironov D.V., 2006: Synopsis of FLake Routines, http://www.flake.igb-berlin.de/docs.shtml.

Mironov, D.V., 2008: Parameterization of lakes in numerical weather prediction. Description of a lake model. COSMO Technical Report, No. 11, Deutscher Wetterdienst, Offenbach am Main, Germany, 41 p.

Mironov, D., Heise, E., Kourzeneva, E., Ritter, B., Schneider, N., and *Terzhevik, A.*, 2010: Implementation of the lake parameterisation scheme FLake into the numerical weather prediction model COSMO. *Boreal Environ. Res. 15*, 218–230.

Shahin, U.M., Holsen, T.M., and *Odabasi, M.*, 2002: Dry deposition measured with a water surface sampler: a comparison to modeled results. *Atmos. Environ. 36*, 3267–3276.

Stelson, A.W. and *Seinfeld, J.H.*, 1982: Relative humidity and temperature dependence of the ammonium nitrate dissociation constant. *Atmos. Environ. 16*, 983–992.

Szilágyi, J. and *Kovács, Á.*, 2011: A calibration-free evapotranspiration mapping technique for spatially-distributed regional-scale hydrologic modeling. *J. Hydrol. Hydromech. 59*, 118–130.

Vörös, M., Istvánovics, V., and *Weidinger, T.*, 2010: Applicability of the FLake model to Lake Balaton. *Boreal Environ. Res. 15*, 245–254.

Weidinger, T., Pinto, J., and *Horváth, L.*, 2000: Effects of uncertainties in universal functions, roughness length, and displacement height on the calculation of surface layer fluxes. *Meteorol. Z. 9*, 139–154.

IDŐJÁRÁS

Quarterly Journal of the Hungarian Meteorological Service
Vol. 118, No. 2, April – June, 2014, pp. 119–132

Homogenization of Hungarian daily wind speed data series

Csilla Péliné Németh[1*], **Judit Bartholy**[2], and **Rita Pongrácz**[2]

[1]*Geoinformation Service of the Hungarian Defence Forces*
Szilágyi Erzsébet fasor 7–9., H-1024 Budapest, Hungary

[2]*Department of Meteorology, Eötvös Loránd University*
Pázmány Péter sétány 1/A, H-1117 Budapest, Hungary

**Corresponding author E-mail: pelinenemeth.csilla@mhtehi.gov.hu*

(Manuscript received in final form October 24, 2013)

Abstract—Reliable long time series have key role in climatological research. Long term observations involve inhomogeneities due to change of measuring methods, sensors, surroundings of stations, or moving into a new location. Therefore, homogenization is necessary in order to make reliable analysis of datasets. In this study, the MASH (Multiple Analysis of Series for Homogenization) procedure developed at the Hungarian Meteorological Service was applied to improve our wind time series. Daily wind datasets were homogenized at 19 Hungarian synoptic stations in the period from 1975 to 2012. This paper discusses the validation of the homogenization process and presents the quality control results.

Key words: wind speed, homogenization, MASH application, Hungarian wind climate, measurement automation

1. Introduction

The existence of long and reliable instrumental climate records is necessary both to assess climate variability and climate change and to validate climate model outputs (*Freitas et al.,* 2013). Analysis of appropriate and good quality datasets may help to mitigate possible negative effects of climate change. Furthermore, besides temperature and precipitation, wind is also a key meteorological element, therefore, it is essential to study average and extreme characteristics and tendencies of present and future wind climate.

Hungarian wind climate research at the Eötvös Loránd University in Budapest is based on the analysis of past, present, and modeled wind field data

sets. Projected wind fields are provided by the adapted and validated RegCM3 regional climate model (*Torma et al.,* 2008) experiments for future periods (2021–2050 and 2071–2100) for the Carpathian Basin.

We analyzed present wind climate using measurements of Hungarian synoptic stations, and gridded reanalysis data (*Péliné et al.,* 2011). Hungarian synoptic measurement network has been developed and installed by the Hungarian Meteorological Service taking into account suggestions of the World Meteorological Organisation (*WMO,* 2011). Because of the last decades' developments of measurement and communication technologies, the wind observing network has changed several times, which is unfortunately quite usual. The most significant change was automation – i.e., change traditional measuring instruments into automated measuring systems – during 1995–1996. This major change introduced large variations in the climate signal, and caused inhomogeneities in the data sets. In fact, long instrumental records are very rarely homogeneous because of the changing surroundings of measuring sites (new buildings, vegetation growth, etc.). To avoid misinterpretation due to this inhomogeneity, the available time series can be divided into subsets. For instance, we used two subsets in case of previous (*Péliné et al.,* 2011) wind climate analysis using wind data originating from traditional (1975–1994) and automated (1997–2012) measuring systems.

In addition to automation other causes may also lead to inhomogeneities such as substitution or relocation of weather stations, changing anemometer type or aging of the instruments, changes in measuring height, surroundings (e.g., urbanization), surface coverage, and roughness. Therefore, documentation of metadata is a crucial issue during any kind of meteorological measurement.

The above-mentioned changes could result in inhomogeneities, which cannot be explained by climatological reasons. Brake points in the data sets coincide with change in the probability distribution function of the measurements. These inhomogeneities must be detected and removed before further analyses. For this purpose mathematical methods are widely used, one of them is the Multiple Analysis of Series for Homogenization, MASH v3.03 (*Szentimrey,* 1999, 2011) developed in HMS. This technique is used here for homogenization of available daily wind speed time series between 1975 and 2012 for records of 19 Hungarian synoptic stations.

2. Homogenization with MASH application

A homogeneous climatological time series can be defined as time series where variability is only caused by changes in weather and climate (*Aguilar et al.,* 2003). To decide whether or not a long time series is homogeneous, there are different detection and correction methods available for possible use. These methods are all based on mathematical formulation and climatological

experience, however, their performances are different. Objective comparison of these existing methods was carried out in the framework of a scientific programme COST Action HOME ES0601: Advances in Homogenization Methods of Climate Series: an integrated approach (*HOME,* 2011; *Szentimrey,* 2013). The HOME tests concluded that MASH was one of the most successful methods (*Domonkos et al.*, 2012, *Domonkos* 2013, *Venema et al.,* 2012), that is why we used it in this study.

MASH application is a relative homogeneity test procedure (*Szentimrey,* 1999). This tool consists of mathematical formulation, climatological station information (metadata), and software development for automation. Application does not assume that the reference series are homogeneous. The candidate series is chosen from the available time series (for example daily wind speed data), and the remaining series are considered as reference series. As running the application, the role of series changes step by step during the procedure. Depending on the climatic element, additive (for temperature) or multiplicative (for precipitation or wind speed) models can be used.

It is possible to homogenize monthly, seasonal, or annual time series. The daily inhomogeneities can be derived from the monthly ones (*Szentimrey,* 2008). The application provides automatically the probable dates of break points for further usage, and the homogenized, completed and quality controlled time series. Although MASH is able to use metadata (for example the date of relocation) during the break point detection, it was not used during this work.

In this study, daily wind speed data sets for 19 stations (*Fig. 1*) were derived from at least 8 hourly wind speed data a day. Before calculating daily wind speed, hourly data was quality controlled and corrected. Metadata of stations is summarized in *Table 1*. Data are available from 1975 to 2012 at most stations. At station Paks (No. 15), measurements started only on May 1, 1979. Altogether more than one year is missing at Zalaegerszeg (No. 11) during 1993 and 1994. It is also important to note that 50 days are missing at Kecskemét (No. 17) in 2009.

A multiplicative model was applied for homogenization of daily wind speed data using the 0.05 significance level. Original series can be described as Eq. (1) affected by climate change, inhomogeneity, and noise effect (*Szentimrey,* 2011).

Original series for multiplicative model is

$$X^*_{O,j}(t) = C^*_j(t) \cdot IH^*_j(t) \cdot \varepsilon^*_j(t), \quad (j = 1,2,\dots,n), \tag{1}$$

where C^* is the climate change, IH^* is the inhomogeneity, ε^* is the noise.

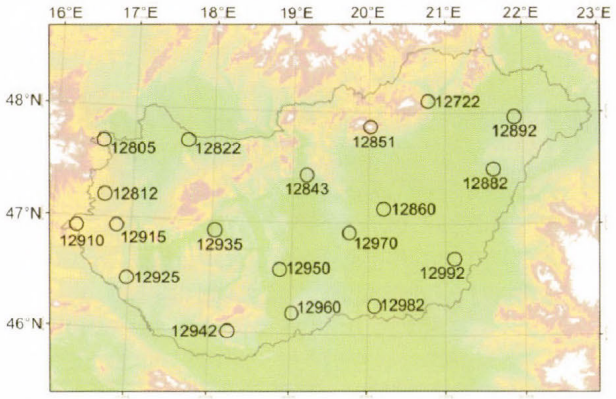

Fig. 1. Hungarian stations used at MASH application for homogenization.

Table 1. Metadata of Hungarian stations used at MASH application for homogenization (in 2012)

No.	WMO	Station name	Lon [° E]	Lat [° N]	Altitude [m]	Anemometer elevation [m]	Missing data [%]
1	12772	Miskolc	20.77	48.10	232.8	16.25	0.0
2	12805	Sopron	16.60	47.68	233.8	18.40	< 0.1
3	12812	Szombathely	16.65	47.20	201.1	10.56	< 0.1
4	12822	Győr	17.67	47.71	116.7	11.16	0.0
5	12843	Budapest Lőrinc	19.18	47.43	139.1	14.68	< 0.1
6	12851	Kékestető	20.02	47.87	1011.3	25.07	< 0.1
7	12860	Szolnok	20.13	47.17	108.1	10.40	< 0.1
8	12882	Debrecen	21.61	47.49	107.6	10.23	0.1
9	12892	Nyíregyháza	21.89	47.96	142.1	15.98	0.2
10	12910	Szentgotthárd	16.31	46.91	311.7	16.61	0.1
11	12915	Zalaegerszeg	16.81	46.93	240.1	10.40	3.3
12	12925	Nagykanizsa	16.97	46.46	139.8	13.69	0.1
13	12935	Siófok	18.04	46.91	108.2	15.10	0.0
14	12942	Pécs	18.23	46.01	202.8	10.55	0.0
15	12950	Paks	18.85	46.57	97.2	9.80	11.4
16	12960	Baja	19.02	46.18	113.0	10.30	0.1
17	12970	Kecskemét	19.75	46.91	114.0	10.40	0.4
18	12982	Szeged	20.09	46.26	81.8	12.25	< 0.1
19	12992	Békéscsaba	21.11	46.68	86.2	6.50	< 0.1

3. Results

MASH v3.03 procedure produces quality control results automatically (e.g., the number of days with error, total number of errors; their dates), identifies problematic series, and gives the estimated error values. First, our input data was

checked with partially automated self-developed computer codes including basic controlling rules and the detected errors were corrected manually before homogenization. As a result, only 2 errors (on two consecutive days) were detected at one of the stations, Szombathely (No. 3). Normally, file of MASH quality control results contains the detected maximal positive and the minimal negative errors and their dates; however minimal negative error was zero in this work (*Table 2*).

Table 2. Quality control results

Dates of the detected errors	Maximal positive error [m/s]
August 9, 1995	0.31
August 10, 1995	0.54

During verification of homogenization, the null hypothesis supposes that the examined series are homogeneous. The homogenization is acceptable if the following condition is true (*Lakatos et al.,* 2013): the test statistic after homogenization (TSA) has to be either near the critical value (20.57, significance level 0.05) or much less than the test statistic before homogenization (TSB). TSA and TSB values are summarized in *Table 3.* Since TSA values are much smaller compared to TSB values, it can be concluded that the homogenizations are acceptable and improve the qualities of the station time series considerably. The smallest TSB value – less than 100.0 – is found in case of station 3 (30.11) where the homogenization could not improve the data quality (station 3 is the only station with this feature among the 19 stations evaluated in this study). In fact, the TSA value of station 3 is larger than the TSB value. The small difference between them suggests that only a slight correction was made in the time series of station 3, since the original time series can be considered homogeneous. However, due to missing data of the original data set at this station, we used the homogenized time series in the analysis.

Table 3. Yearly test statistics for inhomogeneity of series

Station No.	TSA	TSB	Station No.	TSA	TSB
1	151.21	2590.78	11	42.39	953.13
2	26.69	137.10	12	100.19	218.26
3	39.76	30.11	13	69.66	395.84
4	29.49	113.96	14	16.70	492.12
5	23.93	285.97	15	50.67	574.81
6	147.45	229.40	16	47.14	512.55
7	53.85	1715.00	17	35.86	490.28
8	60.62	116.63	18	57.82	178.88
9	49.72	1680.52	19	84.57	359.90
10	36.61	578.96			
			Average	**59.17**	**613.38**

Table 4 lists annual relative estimated inhomogeneities (REI) and annual relative modification of wind speed data sets (RMS). They are proportional to standard fluctuation based on their definitions (*Szentimrey,* 2011).

Fluctuation of series is

$x(t)(>0)y(t)(>0)$ $(t = 1,2, \dots, n)$:

$$F(x) = \left(\prod_{t=1}^{n} max\left(\frac{x(t)}{y(t)}, \frac{y(t)}{x(t)}\right)\right)^{\frac{1}{n}}. \tag{2}$$

Standard fluctuation of series is

$x(t)(>0)$ $(t = 1,2, \dots, n)$:

$$SF(x) = \left(\prod_{t=1}^{n} max\left(\frac{x(t)}{\bar{x}_G}, \frac{\bar{x}_G}{x(t)}\right)\right)^{\frac{1}{n}}, \tag{3}$$

where G is the geometric mean.
Relative estimated inhomogeneity (REI) is

$$SF\left(I\widehat{H}^*\right) \approx SF(X_0^*)^{REI}. \tag{4}$$

Relative modification of series (RMS) is

$$F(X_0^*, X_H^*) \approx SF(X_0^*)^{RMS}. \tag{5}$$

Annual variability of wind speed is definitely smaller than other meteorological parameters such as maximum temperature or sunshine duration. Seasonal REI of daily wind speed time series shows an annual cycle with very small amplitude. Analysis of time dependence of REI suggests that averaged values for all stations are slightly larger in spring (0.46) and summer (0.55) than in winter (0.39) and autumn (0.44). Seasonal REI values vary from zero to 1.01 (*Fig. 2*), the smallest values appear in autumn and summer at stations 3 and 4, respectively, whereas the largest REI values can be found in summer at station 7 (in Szolnok). The maximum difference between the seasonal REI values is in Sopron (station 2), where REI is eight times larger in summer than in spring (the difference is 0.36). Considering the monthly RMS values (*Fig. 3*), the average adjustments were higher during those months when natural variability of wind speed is larger (due to higher thunderstorm frequency). *Fig. 3* illustrates the RMS analysis at three stations, i.e., Szombathely (station 3), Zalaegerszeg (station 11), and Kecskemét (station 17), where annual REI and RMS are minimum, maximum, and around the multi-station mean values, respectively.

Table 4. Annual relative estimated inhomogeneities (REI) and annual relative modification of series (RMS)

Station name	REI	Station name	RMS
Zalaegerszeg	0.90	Zalaegerszeg	1.57
Szolnok	0.90	Szolnok	1.30
Miskolc	0.88	Nyíregyháza	1.07
Nyíregyháza	0.80	Miskolc	1.06
Pécs	0.61	Pécs	0.90
Szentgotthárd	0.60	Siófok	0.77
Paks	0.53	Békéscsaba	0.70
Siófok	0.51	Szentgotthárd	0.67
Kecskemét	0.51	Paks	0.66
Baja	0.51	Kecskemét	0.63
Békéscsaba	0.50	Baja	0.61
Debrecen	0.36	Debrecen	0.58
Nagykanizsa	0.33	Nagykanizsa	0.45
Kékestető	0.23	Szeged	0.31
Szeged	0.19	Kékestető	0.27
Sopron	0.17	Sopron	0.18
Budapest Lőrinc	0.11	Budapest Lőrinc	0.13
Győr	0.06	Győr	0.08
Szombathely	0.06	Szombathely	0.07
Average	**0.46**	**Average**	**0.64**

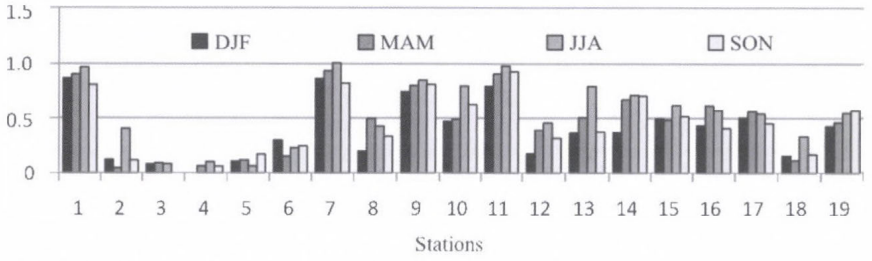

Fig. 2. Seasonal relative estimated inhomogeneity in different stations.

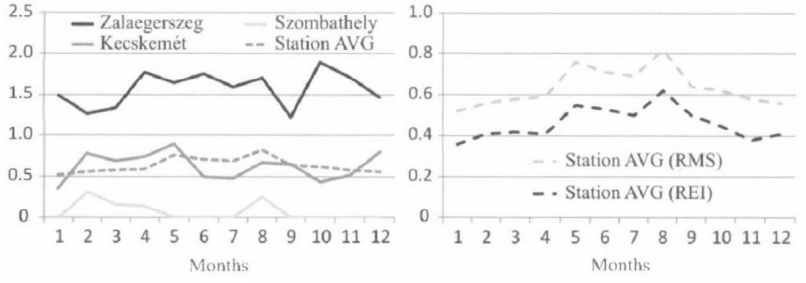

Fig. 3. Monthly RMS at three stations and station average (*left*), and average monthly RMS and average monthly REI calculated from values of the 19 stations (*right*).

During the homogenization process, time series can be modified in any year. Break points usually were found throughout the whole period, however, data series of some stations were corrected only in a shorter period. *Fig. 4* demonstrates annual number of stations where break points were detected.

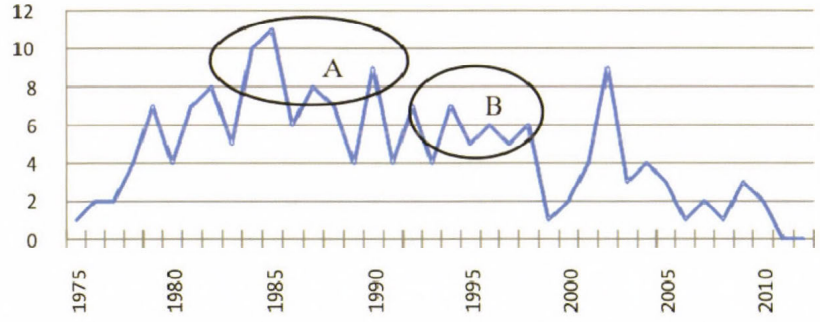

Fig. 4. Number of stations of annually detected break points. (Ellipse A: missing values during the 1980's. Ellipse B: inhomogeneity due to automation.)

In general, there is a decreasing trend towards fewer break points in recent times. Metadata may be valuable either during the homogenization or the validation procedure (*Auer et al.,* 2005). Based on documented metadata, missing values were found frequently mainly at night in most of the analyzed stations in the 1980's (ellipse A). Consequently, daily average wind speed was calculated from less number (at least eight) of measurement records. Automation process obviously caused inhomogeneity in data series at almost every station (ellipse B). Moreover, relocated stations and changed height of the measuring sensors also could cause break points (after 2000). In these latter cases, the modification factors suggest that the inhomogeneity is often more explicit than the effect of automation. Therefore, it is important to take into account these effects in planning and installation of measurement systems, moreover, it is essential to document any changes in meteorological measurement network.

After completing the homogenization process, the distribution of daily wind speed changed considerably. *Fig. 5* shows the relative frequencies of wind speed at three stations before and after homogenization. The REI and RMS at Zalaegerszeg (station 11) are the largest, while the minimum values can be found at Szombathely (station 3). Therefore, the largest difference between pre- and post-homogenized distributions is at Zalaegerszeg, where the distribution shifted to a higher wind speed regime.

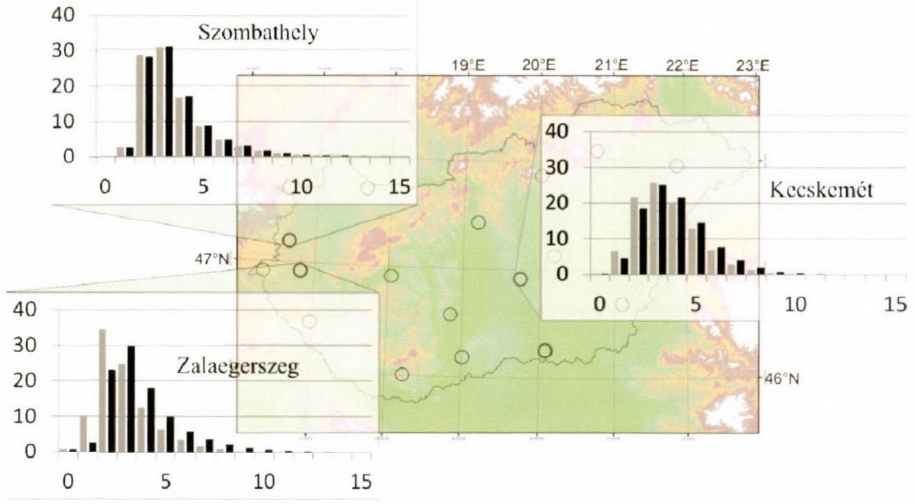

Fig. 5. Relative frequencies [%] of daily wind speed [m/s] at different stations before (grey) and after (black) homogenization (1975–2012).

The original and homogenized average yearly wind speed time series are shown in *Fig. 6* for all analyzed stations. Detected numbers of annual break points are indicated at the upper right corner of each diagram. Most of the break points can be identified from the documented metadata, however, the actual required adjustments cannot be quantified from metadata (*Menne et al.,* 2005).

In many cases (Miskolc, Szolnok, Siófok), time series were modified (see vertical lines in *Fig. 6*) in the first half of the entire period. Measuring station in Miskolc moved to another place in 1990, this change caused a significant increase in wind speed. Other documented changes include the automation, during which both the type of the anemometer (from Fuess to Vaisala) and the method of measurement have changed. Moreover, this modernization usually coincided with change of the sensor's height. For example, stations at Miskolc and Szolnok were automated in 1997, and at Siófok in 1995. At Miskolc, the sensor was installed from 10 meter (standard elevation of anemometers) to 16.25 meter. Station Siófok is located at the waterfront of Balaton (the biggest lake in Central Europe), the measurements were automated in 1995, when the height of the anemometer was lifted to 15.10 meters. After automation in 1997 at Szolnok, the type of the anemometer was changed twice, in 2004 and 2011.

However, there are some stations, such as Szombathely and Sopron, where smaller modifications were applied during the homogenization process. The automation in both stations was completed in 1995. Other effects also influenced the homogeneity, namely, (i) station of Szombathely was moved in 2002 with unchanged sensor's height, (ii) station of Sopron was reinstalled twice, in 2003 and 2005, when height of the anemometer was lifted from 15.64 to 18.40 meter.

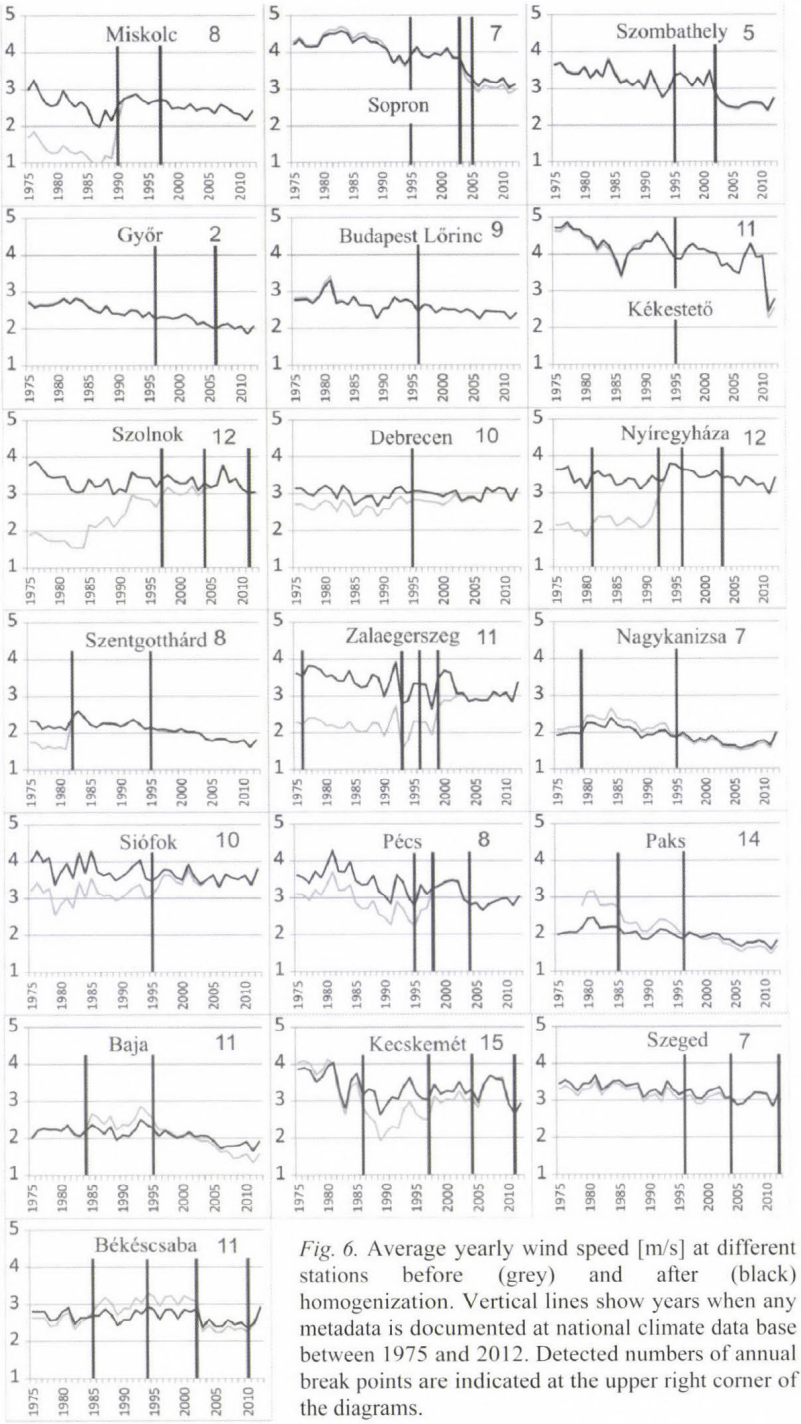

Fig. 6. Average yearly wind speed [m/s] at different stations before (grey) and after (black) homogenization. Vertical lines show years when any metadata is documented at national climate data base between 1975 and 2012. Detected numbers of annual break points are indicated at the upper right corner of the diagrams.

MASH procedure homogenizes monthly and daily time series and completes missing data for further analysis, e.g., extreme value evaluation or model output verification. In this study, different yearly and seasonal percentile values (median, 0.90 and 0.99) were calculated for 19 stations from 38-year-long time series (1975–2012) before and after homogenization. *Fig. 7* and *8* show that the largest difference was found at Zalaegerszeg. At this station the yearly homogenized percentile values (0.50, 0.90, and 0.99) were increased by 131%, 128% and 140%, respectively. The highest decreasing was at station 19 (Békéscsaba), where homogenized percentiles are 98%, 96%, and 95% compared to percentiles of original time series. Median decreased at six stations, 0.90 and 0.99 percentiles were decreased in eight cases each. The smallest correction was applied to station data at Szombathely, No. 3 (100.0%, 99.8% and 98.3%) and in Kékestető, No. 6 (100.0%, 100.4% and 104.5%). Moreover, some smaller differences are demonstrated in *Fig. 8* comparing seasonal percentile values.

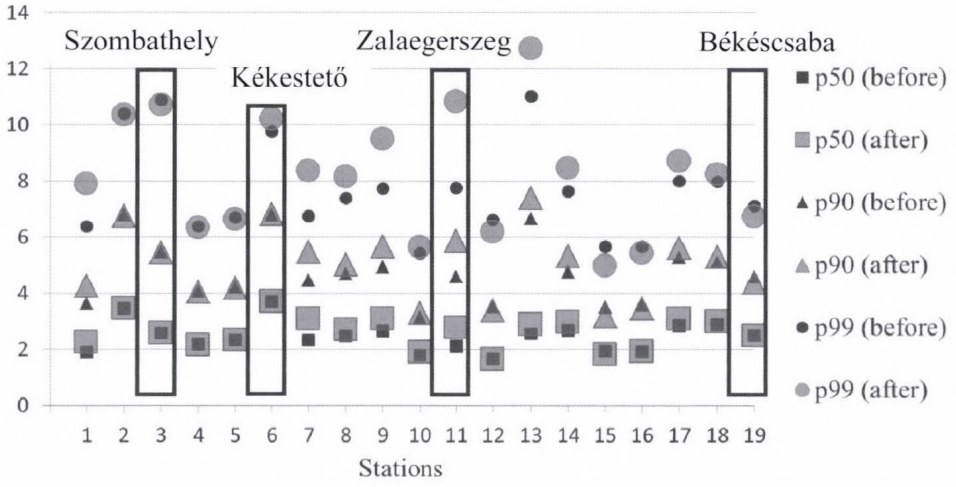

Fig. 7. Different yearly percentile values before and after homogenization for involved 19 stations calculated from 38-year time series (1975–2012).

Average yearly wind speed was modified significantly by homogenization procedure (*Fig. 6*). Consequently, the fitted linear trends of average and different percentile values also changed at many stations. In this paper, three stations (Szolnok, Zalaegerszeg, and Siófok) were chosen to demonstrate these differences emphasizing that inhomogeneities may lead to misinterpretations. *Fig. 9* shows monthly linear trend coefficients of 0.9 percentile values for two periods (1975–2012 and 1997–2012) calculated from daily wind speed data before (left) and after (right) homogenization for the three stations. Decreasing trends dominate in the homogenized datasets analyzing the whole period (1975–2012), and most of

the increasing trends of the non-homogenized data disappeared. Smaller differences were found between homogenized and original data after automation (1997–2012). For instance, in case of Siófok, both in November and December the detected trends are significant and similar for the homogized and non-homogenized times series.

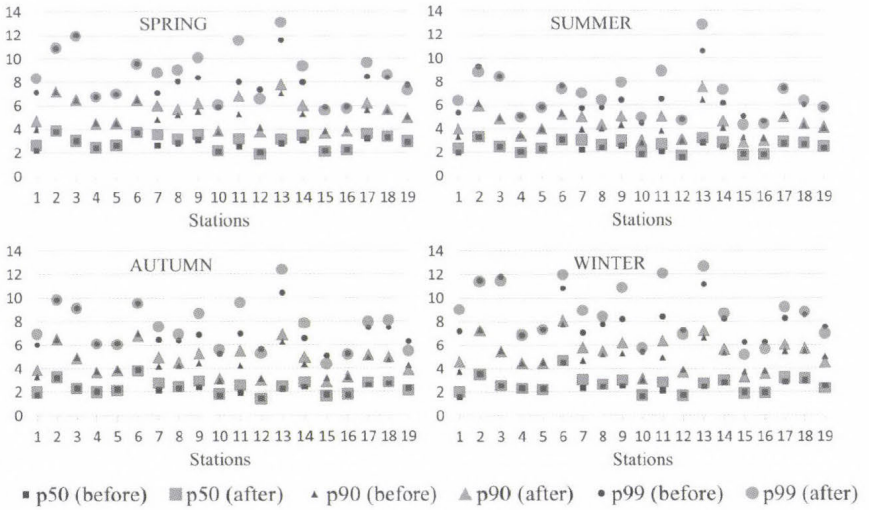

Fig. 8. Different seasonal percentile values [m/s] before and after homogenization for the 19 stations calculated from 38-year time series (1975–2012).

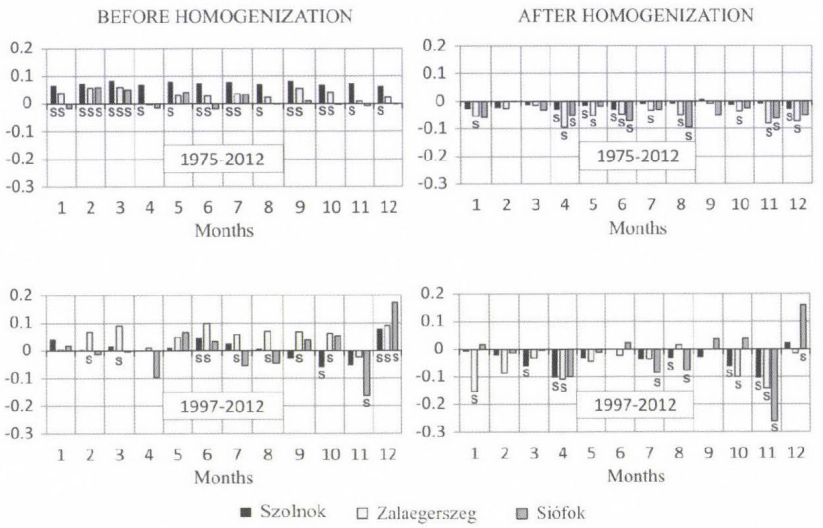

Fig. 9. Monthly linear trend coefficients of 0.9 percentile value for periods 1975–1912 and 1997–2012 calculated from daily wind speed data before (left) and after (right) homogenization for 3 stations. The significant changes are marked with letter "S".

4. Conclusions

Daily wind speed data sets of 19 Hungarian synoptic stations were homogenized for 1975–2012. Our preliminary results are summarized in this paper, based on them the following conclusions can be drawn. (1) Automation, relocated stations, and changed height of measurement sensors could cause break points in time series. Analyzing the modification factors, the inhomogeneity is often larger due to relocations than automation. Therefore, it is important to take into account these effects in planning and installation of measurement systems, moreover, it is essential to document any changes in meteorological measurement network. (2) Homogenization process determined the main break points of stations' time series. Most of the break points could be identified from documented metadata, however, it is not possible to deduce the number of break points from the metadata only. Consequently, non-climatic biases cannot be quantified solely from documented metadata. (3) Spatial variability of wind speed is high, but the temporal variability is small compared to other meteorological parameters (e.g., maximum temperature, sunshine duration). Seasonal relative estimated inhomogeneities of daily wind speed suggest very small changes within the year. (4) Values of RMS are higher when thunderstorm events occur more frequently, i.e., from spring to autumn.

Acknowledgement—We would like to express our very great appreciation to *Tamás Szentimrey* (Hungarian Meteorological Service) for providing MASH application, moreover, for his guidance and help in analyzing the results of homogenization. We are grateful to the Hungarian Meteorological Service and the Geoinformation Service of the Hungarian Defence Forces for the wind data of the Hungarian synoptic meteorological stations. This work was partially supported by the European Union and the European Social Fund through the project FuturICT.hu (grant no.: TÁMOP-4.2.2.C-11/1/KONV-2012-0013). Research leading to this paper has been supported by the Hungarian National Science Research Foundation under grant K-78125, and projects KMR_12-1-2012-0206 and GOP-1.1.1.-11-2012-0164.

References

Aguilar, E., Auer, I., Brunet, M., Peterson, T.C., and *Wieringa, J.,* 2003: Guidelines on climate metadata and homogenization. *WCDMP-No. 53, WMO-TD No. 1186.* World Meteorological Organization, Geneve.

Auer, I., Böhm, R., Jurković, A., Orlik, A., Potzmann, R., Schöner, W., Ungersböck, M., Brunetti, M., Nanni, T., Maugeri, M., Briffa, K., Jones, P., Efthymiadis, D., Mestre, O., Moisselin, J.- M., Begert, M., Brazdil, R., Bochnicek, O., Cegnar, T., Gajić-Čapka, M., Zaninović, K., Majstorović, Ž., Szalai, S., Szentimrey, T., and Mercalli, L., 2005: A new instrumental precipitation dataset for the greater Alpine region for the period 1800–2002. *Int. J. Climatol. 25,* 139–166.

Domonkos, P., Venema, V., and *Mestre, O.,* 2012: Efficiencies of homogenization methods: our present knowledge and its limitation. In *Proceedings of the 7th Seminar for Homogenization and Quality Control in Climatological Databases in press,* www.c3.urv.cat/publicacions/publicacions2012.html

Domonkos, P., 2013: Measuring performances of homogenization methods. *Időjárás 117,* 91–112

Freitas, L., Gonzalez Pereira, M., Caramelo, M., Mendes, M., and *Nunes, L.,* 2013: Homogeneity of monthly air temperature in Portugal with HOMER and MASH. *Időjárás 117*, 69–90

HOME, 2011: Homepage of the COST Action ES0601 - *Advances in Homogenisation Methods of Climate Series: an Integrated Approach* (HOME), http://www.homogenisation.org.

Lakatos, M., Szentimrey, T., Bihari, Z., and *Szalai, S.,* 2013: Creation of a homogenized climate database for the Carpathian region by applying the MASH procedure and the preliminary analysis of the data. *Időjárás 117,* 143–158.

Menne, M.J., and *Williams Jr. C.N.*, 2005: Detection of undocumented changepoints using multiple test statistics and composite reference series. *J. Climate 18*, 4271–4286.

Péliné, N. Cs., Radics, K., and *Bartholy, J.*, 2011: Seasonal Variability of Wind Climate in Hungary. *Acta Silv. Lign. Hung. 7*, 39–48.

Szentimrey, T., 1999: Multiple Analysis of Series for Homogenization (MASH). Proceedings of the Second Seminar for Homogenization of Surface Climatological Data, Budapest, Hungary; WMO, WCDMP-No. 41, 27–46.

Szentimrey, T., 2008: Development of MASH homogenization procedure for daily data, *Proceedings of the Fifth Seminar for Homogenization and Quality Control in Climatological Databases,* Budapest, Hungary, 2006; *WCDMP-No. 68, WMO-TD No. 1434*, 116–125.

Szentimrey, T., 2011: Manual of homogenization software MASHv3.03. *Hungarian Meteorological Service*, Budapest.

Szentimrey, T., 2013: Theoretical questions of daily data homogenization, Special Issue of the COST-ES0601 (HOME) ACTION, *Időjárás 117*, 113–122.

Torma, Cs., Bartholy, J., Pongrácz, R., Barcza, Z., Coppola, E., and *Giorgi, F.,* 2008: Adaptation and validation of the RegCM3 climate model for the Carpathian Basin. *Időjárás 112*, 233–247.

Venema, V., Mestre, O., Aguilar, E., Auer, I., Guijarro, J.A., Domonkos, P., Vertacnik, G., Szentimrey, T., Stepanek, P., Zahradnicek, P., Viarre, J., Müller-Westermeier, G. Lakatos, M., Williams, C.N., Menne, M., Lindau, R., Rasol, D., Rustemeier, E., Kolokythas, K., Marinova, T., Andresen, L., Acquaotta, F., Fratianni, S., Cheval, S., Klancar, M., Brunetti, M., Gruber, C., Duran, M.P., Likso, T., Esteban, P., and *Brandsma, T.,* 2012: Benchmarking monthly homogenization algorithms. *Climate of the Past 8*, 89–115.

World Meteorological Organization, 2011: Guide to Climatological Practices, WMO/No. 100, Geneva.

IDŐJÁRÁS

Quarterly Journal of the Hungarian Meteorological Service
Vol. 118, No. 2, April – June, 2014, pp. 133–145

Spatial modeling of the climatic water balance index using GIS methods

Agnieszka Wypych[1]* and **Ewelina Henek**[2]

[1]*Jagiellonian University, Department of Climatology*
7 Gronostajowa Str., 30-387 Krakow, Poland
agnieszka.wypych@uj.edu.pl

[2]*Institute of Meteorology and Water Management – National Research Institute*
14 Borowego Str., 30-215 Krakow, Poland
ewelina.henek@imgw.pl

**Corresponding author*

(Manuscript received in final form December 13, 2013)

Abstract—The aim of this study is to find the optimal spatialization method to model spatial differentiation of the climatic water balance (CWB). Monthly mean values from the period 1986–2010 for air temperature and precipitation as well as monthly solar radiation totals over Poland were considered in the study. Potential evapotranspiration data were calculated via the Turc formula.

Two simultaneous methods were used in the modeling: simple and multiple linear regression (with latitude, altitude, and distance from the coastline as variables) and the map algebra method. Map algebra was shown to be the better spatialization method; however, its optimization would require a reduction in the research scale and the use of more in-situ data. This would allow more local variables such as landform and land cover to be included in the analysis.

Key-words: spatial analysis, regression model, map algebra, climatic water balance, Poland

1. Introduction

Geographic information systems (GIS) provide a variety of methods for the modeling and presentation of data. GIS provides a powerful research tool for climatology and meteorology, where detailed analysis at different temporal and spatial scales is essential in order to understand processes prevailing in the

atmosphere. Although temperature and precipitation have received the most attention in GIS research, increasingly complex meteorological and climatological indices are also under examination, as they provide information useful in the environmental and social sciences (*Tveito et al.*, 2008).

One such index is the climatic water balance (*CWB*). It focuses on the difference between precipitation (*RR*) and evapotranspiration (*ETP*), presenting a basis for a climatic assessment of water resources in a given geographic area. An understanding of the spatial distribution of the climatic water balance appears to be very important to its comprehensive application in spatial management, agriculture, and hydroclimatological modeling.

Although the *CWB* index seems to be quite simple to compute, it is dependent on many different variables such as solar radiation, relief, land use, and urban development, among others. This creates certain difficulties. It is, first and foremost, a subject involving evapotranspiration, which varies considerably with changes in the natural environment. As data availability is poor, issues arise with proper index interpretation, mainly due to spatial differentiation.

GIS techniques enable the merging of different data processing and integration methods with complex analyses and modeling methods. However, given the complicated nature of the subject, it is no wonder that there exist many GIS methods that attempt to model the spatial differentiation of evapotranspiration (e.g., *Nováky*, 2002; *Xinfa et al.*, 2002; *Fernandes et al.*, 2007; *Vicente-Serrano et al.*, 2007). Remote sensing techniques are also becoming more commonly used to address this research issue and is often used to supplement ground-based observations (*Rosema*, 1990; *Kalma et al.*, 2008).

The purpose of this paper is to describe a new methodology for climatic water balance index implementation using geographic information systems (GIS) in cases when there is no appropriate spatial information given from in-situ observations.

The area under consideration is the territory of Poland, located in Central Europe. Poland was chosen because of its relatively diverse relief from the north (Baltic Sea coast) to the south (the Carpathians), which impacts weather and climate conditions. The lie of the land as well as the country's location suggest that an analysis based on the study area (Poland) seems to be representative of the greater region, e.g., Central and Eastern Europe.

2. *Data and methodology*

As mentioned before, evapotranspiration seems to be the crucial element of climatic water balance index calculations. Regrettably, the complexity of the process (caused by many factors) makes it very difficult to obtain exact values of *CWB* for current meteorological analyses. The alternative solution, the value of ETP, can be calculated to a high degree of precision with the use of simplified

models including meteorological elements that are typically observed by meteorological stations. Therefore, analyses of the climatic water balance (*CWB*) are usually developed for regions where the input data, mainly air temperature and precipitation, can be readily obtained.

The research described herein is based on mean monthly values of air temperature and precipitation totals obtained from 60 meteorological stations as well as monthly totals for solar radiation obtained from 21 actinometric stations. The data cover the periods 1951–2010 and 1986–2010, respectively.

Not all the actinometric stations considered collect the necessary meteorological data, therefore, detailed analyses of the climatic water balance use data obtained only from 16 stations covering the period from 1986 to 2010.

Meteorological data were compiled using topographic information from the SRTM DEM model (*EROS,* 2011).

Given the limited nature of the source data, Turc formula (1961) was used to obtain potential evapotranspiration values. This method was confirmed (*Kowanetz*, 2000) to be suitable for describing the relationship between evapotranspiration and relief. The resulting formula is as follows:

$$CWB = RR - 0.4\frac{t}{t+15}I + 50\,, \tag{1}$$

where *RR* is the monthly precipitation totals [mm], *t* is the monthly average air temperature [°C], and *I* is the monthly sum of total solar radiation [cal cm^{-2} day^{-1}].

Climatic water balance modeling was carried out using two approaches simultaneously. The first approach, examining correlations between environmental elements, used a linear regression method. Statistical relationships between *CWB* and geographic variables such as latitude, elevation, and distance from the coast line were taken into account. The second approach was based on data modeling implementing a map algebra procedure. The results of both approaches were validated using common error estimators.

The *CWB* values calculated for 16 stations were used as reference data (*Fig. 1*). In this study, climatic water balance modeling was conducted using the two methods simultaneously.

An analysis was conducted for the growing season, defined as the time period from May until October. This is consistent with what is frequently considered in agrometeorology.

2.1. Regression models: simple linear regression, multiple linear regression

As mentioned above, the first approach utilized regression models: simple linear regression (SLR) and multiple linear regression (MLR). Close relationships between climatic water balance and geographic factors became the basis for the

model (*Wypych* and *Henek*, 2012), with longitude, latitude, elevation, as well as distance from the coast as explanatory variables.

Fig. 1. Location of the climatic water balance data source stations.

Due to the limited number of samples and also the smallest correlation (from all the analyzed predictors) coefficient between *CWB* values and longitude, it was finally decided to exclude longitude as a variable from regression models, Eqs. (2–4), and not use it in further analyses:

$$Z(s) = \beta_0 + \beta_2 H(s) + \varepsilon(s), \tag{2}$$

$$Z(s) = \beta_0 + \beta_1 \varphi(s) + \beta_2 H(s) + \varepsilon(s)\,, \tag{3}$$

$$Z(s) = \beta_0 + \beta_1 \varphi(s) + \beta_2 H(s) + \beta_3 d(s) + \varepsilon(s)\,, \tag{4}$$

where $Z(s)$ is the dependent variable, $\varphi(s)$ is the latitude, $H(s)$ is the elevation [m a.s.l.], $d(s)$ is the distance from the coast [m], and $\varepsilon(s)$ is the regression residuals.

CWB values were calculated for points on a grid with a spatial resolution of 1 km on the basis of the described linear relationships and using the described regression method.

Data interpolation using radial basis functions (RBF) was used in the final step of creating the climatic water balance spatial differentiation map. RBF is an interpolation technique, which takes into account general tendencies as well as local variability. Research conducted hitherto (*Wypych* and *Ustrnul*, 2011) has confirmed the suitability of RBF as a method for CWB index spatialization.

2.2. Map algebra

The second approach was based on a map algebra application. This type of model requires a process of raster data transformation using GIS tools.

For this study, map algebra was used to create the final CWB spatial differentiation map. First, a series of maps showing the spatial distribution of climatic water balance index components such as air temperature, precipitation totals, and solar radiation, were created using in-situ data.

Component maps of the climatic water balance index were constructed according to a method developed by international research teams dealing with GIS implementation in meteorology and climatology (*Dobesch et al.*, 2007). The method most widely used and commonly considered most effective is kriging (*Dobesch et al.*, 2007).

Temperature spatial differentiation maps were created as the first CWB component using the residual kriging method (*Ustrnul* and *Czekierda*, 2005). Several geographic parameters including elevation, latitude, longitude, and distance to the Baltic coast (for stations located within 100 km), were used as predictor variables.

Precipitation totals were interpolated for the territory of Poland using the kriging method (*Łupikasza et al.*, 2007).

A solar radiation surface was obtained by the application of Solar Analyst ArcGIS. All necessary information such as sunshine duration, altitude at the given location, radiation parameters (diffuse factor and transmittivity), as well as topographic factors such as slope, aspect, and shaded relief based on the SRTM was implemented. Because of element sensitivity to local conditions (astronomical, geographic, meteorological), a variety of different settings in the Solar Analyst application were tested to achieve satisfactory final results. In most cases, the diffuse factor and transmittivity were adjusted. For Poland, the diffuse factor approaches 0.5, while a transmittivity value of 0.4 may also be assumed. In-situ data were used as the reference for parameter selection and model estimation.

All of the layers created were used as input parameters for the potential evapotranspiration model in the Turc formula (air temperature and solar radiation map) and used along with the precipitation map to calculate the climatic water balance for the territory of Poland using the map algebra method. Transformations affected entire layers; all cells of the raster were used as variables. Raster cell values were changed due to previously cited formulas for potential evapotranspiration and the CWB index.

2.3. Validation

The final step was to validate the proposed methods. Due to the limited number of reference points and the use of several different interpolation methods (which are not the typical methods of spatial data interpolation), only simple statistical evaluation measures could be used. The first and most basic measure of model adjustment was the value of the correlation coefficient between the real (from in-situ measurements) and modeled data (R). In addition, bias (RE), percentage error (PE), and absolute error (AE) were calculated and used. Because of the limited number of reference points, it became impossible to evaluate the models using the most common validation methods used for interpolation. Neither cross-validation nor the method of independent sampling could be properly used in this case. However, the suggested estimation factors used for analyzing the results of spatial analyses conducted using different interpolation methods (*ESRI,* 2001) were implemented to assess average real spatial interpolation errors. These include errors for points gained in the first validation step: RMSE (root-mean square error), MPE (mean percentage error), MAPE (mean absolute percentage error). All the model adjustment measures were implemented in relation to values obtained at field measurement sites.

3. Results

Research has shown that the spatial differentiation of the climatic water balance in Poland in the growing season (May – October) amounted to less than –200 mm in the central part of the country and hundreds of millimeters in the high mountain regions of the Carpathians Mountains and the Sudety Mountains (*Fig. 2*).

Most of the territory of Poland is characterized by a moisture shortage. Positive moisture values are typical only in the southern highlands, foothills, and mountain areas (*Fig. 2*). In addition, the spatial distribution of the climatic water balance varies seasonally.

Nevertheless, a detailed analysis of the climatic water balance index distribution shows regional and local differences attributable to the spatialization method implemented as described below.

The regression models used in this research study have shown to be most strongly affected by elevation in a significant correlation. The predominant role of this predictor has been to influence the spatial differentiation of the climatic water balance index in Poland. However, regardless of the regression method, the belt-like distribution of *CWB* index values is still discernible. This pattern holds true mainly in the spring and summer months, but it is less visible in the autumn. The Baltic Sea also affects seasonal differences by limiting evapotranspiration – higher *CWB* values noted between July and October. In May and June, it was not shown to have an important effect.

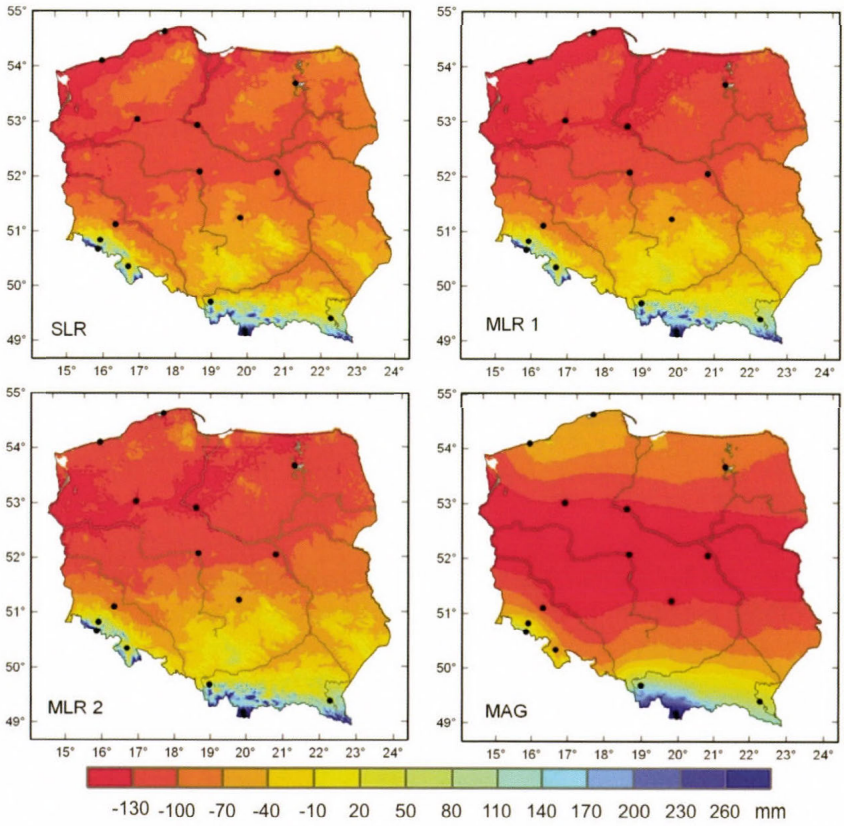

Fig. 2. Spatial differentiation of climatic water balance (*CWB* in mm) in Poland in the growing season (May–October) based on different methods.
SLR – simple regression: f (H), MLR 1 – multiple regression: f (φ, H), MLR 2 – multiple regression: f (φ, H, d), MAG – map algebra

With an understanding of the spatial differentiation of climate conditions in Poland, it can be stated that regression models can slightly deform *CWB* differentiation visualizations, especially in coastal areas, as mentioned previously.

When using the map algebra method (MAG), the belt-like distribution of the *CWB* shows that the index is dependent on geographic parameters such as elevation and latitude. The "distance from the Baltic coastline" variable is indirectly (i.e., by differentiation of temperature values and precipitation totals) implemented in the MAG model. The climatic water balance field shows a significant moisture deficit (the lowest *CWB* index values) in the lowlands of

Central Poland, whereas values estimated much higher than what other models produce can be observed along the coastline. This situation is characteristic of the entire growing season.

Fundamental evidence acknowledging and supporting the MAG approach can be used for a detailed analysis of *CWB* component spatial fields, which serve as the basis of this study. A MAG image is the effect of the spatialization of different elements such as precipitation and evapotranspiration, whereas the latter is a result of integrating solar radiation and temperature maps.

Research results produced using both methods were validated using universal statistical error estimators. *CWB* values calculated for the 16 weather stations considered in the study were used as reference data.

For all 16 weather stations considered, *CWB* values were calculated for the study period. For each point, the deviations of the modeled values were defined by subtracting the true values (*CWBmod – CWBcalc*) for the growing season (May–October) for each month separately. Positive error values (calculated differences) indicate model overestimation, whereas negative error values show undervaluation of predicted values.

Results for the growing period (May–October) clearly show that the map algebra (MAG) method gives the best fitting results in relation to the reference data. The highest (close to 1), correlation coefficient value confirms the best model adjustment. Absolute errors are also significantly smaller than those produced by other research methods (*Table 1*). The MAG model overestimates *CBW* values for northern and central Poland and produces the best predictions for the northeastern part of the country, and the least accurate predictions for the central part of Poland. For southern Poland, modeled values of the climatic water balance are lower than calculated values.

The differences reach an average in the tens of millimeters; however, in extreme cases, the model can give *CWB* index values different from true values by several hundred millimeters. This has been reported for the Kasprowy Wierch and Śnieżka mountain weather stations. Regression models not considering the distance from the Baltic coastline as a predictor (MLR 1) as well as simple regression (SLR) were shown to be the least accurate methods. The correlation coefficient is about 0.5 lower, and other estimators show minimally higher values in both cases (*Table 1*). It is worth noting that the spatial differentiation of the results produced by the methods used in this paper is readily observable. Simple linear regression (SLR) gives better results for areas near the Baltic coast and for the Sudety mountains in southern Poland. On the other hand, in the central Polish lowlands, differences between the methods used cannot be clearly distinguished. Finally, the MLR 1 method performs well in the Carpathian region.

Table 1. Climatic water balance values (*CWB*) with selected model errors at reference points in the growing season (May – October)

Reference stations	*CWB* [mm]	SLR		MLR_1		MLR_2		MAG	
		APE (%)	RE [mm]	APE (%)	RE [mm]	APE (%)	RE [mm]	APE (%)	RE [mm]
Kołobrzeg	–73.3	107.9	–79.2	17.5	12.8	146.1	–107.2	66.4	–48.7
Łeba	–69.4	122.0	–84.7	16.4	11.3	176.6	–122.6	88.9	–61.7
Piła	–155.4	19.5	30.4	14.2	22.0	12.4	19.3	12.4	19.3
Toruń	–160.9	21.7	35.0	13.3	21.4	14.5	23.3	14.5	23.4
Mikołajki	–97.6	1.4	–1.4	5.0	4.8	28.3	–27.6	28.3	–27.6
Koło	–181.8	38.6	70.2	9.5	17.3	39.3	71.5	39.3	71.5
Warszawa	–177.6	38.0	67.5	16.9	30.0	38.5	68.4	38.5	68.4
Legnica	–165.6	37.9	62.7	27.7	45.9	47.4	78.5	47.4	78.5
Sulejów	–157.9	52.8	83.4	13.3	21.0	60.5	95.5	60.5	95.5
Jelenia Góra	–16.1	117.2	18.9	46.7	–7.5	154.3	24.9	154.6	24.9
Śnieżka	271.1	40.7	110.2	55.3	–149.9	50.2	136.0	50.0	135.6
Kłodzko	–44.5	77.3	34.4	38.2	–17.0	139.0	61.8	138.9	61.8
Bielsko-Biała	165.2	88.4	–146.1	26.5	–43.8	75.8	–125.2	75.8	–125.3
Zakopane	378.5	39.7	–150.2	11.0	–41.7	37.0	–140.2	37.0	–140.2
Kasprowy Wierch	819.7	32.0	–262.4	35.7	–292.7	21.6	–177.1	21.5	–176.6
Lesko	86.5	87.5	–75.7	44.1	–38.2	56.0	–48.4	56.0	–48.5
MAE [mm]		82.0		83.0		75.5		48.6	
RMSE [mm]		102.5		95.3		88.3		86.1	
MAPE (%)		57.7		68.6		58.1		24.4	
R		0.940		0.937		0.950		0.988	

RE – bias, APE – absolute percentage error, MAE – mean absolute error, RMSE – root-mean-square error, MAPE – mean absolute percentage error, R – Pearson's correlation coefficient, MAG – map algebra, SLR – simple linear regression: f (H), MLR_1 – multiple linear regression: f (φ, H), MLR_2 – multiple linear regression: f (φ, H, d)

The least accurate results, regardless of method, were observed for Poland's mountain regions. All of the models predict values lower than real values for the Carpathians (*Table 1*). For the Sudety Mountains, significant positive differences were modeled only for Mount Śnieżka. Other weather stations are characterized by errors commonly found in the rest of the country. Coastal areas encountered the same difficulty as mountain areas when it came to the spatialization of the *CWB* index. Regression models significantly lower the

prediction and estimate values close to those recorded for Poland's lake districts and the central part of the country.

As previously mentioned, map algebra images are produced by the spatialization of climatic water balance index components. Therefore, it could be supposed that the final map additionally contains some errors such as precipitation errors, and above all, potential evapotranspiration interpolation errors, since the latter were obtained using map algebra, where the temperature field was integrated with solar radiation. Moreover, solar radiation was modeled using the Solar Analyst tool, and the potential solar radiation field was based primarily on elevation.

4. Discussion

The climatic water balance is a complex index influenced by many different factors. These factors affect both precipitation and evapotranspiration values including solar radiation, relief and slope aspect, land use, and degree of urbanization.

In the course of research and analysis, several problems were identified that could potentially affect further research in this area.

Climatic water balance components such as precipitation and potential evapotranspiration are characterized by considerable spatial and temporal differentiation as well as strong correlations between atmospheric circulation, meteorological conditions, and local factors. Therefore, *CWB* spatial variability is difficult to identify. Current understanding of mesoclimate differentiation, especially that of mountain areas, suggests that many geographic variables should be taken into consideration. In order to accurately describe the spatial distribution of *CWB*, it is necessary to take into account variables such as slope, aspect, land use, and soil type, all of which determine how much solar radiation is available to produce given air temperature values (*Ustrnul* and *Czekierda*, 2005). Both solar radiation and air temperature affect the degree of evapotranspiration. Furthermore, both parameters must be calculated independently for smaller regions – especially regions characterized by specific mesoclimate conditions such as those found in coastal or mountain areas.

In order to determine the value of the *CWB* index, the magnitude of evapotranspiration must be properly estimated. Although Turc formula used in this paper is strongly correlated with geographic factors (especially elevation), it seems insufficiently sophisticated to fully represent evapotranspiration conditions. The purpose of this study was to identify the best spatialization method in a situation with a shortage of data; therefore, Turc formula was chosen as the least demanding. Ultimately, the final results do contain errors.

At least 30 years of daily data are needed in order to analyze the climatology of an element; in this case, the spatial and temporal differentiation of the climatic water balance. The data must address all *CWB* components. As

mentioned before, no evapotranspiration data were available, and the available data required the use of complex formulas that are not completely suitable for long-term data. Furthermore, commonly used formulas providing potential evapotranspiration data only fulfill environmental requirements to a certain extent and tend to produce unreliable data (*Jaworski*, 2004).

The main objective of this research study was to depict *CWB* spatial differentiation using a limited quantity of homogenized data. Recent developments in GIS techniques have produced a wide range of powerful methods for capturing, modeling, and displaying of climate data. Using geospatial analysis seems to be the sensible response to the current research needs for this topic. Nevertheless, even the most advanced data processing methods we use contain failures and problems that need to be solved in order to perform detailed analysis of the climatic water balance index on different temporal and spatial scales.

Using only 16 reference points to create the regression models and validate the data, the results were error laden. The magnitude of the regression model errors cannot be accepted. The weather stations were not representative enough to build the final model. This is why, among other things, the land use factor was removed from the formula. In the regression methods, the most deficient were solar radiation data. It would be possible to use more reference points (however not so many as 60 stations as used for temperature and precipitation data), if modeled data were used instead of in-situ solar radiation data. There exist empirical formulas (*Podogrocki*, 1978) for which daily sums of total solar radiation are obtained using sunshine duration data.

It would also be possible to generate the missing data from, for instance, the Solar Analyst application. Nevertheless, the more generalized or simplified the data, the greater the possibility of error in the final model.

The data deficit problem also concerns the map algebra model and validation section. Model errors generated for "blank" areas (without measuring points) cumulate while being aggregated in the map algebra method. As far as estimating the models, weather stations located in the northeast and east of Poland, as well as in mountain areas are desirable.

The least accurate results were obtained for mountain areas. This is mainly because in the mountains weather systems are strongly affected by the topography, and the modeling of climate conditions requires representative points for different elevations, landforms, aspects, etc. The spatial resolution suggested for mountainous areas is at least one weather station per 1,300 km^2 for temperature, wind velocity, precipitation, and one weather station per 500 km^2 for snow data (*Barry*, 1992). The validation results for climatic water balance variability would be different (more positive) if the Kasprowy Wierch and Śnieżka weather stations were not taken into account. Model errors are also the effects of temporal/seasonal differentiation of particular climate elements included in the CWB index. Local factors are of great importance, especially in the spring and summer months, which is also reflected in the selected estimator values.

Regardless of the validation results, the obtained maps of climatic water balance spatial differentiation in Poland show certain problems with the methods used. Regression models are affected mainly by the lack of data used to create the formulas taking into account long-term and homogenous data series of necessary meteorological elements. The fundamental error source was the irregular location of the data gathering points and subsequently limited representativeness regarding various environmental conditions. This can be more clearly seen along the Baltic coast, but also in the northeastern part of Poland, and of course, in its mountains in the south. On the other hand, solar radiation field data seems to be the vulnerable point of the map algebra method. The limitations of the Solar Analyst application – mainly due to highly variable cloud cover – and the lack of a sufficiently dense network of weather stations failed to ensure good interpolation results.

5. Conclusions

The primary objective of this study was to find the optimal spatialization method to describe spatial differentiation of the climatic water balance (*CWB*) in Poland. Two different approaches employing five spatialization methods were used – regression models (simple linear regression, various multiple linear regression formulas) and map algebra. Climatic water balance values and their spatial distribution are dependent on both atmospheric circulation (i.e., weather conditions) and local environmental conditions. Hence, it was necessary to use many different geographic predictors including coordinates, elevation, and others.

The research confirmed that the application of GIS techniques is a useful and promising tool for constructing maps of different climate elements and indices. At the same time, through a detailed analysis of the research results, certain shortcomings of the proposed method can be reported. Aside from the nature of the method itself, the principal problem can be the lack of source data. As a consequence, there is the risk of performing extrapolation instead of interpolation.

The largest differences between model values and real values were noted for regions with a sparse weather station network. This means that the final results may be the effect of the particular method used in spatial analysis, especially for areas with few measuring points. Such cases warrant a very careful interpretation of the research results.

Regardless of the research method used, the obtained results confirm the role of local factors in CWB modification. Therefore, it is necessary to take into account not only the spatial scale, but also the time scale used for explanatory variables. This is because, depending on the area and the season, their impact on the predictand will vary.

No matter how accurate the results are, research experience and scientific intuition are the keys to the interpretation of research results. Careful and detailed analysis is required as well as thorough knowledge of pertinent physical processes and complexity of the geographic environment. Both types of factors need to be considered when choosing predictors and later in the course of model validation, where a complex series of explanatory variables is used.

References

Barry, R.G., 2008: Mountain weather and climate. Routledge, London-New York.

Dobesch, H., Dumolard, P., Dyras, I. (eds.), 2007: Spatial Interpolation for Climate Data: the Use of GIS in Climatology and Meteorology. ISTE, London.

EROS: Earth Resources Observation and Science Center, 2011: on-line at: http://earthexplorer.usgs.gov/, accessed: December 2011.

ESRI, 2001: ArcGIS Geostatistical Analyst: Statistical Tools for Data Exploration, Modeling and Advanced Surface Generation. ESRI White Paper, New York – Redlands.

Fernandes, R., Korolevych, V., Wang, S., 2007: Trends in land evapotranspiration over Canada for the period 1960–2000 based on in situ climate observations and a land surface model. *J. Hydrometeorol. 8*,1016–1030.

Kalma, J.D., McVicar, T.R., and *McCabe, M.F.*, 2008: Estimating land surface evaporation: A review of methods using remotely sensed surface temperature data. *Surv. Geophys. 29*, 421–469.

Jaworski, J., 2004: Evaporation in hydrological cycle of river basins. Polskie Towarzystwo Geofizyczne, Warszawa (in Polish).

Kowanetz, L., 2000: On the method of determining the climatic water balance in mountainous areas, with the example from Polish Carpathians. *Zeszyty Naukowe UJ, Prace Geograficzne* 105, 137–164.

Łupikasza, E., Ustrnul, Z., Czekierda, D., 2007: The role of explanatory variables in spatial interpolation of selected climate elements. *Roczniki Geomatyki* 5, 55–64.

Nováky, B., 2002: Mapping of mean annual actual evaporation on the example of Zagyva catchment area. *Időjárás 106*, 227–238.

Podogrocki, J., 1978: Spatial distribution of global solar radiation in Poland. *Publ. Inst. Geophys. Pol. Acad. Sc., D5-120*, 17–30.

Rosema, A., 1990: Comparison of Meteosat-based rainfall and evapotranspiration mapping in the Sahel region. *Int. J. Remote Sens. 11*, 2299–2309.

Turc, L., 1961: Evaluation des besoins en eau d'irrigation, évapotranspiration potentielle. *Ann. Agronomiq.12*, 13–49.

Tveito, O.E., Wegehenkel, M., Wel van der, F., and *Dobesch, H.* (eds.), 2008: The use of geographic information systems in climatology and meteorology. Final Report COST Action719, COST Office.

Ustrnul, Z. and *Czekierda, D.*, 2005: Application of GIS for the development of climatological air temperature maps: an example from Poland. *Meteorol. Appl. 12*, 43–50.

Vicente-Serrano, S.M., Lanjeri, S., and *López-Moreno, J.I.*, 2007: Comparison of different procedures to map reference evapotranspiration using geographical information systems and regression-based techniques. *Int. J. Climatol. 27*, 1103–1118.

Wypych, A. and *Ustrnul, Z.*, 2011: Spatial differentiation of the climatic water balance in Poland. *Időjárás 115*, 111–120.

Wypych, A. and *Henek, E.*, 2012: Using GIS in spatial differentiation of the climatic water balance research in Poland. *Przegląd Geofizyczny 57*, 233–244 (in Polish).

Xinfa, Q., Yan, Z., and *Changming, L.*, 2002: A general model for estimating actual evaporation from non-saturated surfaces. *J. Geograph. Sci. 12*, 479–484.

IDŐJÁRÁS

Quarterly Journal of the Hungarian Meteorological Service
Vol. 118, No. 2, April – June, 2014, pp. 147–166

Modification of the Tourism Climatic Index to Central European climatic conditions – examples

Attila Kovács* and **János Unger**

Department of Climatology and Landscape Ecology, University of Szeged
P.O. Box 653, H-6701 Szeged, Hungary

**Corresponding author E-mail: kovacsattila@geo.u-szeged.hu*

(Manuscript received in final form September 18, 2013)

Abstract—Climate is a decisive tourism resource and plays key role in the attractiveness of tourist destinations and the seasonality in tourism demand. The suitability of climate for general tourism purposes (i.e., sightseeing, shopping, and other light outdoor activities) is most frequently expressed by the Tourism Climatic Index (TCI), which combines several tourism-related climatic elements. In this study, the original TCI is modified in two ways. On the one hand, one of the most popular and widely used bioclimatic indices, Physiologically Equivalent Temperature (PET) is applied instead of effective temperature (ET) in the part of the index related to thermal comfort conditions. Furthermore, the TCI is adjusted to a ten-day scale since it is more relevant to tourism than the original monthly averages of the climatic parameters. Using the modified TCI we characterize and compare climatically suitable or even unfavorable places and periods of the year in case of some Hungarian and two other relatively close tourist destinations as examples. Analytical results indicate that the most optimal climatic conditions are in the shoulder seasons in all investigated places. The summer period is more unpleasant for sightseeing activities mainly due to the instense heat load. There are some remarkable differences between the cities in the time of occurence of different tourism climatic conditions and, therefore, in the seasonality conditions.

Key-words: climatic conditions, tourism, modified Tourism Climatic Index, Physiologically Equivalent Temperature, Central Europe

1. Introduction

Tourism is one of the key sectors in Hungarian economy. In 2011, more than 41 million foreign tourists contributed with 1200 billion HUF to the tourism sector. Tourism related industries generate about 5.9% of national gross domestic product (GDP) and employ 8.4% of all workers in Hungary (*KSH,* 2012).

The attractiveness of a tourist destination is influenced by several factors. Together with geographical location, topography, landscape, flora and fauna, climate constitutes the natural tourism resource of a place (*de Freitas,* 2003). Climate can directly affect tourism in many ways. Climate may be a decisive factor in the choice of a destination by determining the time of the year, when climatic conditions are at their optimum, or by designating the area that offers the most suitable climatic conditions (*Mieczkowski,* 1985). Ultimately, it affects tourists' satisfaction with the destination area, thermal comfort, and climatic well-being of visitors. Inter-annual climate variability influences the length and quality of tourism seasons, and thus, the tourism demand (*Scott* and *McBoyle,* 2001; *Scott et al.,* 2008).

Mainly due to the increasing competition between tourist destinations, considerable effort has been put into defining an easily applicable metric in order to investigate the suitability of different tourist activities in terms of climatic conditions. It is generally accepted that tourists respond to the integrated effects of the atmospheric environment, therefore, a comprehensive tourism climatic metric has to integrate all three tourism-relevant aspects of climate identified by *de Freitas* (2003): thermal, physical, and aesthetic (*Matzarakis,* 2006; *Scott et al.,* 2008; *Yu et al.,* 2009; *Perch-Nielsen et al.,* 2010). An overview of these three different facets of climate and their significance to tourists is provided in *Table 1*.

One of the most comprehensive and widely used metrics in tourism climatology is the Tourism Climatic Index (TCI) (*Mieczkowski,* 1985), which attempts to reflect the destination's climatic suitability for "average" tourists engaged in light physical outdoor activities (e.g., sightseeing, shopping). TCI is also capable to characterize global or regional effects of climate change to tourism according to projected scenarios of future climatic conditions. For example, *Scott et al.* (2004) used the TCI to assess its temporal and spatial distribution and seasonal variability in the future focusing on destinations in North America, while *Amelung* and *Viner* (2006) and *Perch-Nielsen et al.* (2010) in Europe. *Zaninović et al.* (2010) studied the influence of climate change on summer tourism potential in the Pannonian lowland (great parts of Hungary and Croatia) by analysing the differences between future and present bioclimatic and tourism climatic conditions based on climate simulations focusing on the changes in single climatic parameters and Physiologically Equivalent Temperature (PET, see in Section 2). The results indicate diverse

changes in summer tourism potential of the area due to the global warming. In addition, *Németh* (2013) analyzed the changes of the tourism climate potential in the Lake Balaton region of Hungary in detail during the last half-century based on the original TCI index. According to the results, the best climatic conditions for tourism purpose can be observed in the summer months. Between three climatological normal periods, significant changes in tourism climatic conditions cannot be detected in the last half-century.

Table 1. Various aspects of tourism climate, their impact, and significance (based on *de Freitas,* 2003)

Facets of climate	**Impact, significance**
Thermal	**Physiological impact**
integrated effects of air temperature, humidity, wind speed, short- and long-wave radiation, personal factors	heat sensation, thermal comfort, physiological stress climate therapy
Physical	**Physical impact**
wind	dust, sand, damage to property
rain	wetting, reduced visibility and enjoyment
snow	winter sports/activities
ice	personal injury, damage to property
air quality	health, allergies, well-being
ultraviolet radiation	health, suntan, sunburn
Aesthetic	**Psychological impact**
sunshine/cloudiness	enjoyment, attractiveness of site
visibility	enjoyment, attractiveness of site
day length	period of activities, convenience

The present study aims a modification of the original TCI in order to reduce its two current serious limitations and reflect a more current state of knowledge. We make an attempt to update the thermal comfort parts of the index and its original temporal scale to the Central European conditions. We present the behavior of the modified index while describing climatically suitable or even unfavorable periods of the year in case of some Hungarian and two relatively close tourist destinations as examples.

2. The Tourism Climatic Index

TCI was developed by *Mieczkowski* (1985) based on previous research related to climate classifications for tourism and human biometeorology. In TCI, monthly averages of seven climate variables relevant for tourism are integrated into five sub-indices, listed in *Table 2*: daytime comfort index (CId), daily comfort index

(CIa), precipitation (R), sunshine (S), and wind (W). All of them are rated on different scales from 0 (unfavorable) to 5 (optimal) values while the thermal comfort sub-indices (CId and CIa) are rated from –3 to 5. By distinct weightings and then combining all weighted sub-indices, the overall TCI is calculated as follows:

$$TCI = 2\times(4\times CId + CIa + 2\times R + 2\times S + W). \quad (1)$$

Table 2. Summary of the sub-indices, their impact, and weigthing in TCI (based on *Scott* and *McBoyle*, 2001)

Sub-index	Monthly averages	Influence on TCI	Weighting
daytime comfort index (CId)	daily maximum temperature (°C) and minimum relative humidity (%)	represents thermal comfort when maximum tourist activity occurs (usually between 12 a.m. and 4 p.m)	40%
daily comfort index (CIa)	daily mean temperature (°C) and mean relative humidity (%)	represents thermal comfort over the full 24-hour period	10%
precipitation (R)	total precipitation (mm)	negative impact on outdoor activities and climatic well-being	20%
sunshine (S)	sunshine duration (hour)	positive impact	20%
wind (W)	wind speed (ms^{-1})	variable impacts depending on its value and the maximum temperature	10%

As all sub-indices have a maximum score of 5, *Mieczkowski* (1985) proposed a rating system of TCI with an overall maximum score of 100, where acceptable scores are above 40, good climatic conditions are above 60, and excellent scores are above 80 (*Table 3*).

Table 3. Tourism Climatic Index rating system (*Mieczkowski*, 1985)

TCI scores	Descriptive categories
90 – 100	ideal
80 – 89	excellent
70 – 79	very good
60 – 69	good
50 – 59	acceptable
40 – 49	marginal
30 – 39	unfavorable
20 – 29	very unfavorable
10 – 19	extremely unfavorable
< 10	impossible

Scott and *McBoyle* (2001) presented a conceptual framework of six possible types of annual TCI distributions; the tourism resource of all destinations can be classified into one of them (*Fig. 1*). In our study, this framework is used to characterize the tourism climatic conditions in the selected cities.

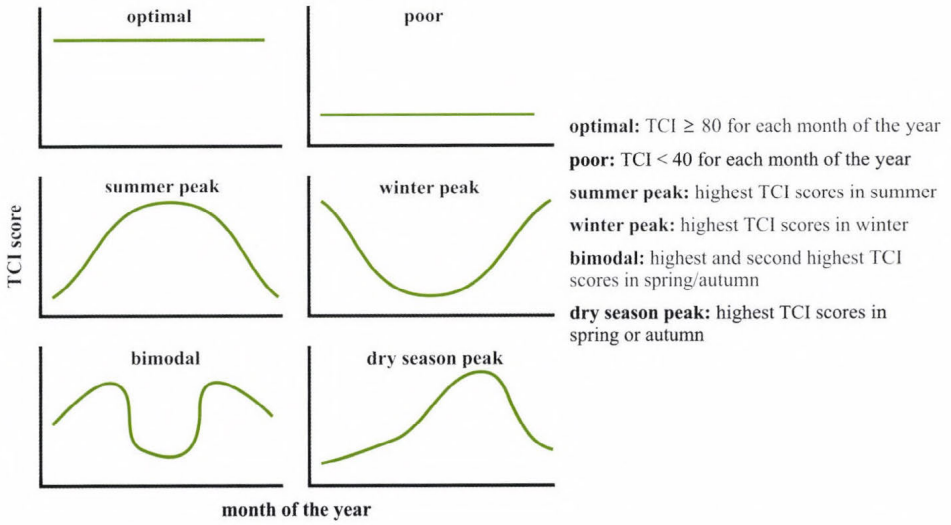

Fig. 1. Conceptual framework of annual tourism climate distributions (based on *Scott* and *McBoyle,* 2001).

The sub-indices of TCI expressing thermal comfort conditions (CId, CIa) are based on the effective temperature (ET), which is a simple empirical index of air temperature/relative humidity combinations (*Houghten* and *Yaglou,* 1923). The optimal comfort zone of ET is between 20 and 27 °C according to *ASHRAE* (1972) rated with maximum point 5. The rating scale then decreases on both sides of the optimal zone with 1 or 0.5 points. However, the rating points of the zones are based on the subjective opinion of the author, they are not empirically tested against the preferences of tourists (*de Freitas,* 2003; *de Freitas et al.,* 2008). A further important shortcoming of ET is that it does not include the effects of such thermal parameters as wind speed, short- and longwave radiation fluxes, in addition, it does not take into account such physiologically, and thus, bioclimatically relevant personal data as age, gender, height, weight, metabolic rate, and clothing. Therefore, it cannot evaluate the thermal conditions of the human body in a physiologically significant manner.

Instead of empirical indices, a full application of rationale indices based on the energy balance of the human body gives detailed information on the effect of thermal environment on humans (*VDI,* 1998). Such indices include all relevant

thermophysiological parameters: air temperature, relative humidity, wind speed, short- and longwave radiation fluxes. One of the most popular and widely used rationale bioclimate indices is the Physiologically Equivalent Temperature (PET), which was developed typically for outdoor applications (*Mayer* and *Höppe,* 1987; *Höppe,* 1999). The interpretation of the index refers to indoor standard reference conditions and the evaluation of the thermal comfort conditions concerns a standardized fictive person. PET is defined as the air temperature at which, in a typical indoor setting, the heat budget of the body is balanced with the same core and skin temperature as those under the prevailing complex outdoor conditions (*Höppe,* 1999). The PET value categories were initially defined according to thermal sensations and physiological stress levels of Western and Central European people, where the thermally neutral heat sensation and stress are indicated by PET value range of 18–23 °C (*Fig. 2*) (*Matzarakis* and *Mayer,* 1996).

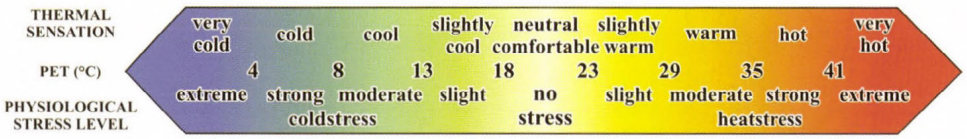

Fig. 2. Categories of the PET values (°C) for different grades of thermal sensation and physiological stress level of Western and Central European people (based on *Matzarakis* and *Mayer,* 1996).

3. Modification methods on Tourism Climatic Index

Despite the comprehensive nature and wide applications of TCI, a number of limitations were addressed and some modification possibilities were suggested by different studies (e.g., *de Freitas,* 2003; *Matzarakis,* 2006; *de Freitas et al.,* 2008; *Perch-Nielsen et al.,* 2010). The rating systems and the weightings of the sub-indices are partly based on human biometeorological literature, but also on the author's subjective opinions. A further important limitation is the application of ET, which was addressed by e.g., *Scott et al.* (2004), *Amelung* and *Viner* (2006) and *Perch-Nielsen et al.* (2010), therefore, they used apparent temperature (AT) (*Steadman,* 1979) instead of ET. However, AT is also based only on temperature/humidity combinations, and it is not really applied in recent human biometeorological research. A further important shortcoming of TCI is its temporal scale since monthly averages of the applied climatic parameters are considered, which are insufficient for tourism climatic purposes because tourists' length of stay during sightseeing is generally shorter (*de Freitas et al.,* 2008; *Scott et al.,* 2008; *Yu et al.,* 2009; *Perch-Nielsen et al.,* 2010).

Based on the above mentioned shortcomings, in the present study two modifications are performed in the structure of the original TCI, which means an initial step forward in the development of an updated index applicable at Central European climatic conditions. Firstly, in order to take into account human thermal comfort conditions more precisely in TCI, we attempted to integrate PET into the thermal sub-indices instead of ET, and for this purpose, a new rating system of PET has been developed, too. Secondly, the TCI is adjusted to a ten-day scale, i.e., ten-day averages of each climatic variables were rated, and then the values obtained in this way were taken at the index calculation.

The annual variations of the modified index and its sub-indices are presented and compared in case of four Hungarian and two other European cities: Szeged-Bajai út (46°15'N, 20°05'E), Siófok (46°54'N, 18°02'E), Debrecen (47°29'N, 21°36'E), Győr-Likócs (47°42'N, 17°40'E), Prague-Libus (50°0'N, 14°26'E), Thessaloniki-Airport (40°31'N, 22°58'E) (*Fig. 3*). The analysis concerns the periods of 1996–2010 and 2000–2010 in the first three and second three places, respectively.

Fig. 3. The investigated Hungarian and other European cities.

For the calculation of PET, hourly air temperature, relative humidity, wind speed, and cloudiness data of Hungarian Meteorological Service were used in the case of the Hungarien cities, while hourly and three-hourly synop report queries were utilized for Prague and Thessaloniki, respectively. PET was

calculated by means of the bioclimate model RayMan (*Matzarakis et al.*, 2007). The measured wind speed data were transformed to the bioclimatological reference height of 1.1 m. Ultimately, the daytime (CId) and daily comfort (CIa) sub-indices of the modified TCI consist of the calculated daily maximum and daily average PET values holding the basic concept of *Mieczkowski* (1985) (see in *Table 2*). In addition to the data necessary for PET, daily precipitation and sunshine duration data obtained from the above mentioned databases were utilized. Concerning the parameters used for the calculation of PET, it is often difficult to access appropriate data, especially the radiation component of PET due to the lack of long-term or fine temporal scale (i.e., hourly) data sets. For example, application of global radiation instead of cloudiness data would be more appropriate, but its availability is often limited due to the uncertain measurement program and the lack of long-term data. Nevertheless, we could select several tourist destinations with complete data sets in different climatic regions, and evaluation and comparison are possible using these datasets representing these regions.

The original rating systems of wind speed (W), precipitation (R), and sunshine duration (S), and the weightings of all TCI sub-indices remained unchanged. (Note: Mieczkowski rated monthly precipitation on a scale from 0 to 5. Because of the ten-day averages, this scheme was changed by simply dividing the monthly values by 3, and these categories were rated by the original scores).

However, for the evaluation of PET, a new rating scheme had to be developed keeping in mind that the rating categories and scores should be based on objective, international standards, and subjective factors should be eliminated. The rating scores of PET were derived based on the principle that the comfortable thermal conditions should get higher scores while in case of intesifying warm or cold thermal stress conditions the values should decrease progressively on both sides of the comfort zone in an objective way.

Therefore, in the derivation of rating scores of PET, we utilized the function relationship declared in *ASHARE* (2004) and *ISO* (2005) between two bioclimatic measures, predicted mean vote (PMV) and predicted percentage of dissatisfied (PPD) (*Fanger,* 1972). PMV derived from the comfort equation of *Fanger* (1972) predicts the mean values of the thermal votes of a large group of persons on a seven-point (later nine-point) thermal sensation scale (from –4 very cold to +4 very hot) based on the heat balance of the human body in an environment characterized by given thermal variables (air temperature, relative humidity, wind speed, mean radiant temperature) (*ASHRAE,* 2004; *ISO,* 2005). Individual votes are obviously scattered around this mean PMV value, i.e., thermal environment characterized by the same PET value does not necessarily evoke the same thermal sensation of all persons. However, the distribution of thermal votes as a function of PMV can be statistically predictable. PPD establishes a quantitative prediction of the ratio of thermally dissatisfied people

who feel too cold or too warm, i.e., do not vote –1, 0, or +1 on the seven-point scale (*ASHRAE,* 2004; *ISO,* 2005). For example, in case of 0, PMV such thermal votes belong to only 5% of the given population, while 95% of them can be considered thermally satisfied. The relationship between PPD and PMV can be given as follows (*ASHRAE,* 2004; *ISO,* 2005) (*Fig. 4*):

$$PPD = 100 - 95 \times \exp(-0.03353 \times PMV^4 - 0.2179 \times PMV^2). \quad (2)$$

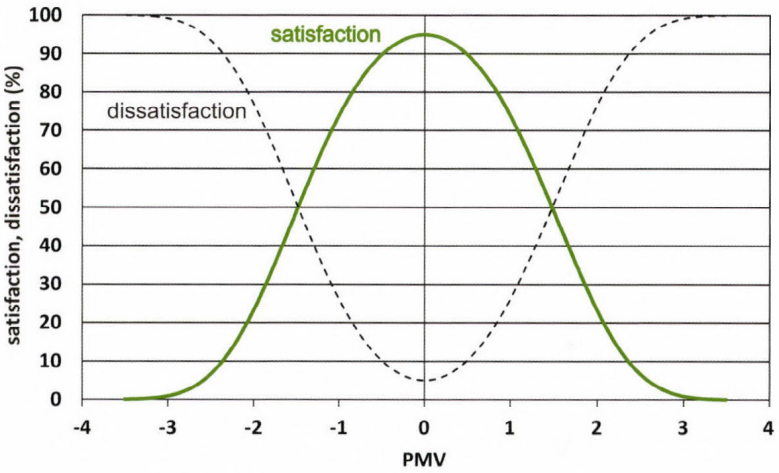

Fig. 4. Relationship between PMV and satisfaction-dissatisfaction with thermal conditions (based on *ASHRAE,* 2004; *ISO,* 2005).

In the derivation of the rating scores we utilized Eq. (2) and assumed that the TCI scores as a function of PET should decrease in the same way as the satisfaction with the thermal environment characterized by PMV declines. Our initial value was 0 PMV related to neutral thermal sensation, which was considered equivalent to the median value (20.6 °C) of the neutral PET category values (18.1–23.0 °C). Towards cold or warm discomfort conditions, decline of satisfaction associated with one-hundredth continuous PMV change was corresponded to decrease of TCI rating score associated with one-tenth PET change. Therefore, we obtained rating scores for all decimal PET values.

In this study, we utilized the widely used PET thermal sensation categories applicable in Western and Central European climatic conditions (*Fig. 2*), and these ranges were rated in case of the selected cities. All categories were characterized by an above derived rating score belonging to the median values of each PET categories. Thus, extreme cold conditions have lower rating scores

than those of the warm extremities, because PET covers a larger range towards cold direction (*Table 4; Fig. 5*).

The above rating system was applied in the rating of the ten-day averages of both thermal comfort sub-indices in TCI.

Table 4. Rating system of PET-based sub-indices (CId, CIa) in the modified TCI (neutral PET category is marked with green)

PET categories (°C)	Median of PET categories (°C)	Rating score
35.1 – 41.0	38.1	1.9
29.1 – 35.0	32.1	3.5
23.1 – 29.0	26.1	4.7
18.1 – 23.0	20.6	5.0
13.1 – 18.0	15.6	4.7
8.1 – 13.0	10.6	3.9
4.1 – 8.0	6.1	2.8
0.1 – 4.0	2.1	1.6
–10.0 – 0.0	–5.0	0.3

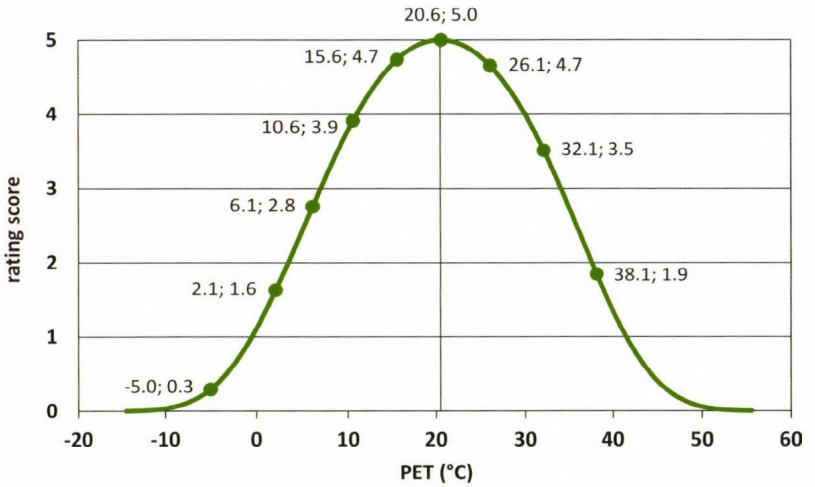

Fig. 5. Medians of PET thermal sensation categories (°C) and their obtained rating scores.

4. *Application of modified TCI in case of European examples*

4.1. Annual variation of ten-day TCI

In the following, the annual variations of the modified TCI and its sub-indices are analyzed in the selected cities. In *Fig. 6*, the annual cycle of the ten-day TCI is presented. In all cities, bimodal type of distribution (see *Fig. 1*) was obtained, that is the most pleasant climate in terms of sightseeing activities in spring and autumn, while in summer, the climatic conditions are rather unfavorable. There are excellent climatic conditions (TCI > 80) in several ten-day intervals of spring and autumn, while in summer more unpleasant but still very good (70 < TCI < 80) conditions prevail. However, in the last decade of July and in early August, TCI often falls below 70 (except Siófok) but it still refers to good conditions. In Thessaloniki, this can be observed as early as mid-June and it lasts till mid-August.

During the winter season, generally unfavorable and marginal conditions (30 < TCI < 50) occur. From the last ten days of February, the climatic conditions are getting acceptable (TCI > 50), which lasts until the end of November or early December. It is remarkable that the conditions of Thessaloniki are suitable for sightseeing almost all winter (TCI > 60) (*Fig. 6*).

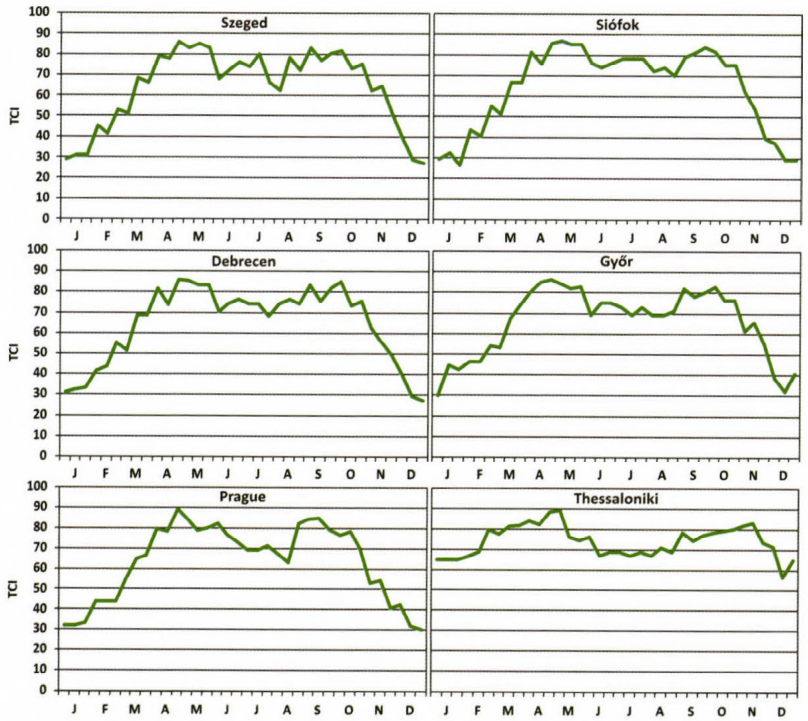

Fig. 6. Annual cycle of the modified ten-day TCI rating scores.

In order to analyze the differences between the cities and their possible causes in details, it is also necessary to examine the contribution of each sub-indices to the overall value of TCI (*Fig. 7*). It is obvious that the daily maximum PET sub-index (CId) is mainly responsible for the bimodal structure of TCI, because in the afternoon hours of summer ten-day intervals, when usually the maximum PET occurs, the prevailing heat stress (slight to strong stress conditions in *Fig. 2*) greatly reduces the rating scores in all cities, particularly in Thessaloniki. In summer and autumn, however, the average maximum values are closer to the comfort zone resulting higher rating scores. Furthermore, CId causes the plesant climate in winter in the Greek city (*Fig. 7*). In early August, a setback in CId in Szeged occurs, which is equal to the CId score of Thessaloniki. Therefore, overall TCI (62.2) barely indicates good climate in Szeged, and this warm load can particularly adversely affect the outdoor activities. It is interesting to note that the Greek city has somewhat higher TCI (66.6) in early August, which is caused by the higher average sunshine duration and lower precipitation conditions; however, the strong warm stress can reduce the comfort level of tourists to such an extent there, that this presumably cannot be fully compensated by the pleasant effects of sun and lack of rain.

The daily average PET (CIa) substantially contributes to TCI only from March to November in Hungary and Prague, while in the summer decades (in the Czech capital only in mid-summer) it falls into the comfort zone providing maximum score. In Thessaloniki, this is limited only to the second and third ten-day intervals of May, while in summer this sub-index indicates slight heat stress. However, CIa has significant effect also in the other periods, because it does not indicate such a level of cold stress conditions there as in the other cities (*Fig. 7*).

From May to August, relatively significant precipitation amount (R) is detected in terms of the ten-day averages in Hungary and Prague, which reduces tourism climatic conditions according to its rating system. Therefore, the contribution of precipitation is less in summer than in the other periods. Thus, in addition to CId, precipitation is also responsible for the bimodal structure shown in *Fig. 6*, even though it has smaller effect than CId because of its lower weight. Thessaloniki has very uneven distribution of rainfall, nevertheless, except in winter, less average precipitation can be detected compared to the other places, therefore it does not influence significantly the outdoor activities in most part of the year as shown in *Fig. 7*.

TCI score is increased the most obviously in summer and the least in winter by the sunshine (S). It should be noted that lower sunshine in Prague can affect adversely, while more hours of sunshine in the Greek city can influence favorably the attractiveness of the place. Significant differences cannot be explored in the averages of wind speed (W) during the year. Their rating scores are somewhat smaller in summer, but there are not any significant monthly or seasonal characteristics and differences between the cities (*Fig. 7*).

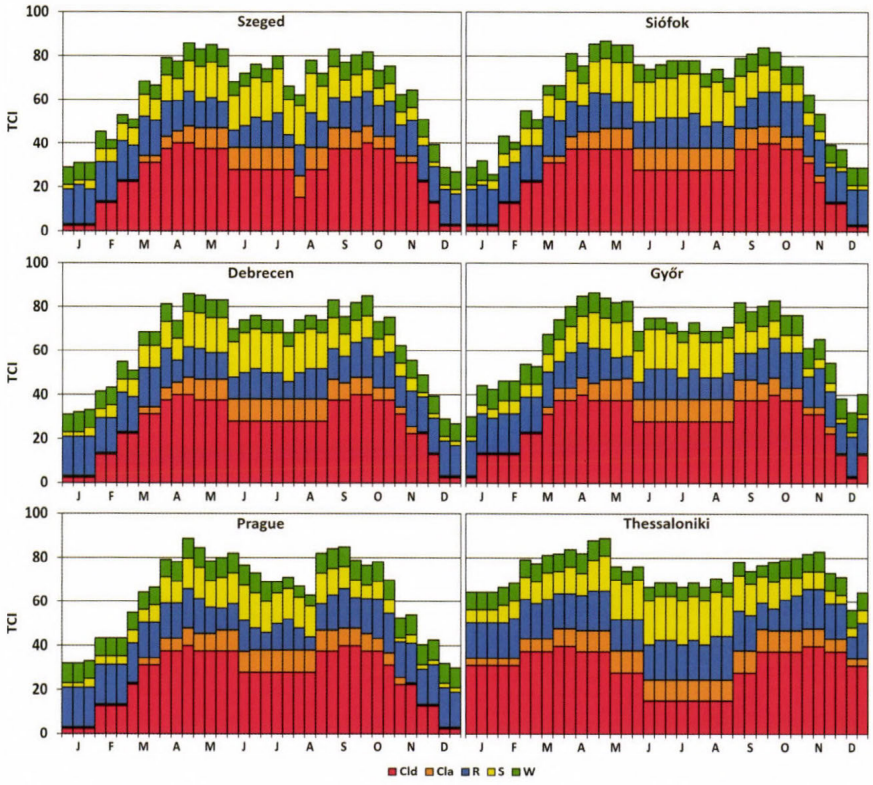

Fig. 7. Ten-day TCI sub-index rating scores (CId: daily maximum PET, CIa: daily mean PET, R: daily precipitation, S: daily sunshine duration, W: daily average wind speed).

4.2. Frequencies of TCI classes per ten-day intervals and seasonality

We have highlighted three distinctive threshold values of TCI (40, 60, 80), and the annual cycle of the average number of days (frequency) per ten-day interval above these thresholds was also investigated. As between the Hungarian cities there are not significant differences, the results are presented in case of Szeged, Prague, and Thessaloniki (*Fig. 8*). Climate is considered to be at least marginal/acceptable, good, and very good in terms of tourism above 40, 60, and 80, respectively.

In Szeged and Prague, all days are at least marginal (TCI > 40) from March to November, while this is valid for the whole year in Thessaloniki. In the distribution of the number of climatologically good days (TCI > 60), a bimodal structure can be recognized, particularly in Szeged. The Greek city has at least good days relatively uniformly throughout the whole year. The distribution of excellent days (TCI > 80) has some interesting characteristics, especially

regarding the time of occurence. Bimodal structure remains in all three places, but while excellent days also occur already from the end of winter until the end of autumn in the Greek city, this starts later and ends earlier in Szeged and Prague. It is remarkable that in the shoulder seasons, one more excellent days can be expected in Prague and Thessaloniki than in the Hungarian city. In the summer period, decline in the number of excellent days can be observed in all cities, but there are significant differences in their temporal occurences. For example, in Thessaloniki, it decreases quickly in spring and reappears only in early autumn, while in Szeged some excellent days occur also in summer. However, in Prague, these rather unpleasant conditions are limited to a very short period in summer: excellent days can be expected even in June and already at the end of summer (*Fig. 8*).

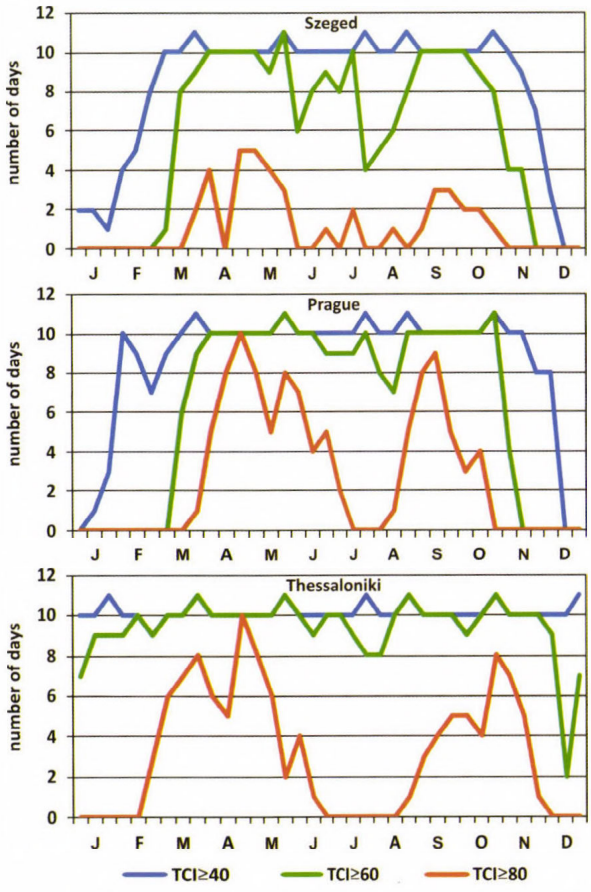

Fig. 8. Average number of days per ten-day interval above different TCI thresholds. At least marginal/acceptable, good, and excellent days are defined as having a TCI above 40, 60, and 80, respectively.

Fig. 9 illustrates the average relative frequencies of all TCI classes (see in *Table 3*) per ten-day interval resulted by the ratio of the average number of days belonging to a given class in a given ten-day interval and the number of days of that unit. According to *Fig. 9*, it can be definitely concluded that the best tourism climatic conditions in terms of the whole year can be observed in Thessaloniki, and the unpleasant climatic conditions occur most commonly in Szeged. In terms of ideal conditions, they appear the least frequently in Szeged and only in some periods of spring. In December and January, very and extremely unfavorable conditions can be often observed there. It should be noted that in summer acceptable and marginal conditions also appear in Szeged to a great extent besides the good categories, which indicates the frequent occurence of warm stress there. It can also be clearly detected that Thessaloniki has the most stable conditions in the whole year without significant diversities: there are almost only good, very good, and excellent days (*Fig. 9*).

The above findings and charts can be associated with the seasonality in tourism, which is one of the most worrisome yet least understood facets of the tourism industry (*Jang,* 2004). We used the "seasonality ratio" (SR), a simple indicator to measure the seasonality in tourism. SR expresses seasonality in a single value, therefore, it is easy to use in tourism climatology. It was initially defined in relation to the ratio of tourist flows (*Yacoumis,* 1980), and the concept was then applied in the context to climate resources characterized by TCI. It is calculated by simply dividing the mean number of good days (TCI > 60) per month by the number of good days in the month with maximum good days (the „best" month) (*Perch-Nielsen et al.,* 2010). The lower the value, the stronger the seasonality, while value 1 indicates equal distribution of good days across all months. We applied this concept in ten-day resolution. SR illustrated in *Fig. 9* indicates approximately moderate seasonality in Prague (SR=0.56) and a slightly higher seasonality in Szeged (SR=0.52) due to their winter and summer conditions. However, Thessaloniki is essentially free of seasonality (SR=0.85), therefore, its SR also confirms that this city offers relatively stable climatic conditions throughout the year.

5. Discussion and conclusions

The applied modifications of Tourism Climatic Index are an initial but significant step towards developing the index for use in Central European climatic conditions. By integrating the PET index into TCI, the thermal comfort sub-indices of TCI are based on more advanced knowledge of bioclimatology than in case of the original index. During the development of the rating system of PET, objective and international standards related to the evaluation of thermal environment were utilized. We assumed that the standardized relationship between the heat sensation of large number of persons evoked by thermal

environment, and their resulting satisfaction with the environment may be appropriate for the rating of the thermal environment of the tourists characterized by PET. The rating system of PET was derived based on this relationship, and the PET thermal sensation ranges used in Western and Central European climatic conditions were applied. By using ten-day averages instead of monthly ones, the climatic conditions can be described suiting better to tourists' length of stay during sightseeing.

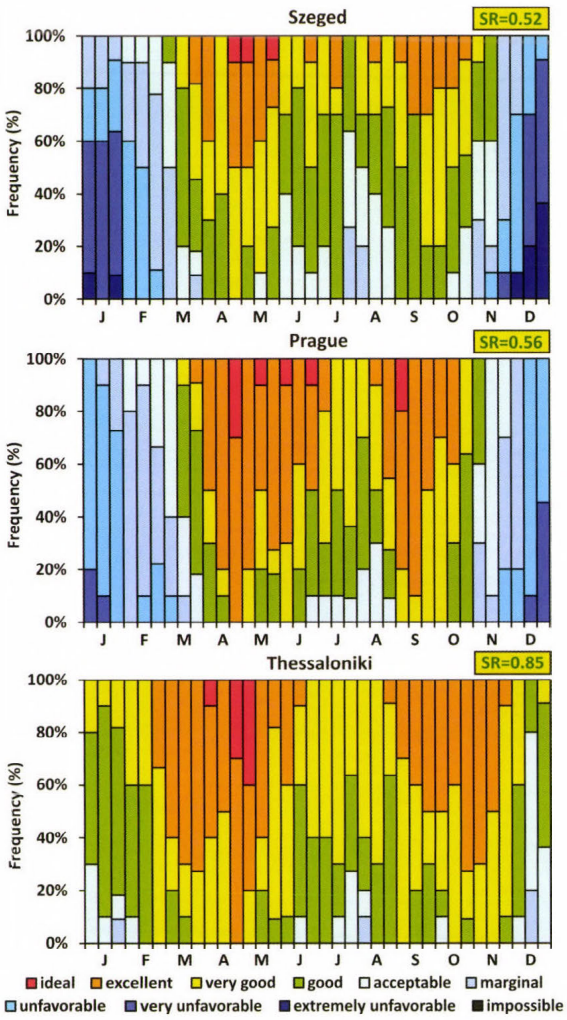

Fig. 9. Average relative frequencies of TCI categories per ten-day interval (see *Table 3* for details). SR indicates the "seasonality ratio".

Our results clearly show the optimal or even unfavorable periods for outdoor (sightseeing) tourism activities in a given place or the comparability of places in a given period. According to the bimodal structure of TCI, summer period has slightly less favorable climatic conditions in all six investigated cities mainly due to the heat load in the afternoon hours, therefore, the shoulder seasons may be the best times for sightseeing. Unlike the other places, in Thessaloniki, winter can also offer suitable climatic conditions. Between the four Hungarian cities only small differences are found, significant and characteristic differences can be detectable only in larger spatial scale. Considering the entire year, Thessaloniki is suitable for sightseeing activities throughout the year without significant seasonality, and it provides pleasant conditions most frequently. Szeged and Prague have higher seasonality and show unfavorable conditions more frequently, but except for winter, these cities are also appropriate for outdoor activities without any doubt, though in Szeged (moreover slightly in Prague, too) warm stress often can impair the level of thermal comfort and well-being of tourists in summer.

It should be noted that it is not sufficient to consider only the overall TCI itself, but it is desirable to analyze individually the contribution of all sub-indices. As an example, Thessaloniki has only a slightly less favorable conditions in summer according to its overall TCI, but if considering each sub-indices, PET sub-indices indicate worse thermal stress conditions by 1–2 categories compared to the other cities, which has a substantial negative impact on the comfort level and well-being of tourists. Presumably, these discomfort conditions cannot be fully compensated by the pleasant (physical-aesthetic) effects of more sunhine and less precipitation there.

During the analysis, basically three drawbacks of the index were identified which would, therefore, need to be changed in order to reflect more accurately and realistically the tourism climatic conditions. Firstly, the precipitation sub-index – particularly in case of convective rainfall – substantially distorts the value of TCI in some ten-day intervals in the calculation of the many-year and ten-day averages, therefore it has such a low rating score compared to other intervals that it rates too unfavorably and unrealistically the climatic conditions. Moreover, such heavy but short rainfalls usually do not have a great effect from a tourist perspective. Some annual differences in rating scores of precipitation can be noticed due to the definite maximum amount in summer and minimum in winter. Nevertheless, if possible, it would be worth changing the applied precipitation variable and its rating system.

Secondly, in the structure of the original TCI, wind speed is rated by means of different scales depending on the value of average maximum temperature and wind speed (as seen in *Table 2*). In case of very cold conditions and high wind speeds, a wind chill rating system has to be used but its rating scores downgrade significantly the relevant ten-day intervals compared to the others. We used this original rating system in this study, but it was developed mainly according to the

thermal effects of wind, which is already expressed by PET in our study, therefore, rather the physical (mechanical) effects of wind should be taken into account in a modified and simplified rating system.

Finally, it would be reasonable to exclude the night hours from the study currently covering the whole day due to the negligible tourist activities at night and to use only the daytime periods, for example the hours between the average sunrise and sunset. Nevertheless, as after sunset the tourist activities often remain significant for a few hours, particularly in summer, this period after sunset would worth being investigated separately.

Our further analysis will be directed to the application of new PET thermal sensation ranges according to an outdoor field survey revealing subjective estimations of thermal environment carried out in Szeged, south Hungary (*Kántor et al.*, 2012). As it is expected, it will provide information on the differences in bioclimatic and tourism climatic conditions of European places for travellers visiting these places but living in south Hungary, therefore accustomed to the thermal conditions prevailing there. By means of the ranges reflecting the thermal sensation of the south Hungarian people, we can compare the results based on the original and new ranges.

References

Amelung, B. and *Viner, D.*, 2006: Mediterranean tourism: exploring the future with the tourism climatic index. *J. Sustainable Tour. 14,* 349–366.

ASHRAE, 1972: Handbook of fundamentals. American Society of Heating, Refrigerating and Air-Conditioning Engineers, Inc., New York

ASHRAE, 2004: Thermal environmental conditions for human occupancy. ASHRAE Standard 55-2004. American Society of Heating, Refrigerating and Air-Conditioning Engineers, Inc., New York

De Freitas, C.R., 2003: Tourism climatology: evaluating environmental information for decision making and business planning in the recreation and tourism sector. *Int. J. Biometeorol. 48,* 45–54.

De Freitas, C.R., Scott, D. and *McBoyle, G.*, 2008: A second generation climate index for tourism (CIT): specification and verification. *Int. J. Biometeorol. 52,* 399–407.

Fanger, P.O., 1972: *Thermal Comfort*. McGraw Hill Book Co., New York

Houghten, F.C. and *Yaglou, C.P.*, 1923: Determining equal comfort lines. *J. Am. Soc. Heat. Vent. Eng. 29,* 165–176.

Höppe, P., 1999: The physiological equivalent temperature – an universal index for the biometeorological assessment of the thermal environment. *Int. J. Biometeorol. 43,* 71–75.

ISO, 2005: Ergonomics of the thermal environment – Analytical determination and interpretation of thermal comfort using calculation of the PMV and PPD indices and local thermal comfort criteria. ISO 7730:2005(E), ISO copyright office, Geneva

Jang, S., 2004: Mitigating tourism seasonality: A quantitative approach. *Ann. Tour. Res. 31,* 819–836.

Kántor, N., Égerházi, L. and *Unger J.*, 2012: Subjective estimation of thermal environment in recreational urban spaces – Part 1: investigations in Szeged, Hungary. *Int. J. Biometeorol. 56,* 1075–1088.

KSH, 2012: Magyarország számokban 2011. Központi Statisztikai Hivatal, Budapest. (In Hungarian)

Matzarakis, A. and *Mayer, H.,* 1996: Another kind of environmental stress: thermal stress. *WHO Newsletter 18,* 7–10.

Matzarakis, A., 2006: Weather- and climate-related information for tourism. *Tourism Hospit. Plann. Dev. 3,* 99–115.

Matzarakis, A., Rutz, F. and *Mayer, H.,* 2007: Modelling radiation fluxes in simple and complex environments – application of the RayMan model. *Int. J. Biometeorol. 51,* 323–334.

Mayer, H. and *Höppe, P.,* 1987: Thermal comfort of man in different urban environments. *Theor. Appl. Climatol. 38,* 43–49.

Mieczkowski, Z.T., 1985: The tourism climatic index: a method of evaluating world climates for tourism. *Can. Geogr. 29,* 220–233.

Németh, Á., 2013: Estimation of tourism climate in the Lake Balaton Region, Hungary. *J. Environ. Geography 6,* 49–55.

Perch-Nielsen, S.L., Amelung, B. and *Knutti, R.,* 2010: Future climate resources for tourism in Europe based on the daily Tourism Climatic Index. *Climatic Change 103,* 363–381.

Scott, D. and *McBoyle, G.,* 2001: Using a 'tourism climate index' to examine the implications of climate change for climate as a natural resource for tourism. In (*Matzarakis, A.* and *de Freitas, C.R* (Eds.)) Proceedings of the First International Workshop on Climate, Tourism and Recreation, International Society of Biometeorology, Commission on Climate, Tourism and Recreation, Halkidi, Greece, 5–10 October 2001, 69–88.

Scott, D., McBoyle, G. and *Schwartzentruber, M.,* 2004: Climate change and the distribution of climatic resources for tourism in North America. *Climate Res. 27,* 105–117.

Scott, D., Gössling, S. and *de Freitas, C.R.,* 2008: Preferred climates for tourism: case studies from Canada, New Zealand and Sweden. *Climate Res. 38,* 61–73.

Steadman, R.G., 1979: The assessment of sultriness. Part I: A temperature-humidity index based on human physiology and clothing Science. *J. Appl. Meteorol. 18,* 861–873.

VDI, 1998: Methods for the human-biometeorological assessment of climate and air hygiene for urban and regional planning. Part I: Climate. VDI 3787, Part 2. Beuth, Berlin

Yacoumis, J., 1980: Tackling seasonality: The case of Sri Lanka. *Int. J. Tourism Manag. 1,* 84–98.

Yu, G., Schwartz, Z. and *Walsh, J.E.,* 2009: A weather-resolving index for assessing the impact of climate change on tourism related climate resources. *Climatic Change 95,* 551–573.

Zaninović, K., Srnec, L., Patarčić, M., Perčec Tadić, M., Mika, J. and *Németh, Á.,* 2010: Influence of climate change on summer tourism potential in the Pannonian basin. In (*Matzarakis, A., Mayer, H.* and *Chmielewski, F-M.* (Eds.)) Proceedings of the 7th Conference on Biometeorology, 12–14 April 2010, Freiburg, Germany. *Berichte des Meteorologischen Instituts der Albert-Ludwigs-Universität Freiburg 20,* 336–341.

IDŐJÁRÁS

Quarterly Journal of the Hungarian Meteorological Service
Vol. 118, No. 2, April – June, 2014, pp. 167–191

Long-term trend of deposition of atmospheric sulfur and nitrogen compounds in Hungary

Andrea Móring*[1,2,3] and **László Horváth**[4]

[1]*University of Edinburgh*
The King's Buildings, Crew Building, West Mains Road,
Edinburgh, EH9 3JN, United Kingdom

[2]*Centre for Ecology and Hydrology, United Kingdom*
Bush Estate, Midlothian, Penicuik, EH26 0Q, United Kingdom

[3]*Hungarian Meteorological Service*
Kitaibel P. u. 1, H-1024 Budapest, Hungary

[4]*Hungarian Meteorological Service*
Gilice tér 39, H-1181 Budapest, Hungary

Corresponding author E-mail: a.moring@sms.ed.ac.uk

(Manuscript received in final form April 11, 2014)

Abstract—Acidification caused serious environmental problems over Europe in the 70's and 80's. The signs of the phenomenon were observed also in Hungary. However, a comprehensive assessment of acidic deposition on long term has not been carried out yet. Therefore, the purpose of this study is to assess the degree of this process and to investigate its long-term change in Hungary based on deposition time series for oxidized sulfur, oxidized nitrogen, and reduced nitrogen compounds. To achieve our goal, we used existing results of atmospheric chemistry transport models, and precipitation chemistry as well as background air pollution measurements at the Hungarian K-puszta site. Comparing the results with national emission datasets, we also made an attempt to interpret the changes in depositions. According to our time series (oxidized sulfur: 1880–2011, oxidized nitrogen: 1982–2012, reduced nitrogen: 1981–2012), the effect of acidification was most likely to intensify before 1980. Since then, the phenomenon presumably has been weakening gradually. In the case of oxidized sulfur and nitrogen compounds, transboundary transport has to be considered while comparing them to depositions. On the other hand, the impact of Hungarian industrial recession as well as the improvement of emission abatement techniques and national emission controlling measures can be observed not just on the emissions, but depositions as well. Moreover, we found that the atmospheric concentration and subsequent deposition of ammonia is strongly affected by the atmospheric concentration of sulfur dioxide, which highlights the need for further refinement of the estimation method for yearly dry deposition of ammonia.

Keywords: acidic deposition, long-term, oxidized nitrogen, oxidized sulfur, reduced nitrogen, ammonia, atmospheric concentration, emission, emission reduction.

1. Introduction

The problem of acidification got wider public and scientific attention at first in the beginning of the 70's, when the reason for the serious damage of Scandinavian lakes and German forests was identified: the decreasing pH of freshwaters and soil (*Almer et al.*, 1974; *Sakamoto et al.*, 1986). It was found that the phenomena had been caused by the excessive emission and subsequent deposition of oxidized sulfur (sulfur dioxide, SO_2 and sulfate, SO_4^{2-}) and oxidized nitrogen compounds (nitric acid, HNO_3, nitrogen oxides, NO_x and nitrate, NO_3^-) (see the quoted references in *Galloway*, 1989). Since then, the problem has been considerably mitigated over Europe, owing to a series of emission control measures (*Grennfelt* and *Hov*, 2005). However, it has been a more and more serious environmental issue in the developing countries of Asia, especially in China (*Duan et al.*, 2013).

The process that leads to acidification consists of three main steps: i) emission of acidifying components or their precursors, ii) their atmospheric transport, simultaneous chemical conversion, phase transition to particles, iii) deposition to the surface. The main source for oxidized sulfur as well as nitrogen compounds is anthropogenic. Most of the oxidized sulfur compounds are emitted during the combustion of fossil fuels (*Seinfeld* and *Pandis*, 2006). These usually contain a certain amount of sulfur, which is oxidized to SO_2 during burning. The primary emission sectors of the oxidized nitrogen compounds are transportation and energy industry (see the same reference). In both cases, nitrogen content of the air is oxidized mainly to nitric oxide (NO) and in smaller amount to nitrogen dioxide (NO_2) at the high burning temperature.

In addition, reduced nitrogen compounds (ammonia, NH_3, and ammonium, NH_4^+) are considered as additional exacerbating factors for acidification. In the soil during nitrification, NH_4^+ ions are oxidized while two equivalent hydrogen-ions (H^+) are produced (*Raven*, 1985). In freshwater ecosystems, algae and macrophyte species release equivalent H^+ when NH_4^+ is consumed (*Goldman* and *Brewer*, 1980). Therefore, further sources must be considered for acidifying components. The largest emission sector of reduced nitrogen compounds is agriculture, releasing gaseous NH_3 to the atmosphere. The primarily source of NH_3 is the breakdown of urea in livestock excreta, but a similar process takes place in the case of urea- and ammonium-based fertilizers as well.

There are two ways for an atmospheric compound to get back to the surface from the atmosphere: by wet or dry deposition. Wet deposition occurs when the compound is washed out from the atmosphere by being dissolved in precipitation, whilst during dry deposition, the substance is transported to the surface by the turbulent flux.

In the atmosphere, SO_2 and NO_x compounds are further oxidized to sulfurous acid (H_2SO_3) and sulfuric acid (H_2SO_4), as well as nitrous acid

(HONO) and nitric acid (HNO_3), respectively. The produced acidic components may be neutralized by dissolved NH_3, forming aerosol particles. These usually act as condensation nuclei; therefore, they can be easily washed out of the atmosphere by precipitation. In addition, during droplet growing as well as rainfall, acidic species and gaseous SO_2 and NH_3 may also dissolve to the droplets. Dry deposition of acidifying compounds is possible as gas molecules as well as in the form of aerosol particles. Deposition of NH_3 and SO_2 in this way is closely related and largely dependent on the pH of the surface wetness (*Flechard et al.*, 1999).

The distance, from the source the atmospheric trace compounds can be transported to, besides meteorological conditions, is basically determined by their atmospheric lifetime. Calculating with a lifetime of 2 days (172 800 s) for SO_2 (*Seinfeld* and *Pandis*, 2006) and an average wind speed of 3 m s^{-1} at 2 m height, the result is more than 500 km. The lifetime of NO_x as well as NO_3^-, SO_4^{2-}, and NH_4^+ aerosols usually ranges also from a few days to weeks, which raises the problem of transboundary air pollution. On the other hand, as a result of their high solubility and reactivity, NH_3 and HNO_3, depending on the surface characteristics and micrometeorological conditions, especially at higher air temperature and lower humidity when dissociation of ammonium nitrate particles into gases is dominant (*Stelson* and *Seinfeld*, 1982), can have a lifetime of a few hours, causing local rather than regional problems.

Beside the damage of surface water and forest ecosystems, high concentration of acidic components can have a severe impact also on human health through inhaling the respirable, fine fraction of formed aerosols (*Pope et al.*, 2002). In addition, in the 70's and 80's, erosion of buildings and statues by "acid rain" was reported (*Lipfert*, 1987). Despite serious acidification caused mainly by excessive emission of SO_2 (*Johnson* and *Reuss*, 1984) has been largely mitigated over Europe, the environmental effect of reactive nitrogen compounds (N_r), such as NH_3, HNO_3, and NO_x, has been still in the focus of scientific research projects (e.g., GRAMINAE, NitroEurope, ENA, ÉCLAIRE). *Sutton et al.* (2011) identified five key threats related to excessive N_r emissions: water quality, air quality, greenhouse balance due to the aerosol particles, ecosystems and biodiversity, and soil quality.

Signs of acidification occurred also in the country: yield reduction of crops, potential forest damage, especially in synergy with other biotic factors, corrosion of historic monuments, and deformation of building ornaments made of limestone were reported (*Várallyay et al.*, 1986; *OKTH/MTA*, 1987). Since then, the impact of acidic compounds, similarly to the whole European region, has been weakening in the country.

Although *Horváth et al.* (2009) published time series of measured atmospheric concentration and wet deposition of NH_3 and NH_4^+ for the period of 1981–2005 for a Hungarian site, for the country a comprehensive assessment of acidic deposition on long term has not been carried out yet. Therefore, the

purpose of this study is to assess the degree of this process and to investigate its long-term change in Hungary based on deposition time series for oxidized sulfur, oxidized nitrogen, and reduced nitrogen compounds. The data sets were compiled from existing atmospheric chemistry transport model results and air concentration as well as precipitation chemistry data measured at the Hungarian K-puszta site.

2. *Methods and data*

2.1. Oxidized sulfur compounds

The long-term deposition data set for oxidized sulfur compounds were compiled from existing results from different versions of the atmospheric chemistry transport model (ACTM) ran by the European Monitoring and Evaluation Programme (EMEP) under the Convention on Long-range Transboundary Air Pollution (CLRTAP). An ACTM calculates atmospheric concentration and deposition fields for a given time and grid from predefined emission fields. Driven by a meteorological model it is capable of simulating the horizontal and vertical transfer of atmospheric trace compounds, as well as the mixing of the different pollutants and the possible chemical reactions between them.

EMEP is a policy driven program for international co-operation to solve transboundary air pollution issues. The model results from their ACTM are used by policy makers Europe-wide. EMEP consists of five Centers and four Task Forces. Among them, the Meteorological Synthesizing Centre-West (MSC-W) is responsible for the modeling of acidifying and eutrophying air pollutants, photochemical oxidants, and particulate matter.

The first part of our deposition data set, for the period 1880–1980, originates from a model experiment (*Mylona*, 1992) for 1880–1991 with an early version of the EMEP model (*Sandnes* and *Styve*, 1992). *Mylona* determined the required SO_2 emission fields based on historical energy and industry statistics. The effect of meteorological variability was disregarded in the experiment, meteorological data for 1991 were used for every year. Depositions were simulated over the 150×150 km^2 EMEP grid, for every fifth year.

From the year 1980 we obtained model results, derived from later versions of the EMEP model, from the open database of MSC-W (*EMEP/MSC-W*, 2013). The main differences compared to the version used by *Mylona* are that these operate on a higher resolution grid (50×50 km^2), and in every year the meteorological data for the given year were fed to the model (for detailed description of the different model versions see the references at *EMEP/MSC-W*, 2013). The data to the second part of our deposition time series, for the period 1980–2011, are originating from the following model versions:

- version rv4.4: for the years 1990, 2000–2011,
- version rv2.5: for the years 1995–1999,
- version rv2.1: 1980, 1985.

During personal communication, Sophia Mylona provided us her model results for the four 150×150 km^2 grid cells in which the fraction of Hungarian area are the largest (the shaded cells in *Fig. 1*). To keep the consistency of the deposition data set for the whole period (1880–2011), we downloaded the gridded version of the model results from the MSC-W database, and then selected the 36 pieces of 50×50 km^2 grid cells covered by the four grid cells provided by Sophia Mylona. All the deposition data were given as flux; therefore, to get the total deposited sulfur over the grid cells, we multiplied the fluxes by the corresponding grid area. According to *Kugler et al.* (2014), the background air pollution in Hungary can be considered homogenous. Therefore, to get country scale depositions, we up-scaled the grid depositions (for 4×150×150=90,000 km^2) for the area of Hungary (93,036 km^2).

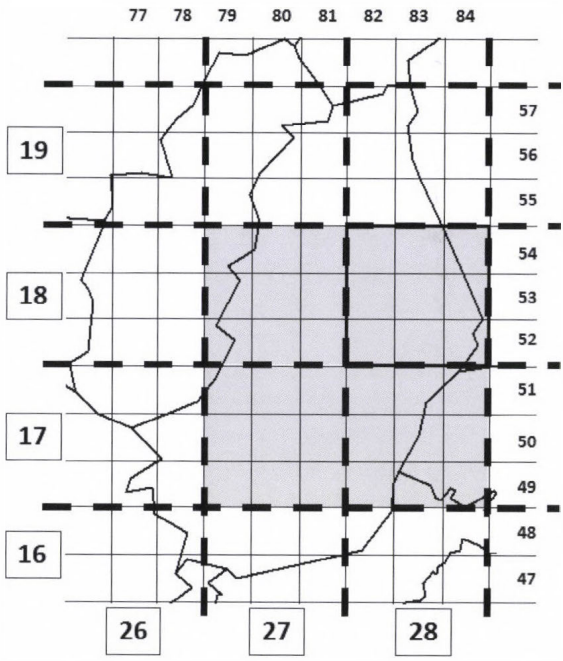

Fig. 1. Hungary on the new EMEP grid with 50×50 km^2 resolution (solid lines), and on the old EMEP grid with 150×150 km^2 resolution (dashed lines). Plain numbers and numbers in boxes indicate the EMEP coordinates for the new and the old grid, respectively. For our sulfur deposition calculations, the shaded grid cells were used from both grids.

2.2. *Oxidized and reduced nitrogen compounds*

The longest available Hungarian atmospheric chemistry data set for oxidized and reduced nitrogen compounds can be obtained from the measurement data base of the Hungarian precipitation chemistry and background air pollution monitoring network maintained by the Hungarian Meteorological Service (HMS). Among the stations of the network, K-puszta has the longest measurement time series; it has been operating since 1974. Therefore, we choose it as the base of our further investigations.

K-puszta (46°58' N, 19°33' E, 136 m a.s.l.) is situated on the Hungarian Great Plain, in the clearing of a mixed coniferous-deciduous forest, far from main anthropogenic emission sources. The site is a part of the network of the Global Atmospheric Watch (GAW) and the EMEP. The starting year of the available data sets for atmospheric concentration and rainwater chemistry (including also precipitation sums) can be seen in *Table 1.*

Table 1. Starting year of the measurements of concentration in air and in precipitation of the depositing nitrogen compounds at K-Puszta station

	Oxidized nitrogen compounds	**Reduced nitrogen compounds**
Atmospheric concentrations	NO_2 : 1974	NH_4^+: 1977
	NO_3^- : 1977	NH_3 : 1981
	HNO_3: 1982	
Concentration in the rain water	NO_3^- : 1974	NH_4^+: 1974

As we attempted to assess the country scale deposition of nitrogen compounds on the base of a single station's measurements, we kept the data in the form of fluxes, rather than calculating the total mass of deposited nitrogen over the country. For simplicity's sake, in the following we will refer to only deposition without 'flux'. We calculated the total deposition as a sum of dry and wet deposition. Calculation of dry deposition was carried out by the inferential method using Eq. (1) for both oxidized and reduced N-compounds:

$$F_{dry} = \sum_i F_{dry,i} = \sum_i c_{air,i} v_{d,i} f \,, \tag{1}$$

where

- F_{dry} – total yearly deposition flux of oxidized/reduced nitrogen compounds (g N m^{-2} $year^{-1}$),

- $F_{dry,i}$ – yearly dry deposition of the oxidized/reduced compound i (g N m^{-2} $year^{-1}$),
- $c_{air,i}$ – yearly average air concentrations of the oxidized/reduced nitrogen compound i (μg N m^{-3}),
- $v_{d,i}$ – yearly average dry deposition velocity of the oxidized/reduced nitrogen compound i (cm s^{-1}), and
- f – conversion factor between the different units (3.1536×10^{-1}).

According to its definition (Eq. (2), *Seinfeld* and *Pandis*, 2006), dry deposition velocity is the reciprocal of the sum of the resistances between the atmosphere and the surface. These are the aerodynamic resistance (R_a), the resistance of the quasi-laminar layer (R_b), and the bulk canopy resistance (R_c). Whilst R_a and R_b account for the atmospheric turbulence, R_c expresses for a given trace substance the absorbing or adsorbing capacity of the canopy that covers the surface. Therefore, v_d is a function of the actual micrometeorological conditions, and it strongly depends on the surface characteristics. For our yearly estimations, however, we used constant yearly average deposition velocities, collected from the literature for selected land-cover types.

$$v_d = \frac{1}{R_a + R_b + R_c}. \tag{2}$$

For both oxidized and reduced compounds we gave estimation for dry deposition on grass, and in the case of oxidized compounds, we calculated it also for mixed land-cover types (grass, forest, arable, urban), giving a closer approach for dry deposition on country level. The same could not been carried out for reduced nitrogen compounds due to the relatively rare occurrence of NH_3 and NH_4^+ dry deposition velocity values in the literature. All the applied dry deposition velocities can be seen in *Table 2*. Data for oxidized nitrogen compounds are originating from the deposition velocity inventory compiled by *Marner* (2003). To get the dry deposition velocities for mixed land coverage, we averaged the data for every oxidized compound using the land-cover fractions (*Table 3*) from the CORINE CLC-50 database over Hungary as weights.

The steps of calculation of yearly wet deposition are described in Eqs. (3), (4), and (5). Daily wet deposition of oxidized and reduced nitrogen compounds can be calculated as a product of the amount of daily precipitation (p_i, dm^3 m^{-2} day^{-1}) and the concentrations of NO_3^- and NH_4^+ ions measured in precipitation samples ($c_{aq,i}$, mg N dm^{-3}), respectively. Summed up these for a month (Eq. (3)), one can get the monthly wet deposition ($F_{wet,j}$, mg N m^{-2} $month^{-1}$).

Table 2. Applied yearly average dry deposition velocities for reduced and oxidized nitrogen compounds (latter from the inventory by *Marner* (2003)) for different surface types, their references and - where applicable – their weighted average, as used in our dry deposition calculations for mixed vegetation (for the weights see *Table 3*)

Compound	Deposition velocity (cm s^{-1})				
	Grass	Arable	Forest	Urban	Weighted average
NH_3	0.99 (*Horváth et al.*,2005)	–	–	–	–
NH_4^+	0.087 (*Gallagher et al.*,2002)				
NO_2	0.16 (*Nicholson et al.*, 2001)	0.16 (*Nicholson et al.*, 2001)	0.26 (*Puxbaum and Gregori*, 1998)	0.08 (*Nicholson et al.*, 2001)	0.17
HNO_3	1.39 (*Marner*, 2003)	2.06 (*Marner*, 2003)	7.33 (*Marner*, 2003)	7.33 (*Marner*, 2003)	3.81
NO_3^-	0.15 (*Slinn*, 1982)	0.26 (*Davidson et al.*, 1982)	1.78 (*Ruijgrok et al.*, 1997)	1.78 (*Ruijgrok et al.*, 1997)	0.77

Table 3. Area of the different land cover types over Hungary and their fraction in the total area of the country, used as weights in our dry deposition calculations

	Grasslands		Forest			Arable	Urban
	Semi-natural	Pasture	Deciduous	Mixed	Coniferous		
Area (10^{10} m^2)	0.58	0.39	1.55	0.08	0.16	5.12	1.42
Fraction	10.43%			19.25%		55.05%	15.27%

The variability of the time series derived in this way is influenced by that of the monthly precipitation amount. According to *Horváth* (1978), there is a positive, strong and significant relationship between the monthly amount of precipitation and the monthly wet deposition. Same was true for our datasets (*Fig. 2*). Based on this, we normalized the monthly wet deposition values applying Eq. (4), where a and b are the slope and the intercept of the regression line, respectively (*Fig. 2*), p_j is the monthly precipitation, and $F_{wet,ave}$ is the wet deposition with the long-term average monthly precipitation (for the values of a, b, and $F_{wet,ave}$ see *Table 4*). Finally, to get the yearly wet deposition (F_{wet}, mg N m^{-2} $year^{-1}$), we summed up the normalized monthly values ($F_{wet,j}^{norm}$ mg N m^{-2} $month^{-1}$) for a year (Eq. (5)).

$$F_{wet,j} = \sum_i c_{aq,i} p_i, \tag{3}$$

$$F^{norm}_{wet,j} = F_{wet,ave} \frac{F_{wet,j}}{ap_j + b}, \tag{4}$$

$$F_{wet} = \sum_{j=1}^{12} F^{norm}_{wet,j}. \tag{5}$$

After calculating the total deposition ($F_{total}=F_{wet}+F_{dry}$) for both the oxidized and reduced nitrogen compounds, to get the total nitrogen load we summed up the two total deposition values over grass. To characterize the change in all of the resulted nitrogen time series, we fitted trends to them. The trends with the best fit were determined by applying the Akaike information criterion (AIC, *Sakamoto et al.*, 1986), as a built-in function in the statistical programming language R.

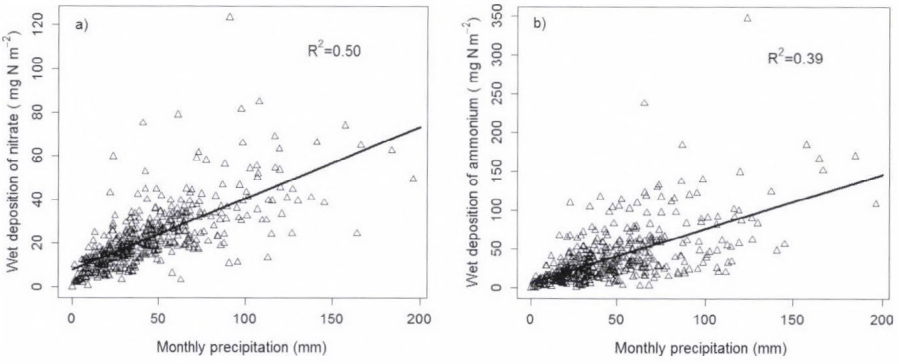

Fig. 2. Regression between monthly precipitation and wet deposition of nitrate (a) and ammonium (b) over the period 1974-2012 at K-puszta. R^2 indicates the square of correlations between the datasets.

Table 4. Parameters of the regression between the monthly precipitation and monthly wet deposition of nitrogen species, where p_{ave} (mm) is the long-term average of the monthly precipitation values, a (mg N dm^{-3} month^{-1}) is the slope, b is the intercept (mg N m^{-2} month^{-1}), and $F_{wet,ave}$ ($a \times p_{ave}+b$) is the wet deposition with the average monthly precipitation (mg N m^{-2} month^{-1})

Ions	p_{ave}	a	b	$F_{wet,ave}$
NH_4^+	44.3	0.70	5.92	36.9
NO_3^-		0.33	7.90	22.4

2.3. Further data sources

During the interpretation of our results, we used further data sources. In the case of oxidized sulfur compounds, we compared the deposition time series to a national emission time series compiled from the historical emission database of A.S.L. & Associates (*Lefohn et al.*, 1999) for the period 1880–1990 and from emissions reported to the EMEP (*CEIP*, 2013) for the period 1990–2011. The emission data obtained from the open database of A.S.L. & Associates (*A.S.L. & Associates*, 1999) are in a good agreement with the emissions published by *Mylona* (1992); however, for illustration purposes the A.S.L. data set is better, as it has a finer, yearly temporal resolution compared to the 5-year resolution of the data set by *Mylona*.

The deposition of oxidized nitrogen species were compared to the national NO_x emissions reported to EMEP that are available in the emission database of EMEP for the period of 1980–2011. In addition, we refined our comparison with data for the total number of cars in Hungary for 1974–2011, from the freely available database (*KSH*, 2013) of the Hungarian Central Statistical Office.

To interpret our results for NH_3 and NH_4^+ depositions, we compiled a national NH_3 emission dataset from *Horváth et al.* (2009) (for 1980–2005) and from the EMEP database (for 2006–2011). As deposition of SO_2 and NH_3 has a strong relationship, for further investigations we calculated also the average yearly SO_2 surface concentrations based on the daily HMS measurements at K-puszta.

3. Results

3.1. Time series of oxidized sulfur compounds

Between 1880 and 1950, deposition of oxidized sulfur compounds over Hungary showed a moderate increase (*Fig. 3*), which was interrupted only by World War II. Over this period, sulfur deposition was mainly under 100 Gg S $year^{-1}$, except in 1940, when it slightly exceeded this limit. From 1950, sulfur deposition was intensifying until it peaked at 381 Gg S $year^{-1}$ in 1980. In the last three decades deposition has been decreasing. Since 2005, the values has been under 100 Gg $year^{-1}$ again.

The emission time series (*Fig. 4*) is very similar to that of the deposition. However, also differences can be noticed between the two time series. In 1880–1950, the increase of emission was not as steady as that of the deposition. Despite it reached its maximum in 1940, there were several other substantial peaks and lows over this period, including a clear minimum after World War II. For this difference more explanations are feasible.

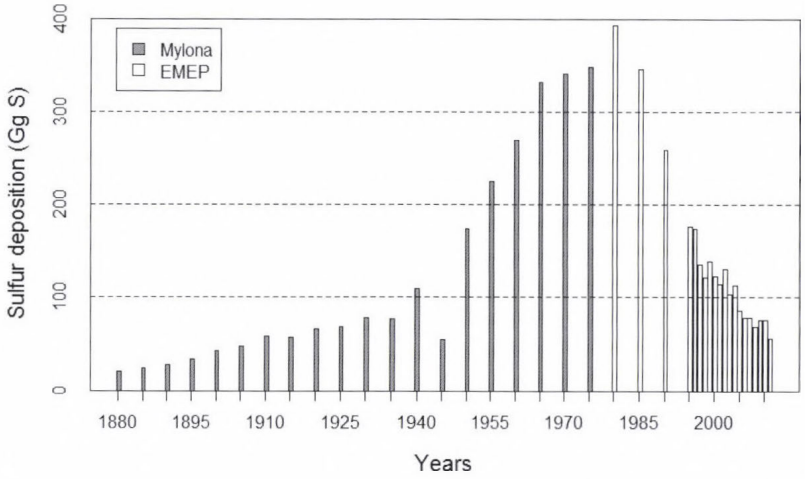

Fig. 3. Sulfur deposition over Hungary between 1880 and 2011 compiled from the two data source: *Mylona* (1992) and the EMEP database (*EMEP/MSC-W*, 2013).

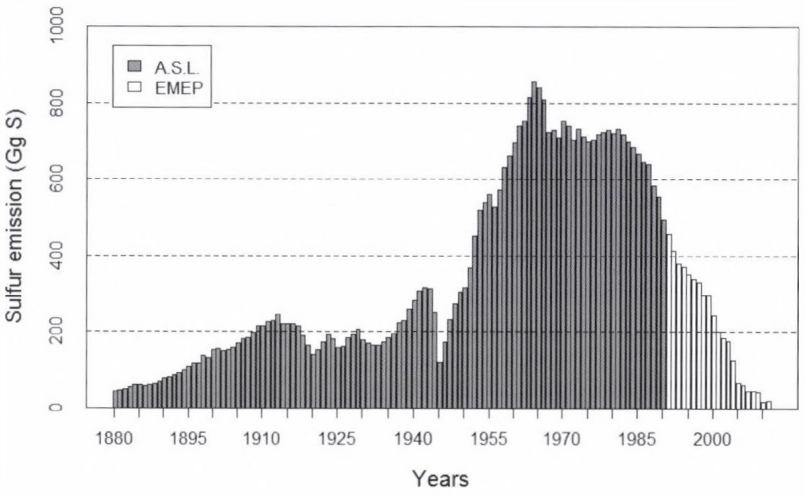

Fig. 4. Sulfur emission in Hungary between 1880 and 2011 compiled from the two data source: *A.S.L. & Associates* (1999) and the EMEP emission database (*CEIP*, 2013).

Firstly, over this period for deposition modeling another emission data set was used. On the other hand, the relationship between emission and deposition of oxidized sulfur compounds on country scale is not linear, as due to their long atmospheric lifetime, their atmospheric transport is transboundary. Consequently, not all of the sulfur emitted in Hungary deposits over the country, and similarly, a part of the deposited sulfur originates from the neighboring countries. As a consequence, even an intense increase in national emission can lead to a more moderate change in national depositions.

Emission reached its absolute maximum in 1964, 16 years earlier than deposition. Same is true for the emission dataset published and used in the model runs by *Mylona* (1992) (not presented here): the most sulfur was emitted in 1960. This could imply that the later maximum in deposition is a result of the imperfect match of the two deposition data sets. However, in the whole deposition time series derived by *Mylona* for 1880–1991, the highest value occurred also in 1980. The difference can be explained only by the above described phenomena of transboundary air-pollution, i.e., the emission tendencies on a larger scale in Europe suppressed the local emission trends. This is supported by the European total emission time series by *Mylona*, that shows an absolute maximum in 1980, at the same time with the highest deposition in Hungary.

It is difficult to qualify the strength of acidification, because it depends, among others, on the buffering capacity of the surface. However, based on the observations – the higher deposition, the stronger the effect of acidification – it can be concluded that during 1950–1980, Hungary was the most exposed to the harmful effects of acidification triggered by the deposition of oxidized sulfur compounds. In the last 3 decades, sulfur emissions has been reducing presumably due to the recession of Hungarian industry as well as the more conscious handling of European industrial emissions as a result of – among other international conventions on air pollution – the 1979 Geneva Convention on Long-range Transboundary Air Pollution. Consequently, the oxidized sulfur deposition has been also decreasing over the last 30 years, possibly leading to gradually weakening acidification.

3.2. Oxidized nitrogen compounds

The wet deposition of oxidized nitrogen compounds (*Fig. 5*) in the period of 1974–2012 ranged between 150 and 350 mg N m^{-2}, except in 1975, when it reached an extreme high value of 446 mg N m^{-2}. Two waves of the tendency can be distinguished: one in 1974–1998 with the highest values during the middle of the 80's, and another from 1998 to 2012 with the largest values in the middle of the last decade. However, the fitted 2nd order polynomial trend shows a steady decline over the whole period (for a summary of our results for nitrogen species see *Table 5*).

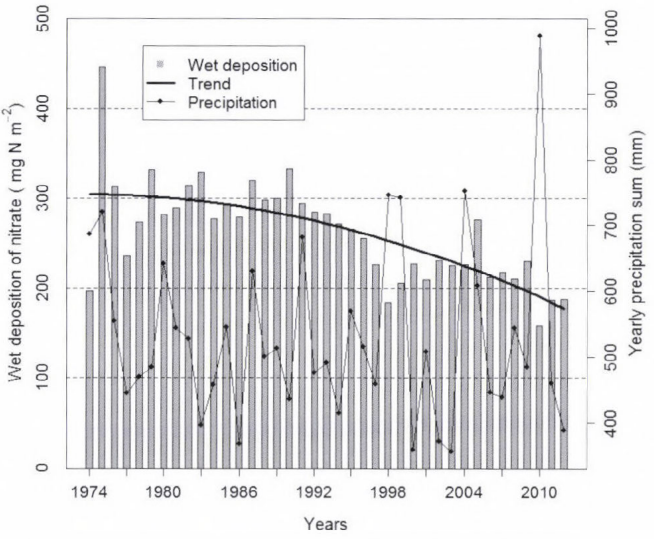

Fig. 5. Wet deposition of oxidized nitrogen compounds between 1974 and 2012 at K-puszta, the best fit line, and the yearly precipitation sum.

Table 5. Summary of our results for the deposition time series of the nitrogen compounds, with their starting year (the last year was 2012 in every case) and the order of the best fit trends

Compounds	**Deposition**	**Beginning of the time series**	**Order of the fitted trend**
Oxidized nitrogen compounds	Wet	1974	2
	Dry[g]	1982	4
	Dry[m]	1982	1
	Total[g]	1982	4
	Total[m]	1982	1
Reduced nitrogen compounds	Wet	1974	3
	Dry[g]	1981	4
	Total[g]	1981	1
Total nitrogen load[g]		1982	1

[g] calculated for grass, [m] calculated for mixed vegetation

For grass the dry deposition ranged from 200 to 500 mg N m^{-2}, whilst for mixed vegetation it varied mostly between 400 mg and 800 N m^{-2}, except in four years (1982, 1983, 1993, and 1994), when deposition was around or over 1,000 N m^{-2} (*Fig. 6*). Despite that the atmospheric concentration of NO_2 (*Fig. 7*) was the highest over the whole period, dry deposition of HNO_3 particles was predominant for both surface types. This is a result of the high reactivity and solubility of HNO_3 and consequently its deposition velocity, that is larger by one order of magnitude compared to those of the other two compounds. This led also to

the above mentioned four peak values in dry deposition for mixed vegetation, as HNO_3 concentrations were relatively high in these years. The higher dry deposition for mixed vegetation compared to grass was caused mostly by the almost three times larger average HNO_3 deposition velocity applied for this surface type.

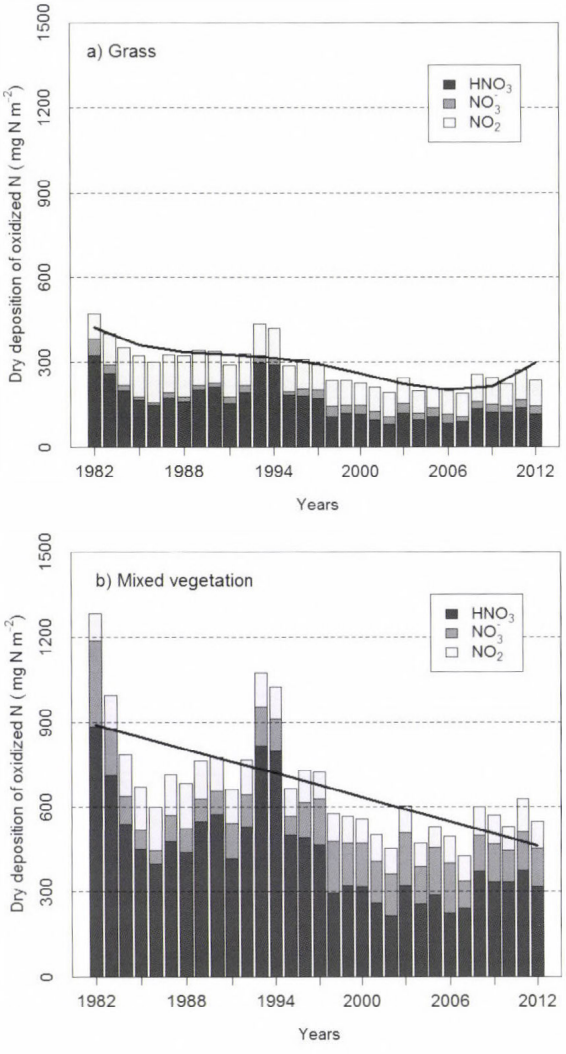

Fig. 6. Dry deposition of oxidized nitrogen compounds over grass (a) and mixed vegetation (b) between 1982 and 2012 at K-puszta, and the best fit lines to the total dry depositions.

In the case of grass, the year-to-year variability was smaller than for mixed vegetation. The fitted 4th order polynomial trend shows a moderate decrease

over most of the period with an increase over the last four years. However, the significance of this rise can be considered low, regarding that the length of the period is quite short and the depositions over the four year do not change consistently. For mixed vegetation the decreasing is much clearer, the best fit trend is linear with a slope of 14 mg N m^{-2} $year^{-1}$.

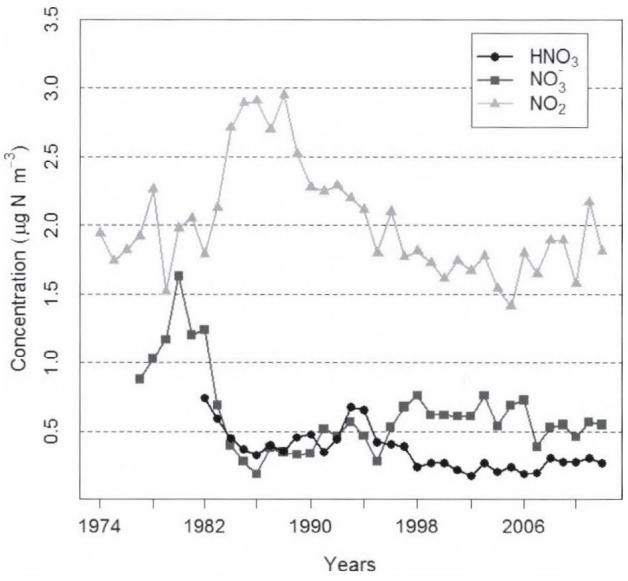

Fig. 7. Atmospheric concentration of oxidized nitrogen species between 1974 and 2012, measured at K-puszta.

Since the variability in wet deposition was smaller, the tendency of total deposition followed that of the dry deposition for both surface types (*Fig. 8*). The ranges of total deposition were 200 mg N m^{-2} higher than for dry deposition for both grass and mixed vegetations. The fitted trends are of the same order like the trends of dry depositions: 1st for mixed vegetation with a yearly reduction of 18 mg N m^{-2} $year^{-1}$, and 4th for grass with a slightly stronger decrease than in dry deposition.

Apparently, the relationship between national NO_x emissions (*Fig. 9*) and depositions is not as clear as in the case of oxidized sulfur compounds. A possible reason for that could be that we are comparing national emissions to depositions calculated from the data of a single station. On the other hand, due to the relatively long atmospheric lifetime of oxidized nitrogen compounds, transboundary transport of pollutants also has a strong influence on depositions. Finally, *Fowler et al.* (2007) suggested, that such non-linearity between emissions and depositions for oxidized nitrogen compounds grows with

distance from the main European source region of the highly populated northern Europe, stretching from the Czech Republic to South East England.

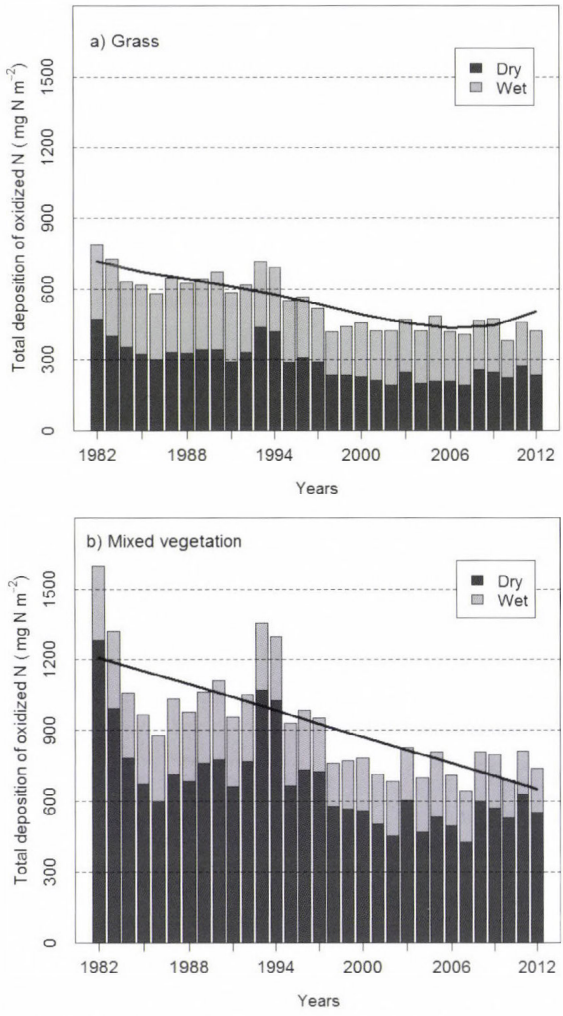

Fig. 8. Total deposition (dry + wet) of oxidized nitrogen species over grass (a) and mixed vegetation (b) between 1982 and 2012 at K-puszta, and the best fit lines to the total depositions.

The approximately 25% decrease in NO_x emission since the beginning of 90's is due to the breakdown of heavy industry after political changes. However, the steadily growing number of cars over the whole period (*Fig. 9*) comparing to the decreasing trend both of emission and total deposition may suggest the impact of technical improvements and national measures in abatement of oxidized

nitrogen emission and resulting deposition – from 1990 the usage of catalyst in cars is ordered by the Hungarian law for newly sold vehicles.

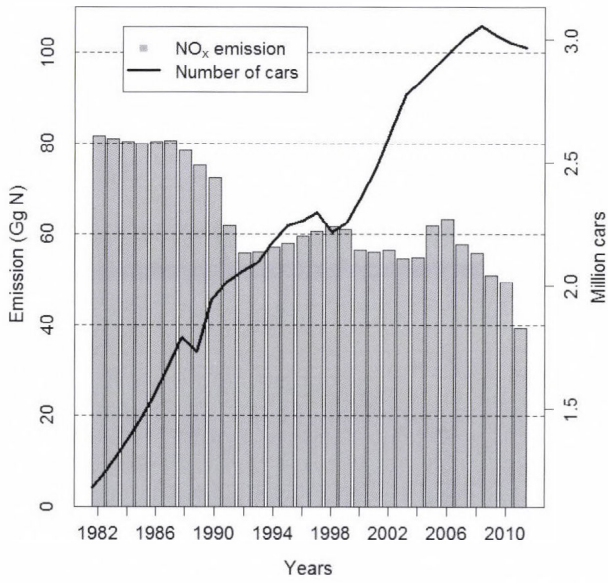

Fig. 9. National emission of NO_x and the number of cars in Hungary between 1982 and 2011.

3.3. Reduced nitrogen compounds

Yearly wet deposition of NH_4^+ ion between 1974 and 1982 (*Fig. 10*) varied from 800 to 1,600 mg N m^{-2}, then the values were under 800 mg N m^{-2}. The best fit trend was a 3rd order polynomial, showing a strong decrease in the first 20 years, and then a moderate further reduction until the end of the period.

Yearly dry deposition (*Fig. 11*) ranged mostly between the values of 200 and 400 mg N m^{-2} before 1996, then the great majority of deposition ranged between 300 and 500 mg N m^{-2}. The fitted 4th order polynomial trend shows a wave-like tendency, with a period of decrease before 1986, followed by a 20-year long increasing period and then a subsequent reduction until 2012. Despite that atmospheric concentration of NH_4^+ was higher in the first 20 years (*Fig. 12*), dry deposition was dominated by NH_3 deposition over the whole period. The cause of that is that NH_3 is highly soluble, resulting in a one order of magnitude higher dry deposition velocity than that of NH_4^+. Moreover, majority of ammonium are in the range of fine particles ($PM_{2.5}$) (*Horváth*, 2003), where deposition velocity has smaller rate than that of ammonia gas.

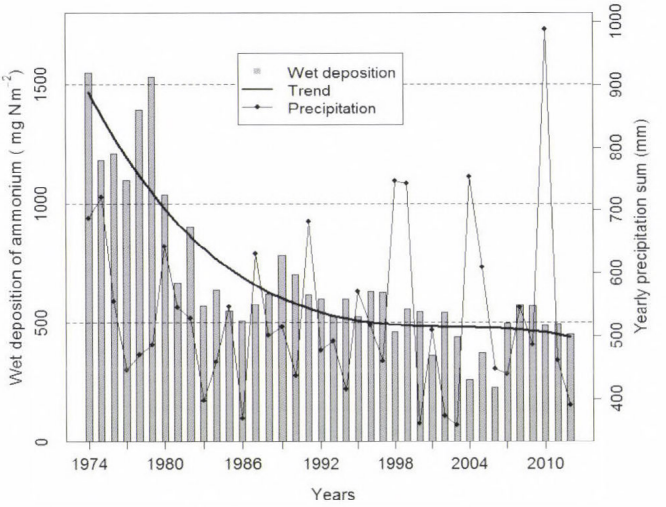

Fig. 10. Wet deposition of reduced nitrogen compounds between 1974 and 2012 at K-puszta, the best fit line, and the yearly precipitation sum.

Total deposition (*Fig. 13*) is mainly dominated by wet deposition, especially in the first half of the period. As the difference between wet and dry deposition is not too large, the opposite tendencies compensated each other, resulting in a balanced total deposition. The best fit, linear trend shows a weak decline of 1.7 mg N year^{-1}.

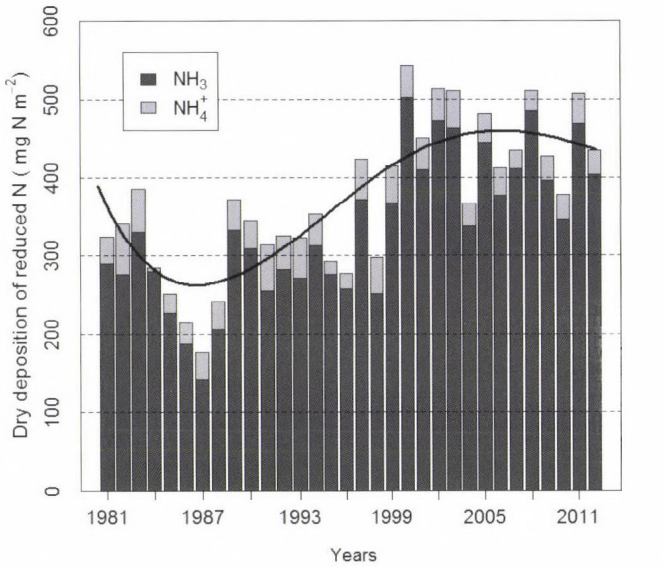

Fig. 11. Dry deposition of reduced nitrogen species between 1981 and 2012 at K-puszta, and the best fit line to the total dry deposition.

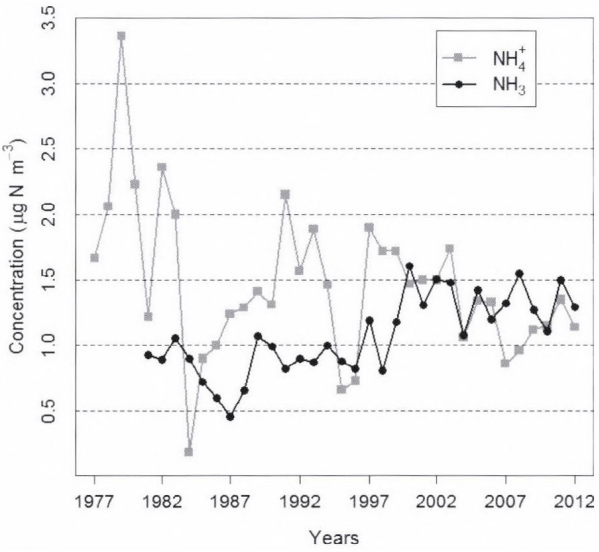

Fig. 12. Atmospheric concentration of reduced nitrogen species between 1974 and 2012, measured at K-puszta.

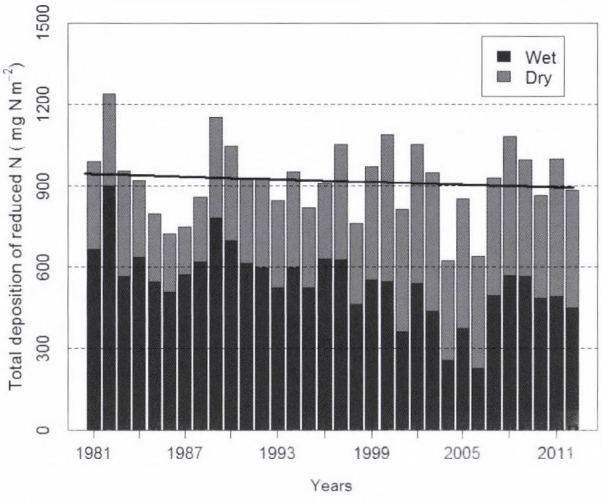

Fig. 13. Total deposition (dry + wet deposition) of reduced nitrogen species between 1981 and 2012 at K-puszta, and the best fit line to the total deposition.

In the national NH_3 emissions (*Fig. 14*), a rapid decrease can be seen between 1989 and 1994, with a close-to-constant emission before and after it. This is mainly parallel with the tendency of wet deposition, but apparently it is

the opposite of the trend in dry deposition. This raises the obvious question: how can the dry deposition grow if emission is reducing? Considering that in our approach the atmospheric concentration and deposition of NH_3 differ only in a constant multiplying factor, the question is the same for concentrations and emissions. Since gaseous NH_3 after emission dissolves quickly on the surface, in this case the influence of long-range transport is presumably weak.

As an alkaline compound, dry deposition of NH_3 is largely dependent on the acidity of the surface water (water film on the surface). Therefore, its deposition is influenced by the deposition of atmospheric acidic components (*Flechard et al.*, 1999). According to *Erisman et al.* (2001) and *Fowler et al.* (2001), the lower the ratio of atmospheric concentration of SO_2 to NH_3 (i.e., SO_2 concentration is relatively low or NH_3 concentration is relatively high), the higher the surface resistance to NH_3 deposition. Consequently, even if the atmospheric input of ammonia decreases with a decreasing SO_2 concentration, it cannot be removed from the atmosphere as the higher pH of the surface water film, caused by the less dissolved SO_2, hampers NH_3 dissolution. As a result, the emitted NH_3 remains in the atmosphere raising its atmospheric concentration, as it was observed earlier by *Horváth et al.* (2009).

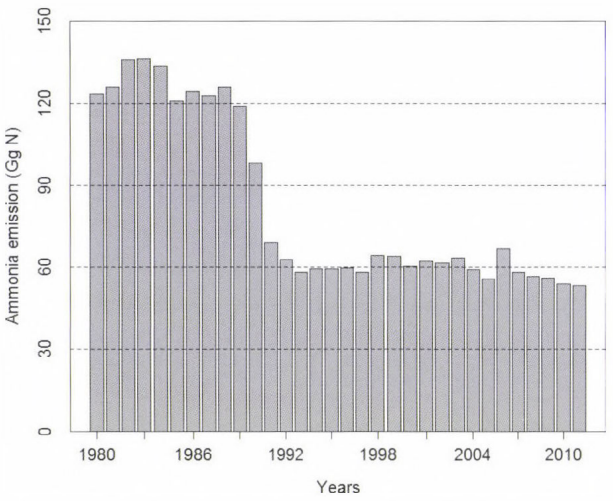

Fig. 14. National emission of ammonia in Hungary between 1980 and 2011.

According to *Fig. 15*, the above described process, referred as the co-deposition of NH_3 and SO_2, was most likely the key process in Hungary as well. On the other hand, this founding highlights the weakness of our simple estimation approach for dry deposition of NH_3, as the process, preventing NH_3

removal from the atmosphere, could lead to lower deposition than our calculations. Therefore, the estimation of NH_3 dry deposition requires further investigation.

In addition, the transfer of ammonia between atmosphere and surface is bi-directional, i.e., not just deposition but also emission can occur depending on the difference between the atmospheric NH_3 concentration and above the surface (*Farquhar et al.*, 1980). Further influencing factors on the magnitude of NH_3 exchange are, among others, temperature, wind speed, and relative humidity, which were all neglected during our approach.

However, considering bi-directional exchange would require a much complex estimation, which has not been applied either in operational ACTMs (*Sutton et al.*, 2013). ACTMs nowadays calculate dry depositions based on the same formula we used, that – even if the calculations are more detailed in an ACTM – supports the relevance of our simple approach.

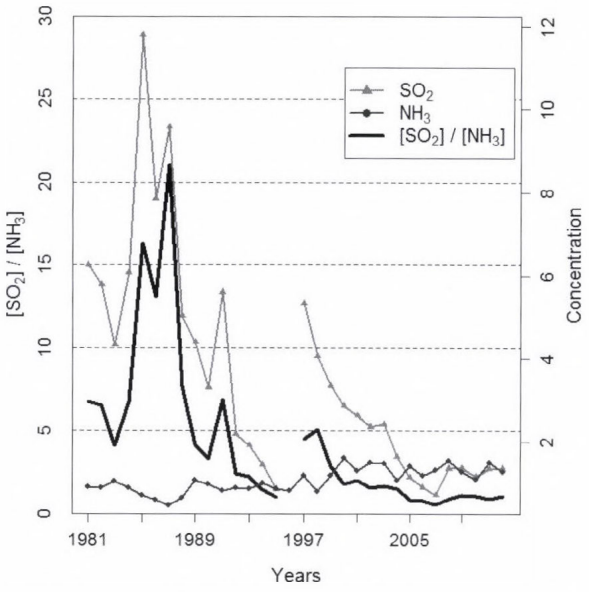

Fig. 15. Atmospheric concentration of SO_2 (μg S m^{-3}, triangles) and NH_3 (μg N m^{-3}, dots), and their ratio (thick line) between 1981 and 2012 at K-puszta.

3.4. Total nitrogen load

Summing up the total depositions of oxidized and reduced nitrogen compounds for grass, we got the total nitrogen load over grass-covered surface (*Fig. 16*). In the period of 1982 and 2012, it varied mainly between 1,000 and

1,600 mg N m^{-2}. According to the measurement practice of air concentration and dry deposition velocity, we estimated the uncertainty of the total nitrogen load ±10% shown as error bars in *Fig. 16*. This uncertainty covers much possibly the year-to-year variability of yearly dry deposition velocities. Compared to the oxidized compounds, deposition of reduced nitrogen compounds had a larger fraction in the total load. As we showed it, both of them had a slow decreasing trend, resulting in a moderate decrease in the total load as well. The fitted trend is linear, with a slope of 12 mg N m^{-2} $year^{-1}$.

Likewise in the case of oxidized sulfur compounds, it is difficult to quantify the acidifying effect of the nitrogen compounds examined above. In addition, in this case the neutralizing effect of dissolving gaseous NH_3 has to be also considered. However, even if dry deposition of reduced nitrogen compounds is highly dominated by NH_3 deposition, in the total load the other components overcame it. Overall, the declining trend of the total nitrogen load implies a mitigating tendency of acidification.

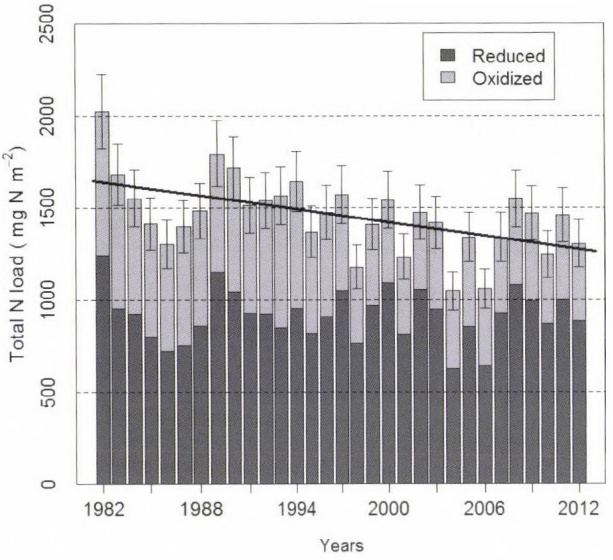

Fig. 16. Total nitrogen load (as a sum of the total deposition of reduced and oxidized nitrogen compounds) over grass between 1982 and 2012 at K-puszta.

4. Conclusions

The purpose of this work was to compile long-term deposition time series for Hungary for acidifying compounds, such as oxidized sulfur, as well as oxidized and reduced nitrogen compounds. To achieve our goal, we used existing results from ACTMs and precipitation chemistry as well as background air pollution

measurements. Comparing the results with national emission datasets, we also made an attempt to interpret the changes in depositions. Finally, we gave a qualitative estimation for the strength of acidification on long term.

In the case of oxidized sulfur compounds, according to the 132-year long deposition time series, 1980 was a changing point: until this year, deposition was steadily increasing, and since then it has been decreasing rapidly. For deposition of oxidized nitrogen compounds, we got declining trend between 1982 and 2012; however, in the case of grass, a non-significant increase occurred in the last four years of the period. We found that the deposition of reduced nitrogen compounds has been also decreasing since 1982. Consequently, our calculation showed that also the total nitrogen load followed a slowly declining tendency.

Despite that the transboundary transport of both oxidized sulfur and nitrogen compounds, influences the national depositions, in the case of the oxidized sulfur compounds the relationship between the emissions and depositions was clearer than for the oxidized nitrogen compounds. On the other hand, we found that the decrease of total deposition of oxidized nitrogen compounds is most likely a sign of the improvement of emission abatement techniques and national emission controlling measures. Same is true for the total deposition of oxidized sulfur species; however, in this case, also the Hungarian industrial recession could be a substantial influencing factor. The total deposition of reduced nitrogen compounds showed only a weak declining tendency in contrast with drastically weakening NH_3 emissions. Moreover, atmospheric NH_3 concentration is nearly constant in spite of emission reduction. We showed that this trend in atmospheric concentration and – in our approach – dry deposition of NH_3 is possibly a result of the declining surface concentration of SO_2. Considering this effect, estimation of dry deposition of NH_3 requires further investigation.

Based on our results, only qualitative conclusions can be drawn regarding the progress of acidification in Hungary: the effect of acidification was most likely to intensify before 1980, since then the phenomenon presumably has been weakening gradually. On the other hand, if atmospheric concentration of NH_3 continuously grows in Hungary, in spite of its potential neutralizing effect in the atmosphere, it may raise new environmental issues in the future due to its key role in the cycle of reactive nitrogen compounds (*Galloway et al.*, 2008).

Acknowledgement – The authors are grateful to Sophia Mylona for providing her model results and to László Haszpra, who contacted her. In addition, we would like to express our appreciation to Ben Marner for sending us his PhD thesis.

References

Almer, B., Dickson, W., Ekstrom, C., Hornstrom, E. and *Miller, U.*, 1974: Effects of acidification on Swedish lakes. *Ambio 3*, 30–36.

A.S.L. & Associates, 1999: Sulfur emissions by country and year. Available: http://www.asl-associates.com/sulfur.htm [Accessed: 15 Novemeber 2013].

CEIP, 2013: Officially reported emission data.

Davidson, C., Miller, J. and *Pleskow, M.*, 1982: The influence of surface structure on predicted particle dry deposition to natural grass canopies. *Water Air Soil Poll.18*, 25–43.

Duan, L., Liu, J., Xin, Y. and *Larssen, T.*, 2013: Air-pollution emission control in China: Impacts on soil acidification recovery and constraints due to drought. *Sci. Total Environ. 463–464*, 1031–1041.

EMEP/MSC-W, 2013: EMEP MSC-W modelled air concentrations and depositions. Available: http://emep.int/mscw/index_mscw.html [Accessed: 12 December 2013].

Erisman, J.W., Hensen, A., Fowler, D., Flechard, C.R., Grüner, A., Spindler, G., Duyzer, J.H., Weststrate, H., Römer, F., Vonk, A.W. and *Jaarsveld, H. v.*, 2001: Dry Deposition Monitoring in Europe. *Water Air Soil Poll. Focus 1*, 17–27.

Farquhar, G.D., Firth, P.M., Wetselaar, R. and *Weir,B.*, 1980: On the Gaseous Exchange of Ammonia between Leaves and the Environment: Determination of the Ammonia Compensation Point. *Plant Physiol. 66*, 710–714.

Flechard, C,R., Fowler, D., Sutton, M.A. and *Cape, J.N.*, 1999: A dynamic chemical model of bi-directional ammonia exchange between semi-natural vegetation and the atmosphere. *Q. J. Roy. Meteorol. Soc. 125*, 2611–2641.

Fowler, D., Smith, R., Muller, J., Cape, J., Sutton, M., Erisman, J. and *Fagerli, H.*, 2007: Long Term Trends in Sulphur and Nitrogen Deposition in Europe and the Cause of Non-linearities. *Water Air Soil Poll. Focus 7*, 41–47.

Fowler, D., Sutton, M.A., Flechard, C.R., Cape, J.N., Storeton-West, R., Coyle, M. and *Smith, R.I.*, 2001: The control of SO_2 dry deposition on to natural surfaces and its effects on regional deposition. *Water Air Soil Poll. Focus 1*, 39–48.

Gallagher, M.W., Nemitz, E., Dorsey, J.R., Fowler, D., Sutton, M.A., Flynn, M. and *Duyzer, J.*, 2002: Measurements and parameterizations of small aerosol deposition velocities to grassland, arable crops, and forest: Influence of surface roughness length on deposition. *J. Geophys. Res. Atmos.107*, AAC 8-1-AAC 8-10.

Galloway, J. N., 1989: Atmospheric Acidification: Projections for the Future. *Ambio 18*, 161–166.

Galloway, J.N., Townsend, A. R., Erisman, J.W., Bekunda, M., Cai, Z., Freney, J.R., Martinelli, L.A., Seitzinger, S.P. and *Sutton, M.A.*, 2008: Transformation of the Nitrogen Cycle: Recent Trends, Questions, and Potential Solutions. *Science 320*, 889–892.

Goldman, J.C. and *Brewer, P.G.*, 1980: Effect of Nitrogen Source and Growth Rate on Phytoplankton-Mediated Changes in Alkalinity. *Limnol Oceanog. 25*, 352–357.

Grennfelt, P. and *Hov, Ø.*, 2005: Regional Air Pollution at a Turning Point. *Ambio 34*, 2–10.

Horváth, L., 1978: A csapadékvíz kémiai összetétele és a légköri nyomanyagok depozíciója Budapesten. *Időjárás 82*, 211–224. (in Hungarian)

Horváth, L., 2003: Dry deposition velocity of PM2.5 ammonium sulfate particles to a Norway spruce forest on the basis of S- and N-balance estimations. *Atmos. Environ. 37*, 4419–4424.

Horváth, L., Asztalos, M., Führer, E., Mészáros, R. and *Weidinger, T.*, 2005: Measurement of ammonia exchange over grassland in the Hungarian Great Plain. *Agric. Forest Meteorol.* 130, 282–298.

Horváth, L., Fagerli, H. and *Sutton, M.A.*, 2009: Long-term record (1981–2005) of ammonia and ammonium concentrations at K-puszta Hungary and the effect of SO_2 emission change on measured and modelled concentrations. In (Eds.:*M.A., S., Reis, S.* and *Baker, S.M.H.), Atmospheric Ammonia – Detecting Emission Changes and Environmental Impacts. Results of an Expert Workshop Under the Convention on Long-range Transboundary Air Pollution.* Springer Science + Business Media B.V.

Johnson, D.W. and *Reuss, J.O.*, 1984: Soil-mediated effects of atmospherically deposited sulphur and nitrogen. *Philosop. Transac. Roy.Soc. London Series B-Biol. Sci.305*, 383–392.

KSH, 2013: *Szállítás (1960–)*. Available: http://www.ksh.hu/docs/hun/xstadat/xstadat_hosszu/h_odme001.html [Accessed: 15 August 2013].

Kugler, Sz., Horváth, L. and *Weidinger, T.*, 2014: Modeling dry flux of ammonia and nitric acid between the atmosphere and Lake Balaton. *Időjárás 118*, 93–118.

Lefohn, A.S., Husar, J.D. and *Husar, R.B.*, 1999: Estimating historical anthropogenic global sulfur emission patterns for the period 1850–1990. *Atmos. Environ. 33*, 3435–3444.

Lipfert, F.W., 1987: Effects of acidic deposition on the atmospheric deterioration of materials. *Materials Perform. 26*, 12–19.

Marner, B.B., 2003: Atmospheric nitrogen deposition to a nitrate vulnerable zone. Ph.D. Thesis. University of Birmingham, UK.

Mylona, S., 1992: Trends of sulphur dioxide emissions, air concentrations and depositions of sulphur in Europe since 1880. *EMEP/MSC-W Report 2/93.* EMEP/MSC-W, Oslo, Norway.

Nicholson, J.P., Weston, K.J. and Fowler, D., 2001: Modelling horizontal and vertical concentration profiles of ozone and oxides of nitrogen within high-latitude urban areas. *Atmos.Environ.*35, 2009–2022.

OKTH/MTA, 1987: A környezet erősödő savasodása. *Környezet és természetvédelmi kutatások 7.* OKTH, Budapest, Hungary.(In Hungarian)

Pope, C.A., III, Burnett, R.T., Thun, M.J., Calle, E.E., Krewski, D., Ito, K. and *Thurston, G.D.,* 2002: Lung cancer, cardiopulmonary mortality, and long-term exposure to fine particulate air pollution. *J. Am. Medic. Ass. 287*, 1132–1141.

Puxbaum, H. and *Gregori, M.,* 1998: Seasonal and annual deposition rates of sulphur, nitrogen and chloride species to an oak forest in north-eastern austria (wolkersdorf, 240 m a.s.l.). *Atmos. Environ. 32*, 3557–3568.

Raven, J.A., 1985: Regulation of pH and generation of osmolarity in vascular plants: a cost-benefit analysis in relation to efficiency of use of energy, nitrogen and water. *New Phytologist 101*, 25–77.

Ruijgrok, W., Tieben, H. and *Eisinga, P.,* 1997: The dry deposition of particles to a forest canopy: A comparison of model and experimental results. *Atmos. Environ. 31,* 399–415.

Sakamoto, Y., Ishiguro, M. and *Kitagawa, G.,* 1986: Akaike Information Criterion Statistics. D. Reidel Publishing Company, Dordrecht, Netherlands.

Sandnes, H. and *Styve, H.,* 1992: Calculated Budgets for Airborne Acidifying Components in Europe, 1985, 1987, 1988, 1989, 1990 and 1991. *EMEP/MSC-W Report 1/92.* EMEP/MSC-W, Oslo, Norway.

Seinfeld, J.H. and *Pandis, S.N.,* 2006: Atmospheric Chemistry and Physics: From Air Pollution to Climate Change. John Wiley & Sons, New York, USA.

Slinn, W.G.N., 1982: Predictions for particle deposition to vegetative canopies. *Atmos. Environ. 16*, 1785–1794.

Stelson, A.W. and *Seinfeld, J.H.,* 1982: Relative humidity and temperature dependence of the ammonium nitrate dissociation constant. *Atmos. Environ. 16*, 983–992.

Sutton, M.A., Howard, C.M., Erisman, J.W., Bealey, W.J., Billen, G., Bleeker, A., Bouwman, A.F., Grennfelt, P., van Grinsven, H. and *Grizzetti, B.,* 2011: The challenge to integrate nitrogen science and policies: the European Nitrogen Assessment approach. In (Eds.: *Sutton, M.A., Howard, C.M., Erisman, J.W., Billen, G., Bleeker, A., Grennfelt, P., Van Grinsven, H.* and *Grizzetti, B.*) The European Nitrogen Assessment: Sources, Effects and Policy Perspectives. Cambridge, UK.

Sutton, M.A., Reis, S., Riddick, S.N., Dragosits, U., Nemitz, E., Theobald, M.R., Tang, Y.S., Braban, C.F., Vieno, M., Dore, A.J., Mitchell, R.F., Wanless, S., Daunt, F., Fowler, D., Blackall, T.D., Milford, C., Flechard, C.R., Loubet, B., Massad, R., Cellier, P., Personne, E., Coheur, P.F., Clarisse, L., Van Damme, M., Ngadi, Y., Clerbaux, C., Skjøth, C. A., Geels, C., Hertel, O., Wichink Kruit, R.J., Pinder, R.W., Bash, J.O., Walker, J.T., Simpson, D., Horváth, L., Misselbrook, T.H., Bleeker, A., Dentener, F. and *de Vries, W.,* 2013: Towards a climate-dependent paradigm of ammonia emission and deposition. *Philosop. Transact. Roy. Soc. B: Biol.Sci. 368*, 20130166.

Várallyay, G., Rédly, L. and *Murányi, A.,* 1986: A savas ülepedés hatása a talajra Magyarországon. *Időjárás 90*, 169–190. (In Hungarian)

INSTRUCTIONS TO AUTHORS OF *IDŐJÁRÁS*

The purpose of the journal is to publish papers in any field of meteorology and atmosphere related scientific areas. These may be

- research papers on new results of scientific investigations,
- critical review articles summarizing the current state of art of a certain topic,
- short contributions dealing with a particular question.

Some issues contain "News" and "Book review", therefore, such contributions are also welcome. The papers must be in American English and should be checked by a native speaker if necessary.

Authors are requested to send their manuscripts to

Editor-in Chief of IDŐJÁRÁS
P.O. Box 38, H-1525 Budapest, Hungary
E-mail: journal.idojaras@met.hu

including all illustrations. MS Word format is preferred in electronic submission. Papers will then be reviewed normally by two independent referees, who remain unidentified for the author(s). The Editor-in-Chief will inform the author(s) whether or not the paper is acceptable for publication, and what modifications, if any, are necessary.

Please, follow the order given below when typing manuscripts.

Title page: should consist of the title, the name(s) of the author(s), their affiliation(s) including full postal and e-mail address(es). In case of more than one author, the corresponding author must be identified.

Abstract: should contain the purpose, the applied data and methods as well as the basic conclusion(s) of the paper.

Key-words: must be included (from 5 to 10) to help to classify the topic.

Text: has to be typed in single spacing on an A4 size paper using 14 pt Times New Roman font if possible. Use of S.I. units are expected, and the use of negative exponent is preferred to fractional sign. Mathematical formulae are expected to be as simple as possible and numbered in parentheses at the right margin.

All publications cited in the text should be presented in the *list of references*, arranged in alphabetical order. For an article: name(s) of author(s) in Italics, year, title of article, name of journal, volume, number (the latter two in Italics) and pages. E.g., *Nathan, K.K.,* 1986: A note on the relationship between photo-synthetically active radiation and cloud amount. *Időjárás 90,* 10-13. For a book: name(s) of author(s), year, title of the book (all in Italics except the year), publisher and place of publication. E.g., *Junge, C.E.,* 1963: *Air Chemistry and Radioactivity.* Academic Press, New York and London. Reference in the text should contain the name(s) of the author(s) in Italics and year of publication. E.g., in the case of one author: *Miller* (1989); in the case of two authors: *Gamov* and *Cleveland* (1973); and if there are more than two authors: *Smith et al.* (1990). If the name of the author cannot be fitted into the text: *(Miller,* 1989); etc. When referring papers published in the same year by the same author, letters a, b, c, etc. should follow the year of publication.

Tables should be marked by Arabic numbers and printed in separate sheets with their numbers and legends given below them. Avoid too lengthy or complicated tables, or tables duplicating results given in other form in the manuscript (e.g., graphs).

Figures should also be marked with Arabic numbers and printed in black and white or color (under special arrangement) in separate sheets with their numbers and captions given below them. JPG, TIF, GIF, BMP or PNG formats should be used for electronic artwork submission.

Reprints: authors receive 30 reprints free of charge. Additional reprints may be ordered at the authors' expense when sending back the proofs to the Editorial Office.

More information for authors is available: journal.idojaras@met.hu

Published by the Hungarian Meteorological Service

Budapest, Hungary

INDEX 26 361

HU ISSN 0324-6329